AD NUMBER

AD835581

NEW LIMITATION CHANGE

TO

Approved for public release, distribution unlimited

FROM

Distribution authorized to U.S. Gov't. agencies and their contractors; Critical Technology; 11 AUG 1959. Other requests shall be referred to Space and Missile Systems Organization, Los Angeles, CA.

AUTHORITY

SAMSO ltr, 28 Feb 1972

CONFIDENTIAL

REPORT NO. 7B 2124-1
DATE 11 August 1959
NO. OF PAGES 65

CONVAIR | ASTRONAUTICS

CONVAIR DIVISION OF GENERAL DYNAMICS CORPORATION

AD 835581

UNCLASSIFIED

# CONVAIR - ARMA BENCH TEST COMPATIBILITY PROGRAM

REPORT NO. 7B 2124-1



This document is subject to special export controls and each transmittal to foreign governments or foreign nationals may be made only with prior approval of: Hq.SAMSO, LA., Ca. 90045 Attn: SMSD

PREPARED BY W. S. Curry D. E. Carson
W. S. Curry D. E. Carson

APPROVED BY F. Walley for W. C. Hardy
Test Lab Group Mgr.

CHECKED BY E. Godenschwager
E. Godenschwager

APPROVED BY R. S. Campbell
R. S. Campbell
Chief of Test Labs

CHECKED BY H. E. Shaw
H. E. Shaw

Classification Changed To:
UNCLASSIFIED

Authorized By: D D 254 MSCG
Date 5-14-65 WS107A

Reclassified By: Richard J. Cook
Dept. 130-1
Date -65

REVISIONS

| NO. | DATE | BY | CHANGE | PAGES AFFECTED |
|---|---|---|---|---|
| jn | | | | |
| | | | | |
| | | | | |

UNCLASSIFIED



FORM NO. A-700-2

TABLE OF CONTENTS

## 1.0 INTRODUCTION:

With reference to STL Document GM437-335 Engineering Bench Compatibility Test Plan and Arma Document DAG 4562 Laboratory Compatibility Program, STL requested that engineering bench compatibility tests between Convair Autopilot and Arma Inertial Guidance System Components be conducted. Accordingly, the Servo-Mechanisms Group requested that these tests be performed in the Systems Test Laboratory, as specified in Convair Report AZM-27-073, dated 27 October 1958.

The purpose of the bench tests was to determine any system incompatibilities as early in the D/AIG program as possible. Primarily, these tests were made to determine the nature and cause of any interface problems that might exist between the available Convair and Arma equipment. Overall missile system compatibility is to be determined during the 30D Tests.

The bench tests were divided into two categories; measurements to determine that interface signal requirements were met, and measurements to determine if the systems component power requirements were compatible with the airborne power supply.

This report is therefore divided in two sections. The first section contains Guidance-Autopilot signal compatibility information, while the second section contains the data on the compatibility of the guidance system with the airborne power supply. The first part of this report is based primarily on information supplied by Arma, and on information contained in reports issued by the Servo-Mechanisms Group as listed under referenc .

## 2.0 SECTION I: Summary of Arma/AIG Autopilot Compatibility Tests.

### 2.1 OBJECTIVES:

Determine -

2.1.1 Signal compatibility between Convair AIG Autopilot and Arma MGS.

2.1.2 Operational characteristics of the guidance system on the airborne power supply.

2.1.3 Operational characteristics of the guidance system during power changeover.

UNCLASSIFIED



FORM NO. A-702-2

2.2 CONCLUSIONS:

2.2.1 No serious incompatibilities were detected between the Convair Autopilot system and the Arma MGS during these tests.

2.2.2 The guidance system performed correctly on both ground and airborne power supplies over a wide range of power system load conditions.

2.2.3 The operational status of the AIG Autopilot was recovered within a fraction of a second after power changeover, while the Arma equipment was fully operational within five seconds in all tests run.

2.3 TEST SPECIMENS:

2.3.1 Convair D/AIG Autopilot Components
Gyro Package
Servo Amplifier Package
Digital Programmer Package

2.3.2 Convair special test equipment
Control Maneuvers Servo Table
Package Control Units

2.3.3 Convair Power Supply Components
Inet-Palmer ground power unit
Airborne Inverter power unit

For a more detailed description of these units, refer to the Electrical Section of this report.

2.3.4 Arma Lot II Missile Guidance System
Computer
Inertial Platform
Analog Signal Converter
Digital Signal Converter
Control Central

2.3.5 Arma Special Test Equipment
ET-1 MGS Test Racks
Computer Test Kit
Simulated Break Away Panel

2.4 TEST PROCEDURES:

2.4.1 Initial Installation

A walled in, limited access area at Columns J, K-1, Bldg. 5 was created for equipment security, 25 January 1959. The Arma Test hardware was then installed and connected. Power lines, control boxes and outlets were installed, furnishing as necessary:

2.4 TEST PROCEDURES: (Continued)

2.4.1 Initial Installation (Continued)

440 volts, 60 cps, 3 phase

117 volts, 400 cps, 3 phase

117 volts, 60 cps, 1 phase

28 volts, DC

Forced air, dry ice equipment coolers were designed and built for Arma equipment, as were a few minor pieces of special test equipment. The required test instruments were obtained and the area was checked out and operational by 9 February 1959. See Figures 1 through 5.

2.4.2 Initial Arma/AIG Gyro Canister Compatibility Tests -

2.4.2.1 On 9 February 1959 the first prototype AIG gyro canister was tested for compatibility with the Arma MGS. The object of this test was to determine if any discrepancies existed when pitch and yaw steering signals were supplied to the gyro canister.

2.4.2.2 In the first test pitch steering signals from the pitch gimbal synchro of the Arma Inertial Platform were supplied to the pitch guidance input of the torquer amplifier in the gyro canister. Signals ranging from +5.0 to -5.0 volts in 1 volt increments were used as inputs. The parameters recorded on a Sanborn recorder were as follows: Input Signal, Pitch Gyro Output, Pitch Amplifier Output and Pitch Torque Current. At each voltage input level, the pitch guidance was disabled through an electronic switch in the gyro canister and the gyro was electrically nulled. The nulling loop was then opened and the pitch guidance was enabled, allowing the signal to torque the gyro. The resulting ramp outputs and torquing current were recorded at that time.

2.4.2.3 The second test was to apply yaw steering signals from the computer to the yaw guidance input of the torquer amplifier in the gyro canister. The inputs ranged from +3 volts to -3 volts in 0.5 volt increments. The parameters recorded on the Sanborn recorder were as follows: Input Signal, Yaw Gyro Output, Yaw Signal Amplifier Output, and Yaw Torque Current. As in the case of the pitch channel, the yaw guidance was disabled through the electronic switch, and the gyro was electrically nulled,

2.4 TEST PROCEDURES: (Continued)

2.4.2.3 (Continued)

The nulling loop was then opened and the yaw guidance was enabled, allowing the signal to torque the gyro.

2.4.2.4 In phase and quadrature components of Arma pitch and yaw steering signals were measured.

2.4.2.5 Arma-Convair guidance interface impedances were investigated.

2.4.2.6 The efficiencies of the torquer amplifier guidance enable switches were evaluated by noting their attenuation of the guidance input in the disable mode.

2.4.3.0 After these initial checks, the detailed testing program was undertaken, and completed by 8 May 1959. The following areas were investigated:

2.4.3.1 Pitch and Yaw Steering

a) Open Autopilot gyro loop
b) Closed Autopilot gyro loop
c) Closed Autopilot gyro loop about a flight maneuvers servo table.

2.4.3.2 The pitch and yaw steering tests were conducted to determine the compatibility of the Arma system with the autopilot gyro canister as well as to compare gyro torquing rates measured three separate ways; open and closed gyro loop, and closed loop through the maneuvers table.

Autopilot gyro package servo loop parameters were also investigated.

2.4.3.3 Pitch gyro drift due to pitch steering null signal was investigated.

2.4.3.4 Yaw gyro drift due to yaw steering null signal was investigated.

2.4.3.5 Effect of yaw steering signal ripple on gyro amplifier output was measured.

2.4 TEST PROCEDURES: (Continued)

2.4.3.6 A normal Lot B 1-G problem yaw steering signal was fed from the Arma Computer to the Autopilot while the computer cutoff signals were sent to the programmer. The tests were run on ground power and repeated using the airborne power supply. The autopilot was operated closed loop using an external nulling amplifier.

2.4.3.7 Simulated Lot C 1-G Test - closed loop. Lot C is a more advanced form of the Arma MGS. A simulated Lot C yaw steering profile was generated by manually setting the yaw steering signal levels in the proper time sequence with the Arma computer test kit. The tests conducted with the simulated Lot C sequence profile were the same as for the normal 1-G profile with the exception that cut-off signals were not available.

2.4.3.8 Sensitivity of discrete signal circuits to over and under supply voltages was measured.

2.4.3.9 The effect of switching on and off the simulated loads on the guidance system power supply was investigated. Arma MGS operation at the specification limits of power supply amplitude and frequency was measured.

2.4.3.10 Effects of power changeover, from ground to airborne, on the guidance system was measured.

2.5 TEST RESULTS:

2.5.1.0 Initial Arma/AIG Gyro Canister Compatibility Tests.

2.5.1.1 The results of the pitch steering tests may be seen in Figure 6 where input voltage is plotted versus Autopilot gyro output, amplified gyro output, and torque current. This data appeared to be consistent with what was expected.

2.5.1.2 Figure 7 shows the results of the yaw steering tests. The null voltage input was 60mv total with negligible phase sensitive component. The recorded gyro drift at this time was approximately 0.005 volts/second or 25 degrees/hour using the nominal gyro sensitivity of 0.7 volts/degree.

2.5.1.3 The in-phase and quadrature components of Arma MGS yaw and pitch output steering signals were measured and recorded by Arma at this time also. Their results are shown in Figures 8, 9, 10 and 11.

2.5 TEST RESULTS: (Continued)

2.5.1.4 The tests of Figures 6 and 7 were made by adjusting the Arma outputs to the desired torquer amplifier input voltage levels. This cancelled any loading effects on the Arma equipment which may have existed. However, Arma supplied the following information on its pitch and yaw source impedances:

| | |
|---|---|
| Pitch | 370 ± 20% + j250±20% ohms |
| Yaw | 6000 ohms |

These impedances drive the pitch and yaw guidance input circuits of the gyro torquer amplifiers, each of which offers a load of 100,000 ohms with guidance disabled and about 190,000 ohms with guidance enabled ensuring a good impedance match with Arma.

2.5.1.5 The enable - disable guidance switches appeared to function efficiently. With 3 volts RMS steering signal applied to the guidance input, and with the switch in the disable condition, .00417 volts per second appeared at the amplifier output. Using a sensitivity of 4.5 volts/degree this is equivalent to a drift rate of 3.34 degrees/hour.

2.5.2 Results of Main Testing Program -

2.5.2.1 Pitch and yaw steering

The pitch steering tests were similar to those run in the initial checks, with signals ranging from null to ±4 volts used as inputs. All testing was done on both ground and airborne power. With the Autopilot gyro loop open, the ramp output from the signal amplifier was recorded at each voltage level after initially nulling the gyro and disabling the guidance input. Simultaneously, the nulling loop was opened and the guidance was enabled allowing the gyro to slew to its stop.

For the second test, the gyro nulling loop was left closed, and the guidance was enabled, while the gyro displacement was measured at the nulling amplifier output for each steering input level. The third test was to close the loop about the control maneuvers servo table and monitor the table rate at each input level. Sample recordings of these tests can be seen in Figures 12 and 13. With the servo loop closed, the rate gyro output was recorded to determine whether any inconsistencies existed in table rate.

2.5 TEST RESULTS: (Continued)

2.5.2.1 Pitch and yaw steering (Continued)

The yaw steering tests were run in a similar manner, with signals ranging from null to ±3 volts used as inputs. The open loop tests were performed as before by applying the yaw steering signals to the guidance input after which the nulling loop was opened and the guidance enabled allowing the gyro to slew to its stop. The ramp output from the gyro signal amplifier was recorded as shown in Figure 14. The same test was repeated with the nulling loop closed and the output of the nulling amplifier recorded, also shown in Figure 14.

2.5.2.2 Autopilot Gyro Package Torquing Rates and Parameters -

Figure 16 is a block diagram of a floated rate integrating gyro and its associated circuitry. The blocks inside the dotted lines represent the components of a floated rate gyro, while those outside represent needed circuitry for open or closed loop operation. Open loop torquing is accomplished with S1 and S2 open, and with the signal applied to the guidance input. Closed servo table loop torquing is accomplished with S1 closed and S2 open. Closed gyro loop torquing is accomplished with switch S1 open and switch S2 closed.

The gyro open loop torquing rate may be defined by

$$\frac{s\theta_o}{E_i} = \frac{\dot{\theta}_o}{E_i} = \frac{K_t \; S_t}{C} \quad \frac{\text{deg/sec}}{\text{volt}}$$

Where $K_t$ = torquer amplifier gain in volts/volt
$S_t$ = torque generator transfer function in volts/deg.
$C$ = viscous damping torque of the gyro in dynes - cm/deg/sec

The open loop torquing rate is calculated from the voltage ramp output of the signal amplifier using the displacement sensitivity which is calibrated to ±5.5%.

Closing the loop about a servo table on which the gyro package is mounted, the torquing rate becomes

$$\frac{s\theta_o}{E_i} = \frac{\dot{\theta}_o}{E_i} = \frac{K_t \; S_t}{H}$$

where H is the gyro angular momentum.

2.5 TEST RESULTS: (Continued)

2.5.2.2 (Continued)

It can be seen that the torquing rates obtained using these two methods of measurement could differ considerably especially if the damping should vary some percentage over a specified temperature range. Figure 17 does show, however, a fairly good correspondance between open and closed servo loop torquing rates.

The third method tried was to close the loop about the gyro itself, torque the gyro electrically with the Arma steering signals, and record the output of the nulling amplifier for each input level. Since the input summing resistors at the input to the torquer amplifier are in the ratio of 1.21 to 1, the voltage $E_n$ should be 1.21 X $E_i$ at any input level. This is verified in Figure 17.

The predominate time constant of the Autopilot gyro nulling loop was computed to be 0.5 second. This seems to agree with the time constant recorded in the simulated Lot C 1-G Test shown in Figure 8. In this test the gyro loop was closed and the nulling amplifier output was recorded, showing a nulling loop time constant of about 0.5 seconds. If necessary, the loop gain could probably be increased sufficiently to lower the time constant, as the loop possesses an ample gain margin.

Summarizing, the gyro nulling loop had a computed natural frequency of 3.5 cps, a damping ratio of 5.62, and a time constant of 0.5 seconds. All these parameters are a function of loop gain which can be controlled by adjusting the gain of the nulling amplifier.

2.5.2.3 The pitch steering signal was nulled by pinning the inertial platform pitch gimbal with a zero pin.

The effect of the Arma pitch steering null signal on the apparent Autopilot gyro drift was then recorded as shown in Figure 18. This null drift was recorded for six minutes. The drift in degrees per hour was calculated using the pitch displacement sensitivity which was calibrated to 3.5 volts/degree. This calculated drift is shown as follows:

2.5 TEST RESULT: (Continued)

2.5.2.3 (Continued)

| | |
|---|---|
| Drift at the end of six minutes | 0.9 volts |
| Drift per hour | 9 volts/hour |
| Drift in degrees/hour | $\frac{\text{9 volts/hour}}{\text{3.5 volts/deg.}}$ = 2.57 deg/hr. |

2.5.2.4 The Arma yaw steering signal was nulled by use of the computer test kit in the "zero subtract" position. The effect of the yaw steering null signal on the apparent Autopilot gyro drift is shown in Figure 19. The gyro drift was recorded for three minutes in each direction by reversing the Arma computer reference voltages' phase. In either direction the drift appeared to be low, 2.27 deg/hr. to 3.46 deg/hr., both within tolerance. The difference between these two drift rates is 1.19 deg/hr. which is the true gyro drift rate caused by the imperfect null signal.

2.5.2.5 The 2 cps ripple on the yaw output of the Arma computer did appear at the output of the nulling amplifier as a 0.1 volt peak-peak signal. The amplitude of the 2 cps ripple is dependent on the steering input signal level. As shown in Figures 14 and 15, the input signal level for 1.1 volts peak-peak was about 3 volts RMS. To determine the effect of the 2 cps ripple on the entire Autopilot system including the sustainer and vernier engines, the resulting 2 cps ripple was recorded at the output of the yaw signal amplifier. See Figure 20. With a 3 volts RMS input signal, the peak-peak voltage appearing at the output of the signal amplifier was 0.2 volts. The sustainer and vernier engine deflection for a peak-peak input of 0.2 volts can be calculated as follows: the end to end sustainer pitch and yaw displacement gain is 1.85 deg/deg. The yaw vernier displacement gain is 15.3 deg/deg. A one degree displacement input produces 3.5 volts signal amplifier out. It follows that the sustainer displacement sensitivity is

$$\frac{\text{1.85 deg/deg.}}{\text{3.5 volts/deg.}} = \text{0.53 deg/volt}$$

2.5 TEST RESULTS: (Continued)

2.5.2.5 Therefore a 0.2 volt peak-peak signal amplifier output produces a sustainer deflection of

$$0.53 \times 0.2 = 0.106 \text{ degrees peak-peak at 2 cps.}$$

The vernier displacement sensitivity is

$$\frac{15.3}{3.5} = 4.37 \text{ deg/volt.}$$

Thus a 0.2 volt peak-peak signal amplifier output produces a vernier deflection of

$$4.37 \times 0.2 = 0.874 \text{ degrees peak-peak at 2 cps.}$$

From the above calculations, it appears that these small engine deflections will not be detrimental to the autopilot control system. The calculated sustainer deflection should be within the dead zone of the engine servo system.

The third test performed with yaw steering input signals was to close the loop about the control maneuvers servo table. This test is shown in Figure 15 where the rate gyro output shows a 0.04 volt peak to peak 2 cps oscillation. This is equivalent to 0.2 deg/sec. peak-peak modulation upon the table rate of 1.24 deg/sec.

2.5.2.6 The normal Lot B 1-G yaw steering profile using airborne power is shown in Figure 21. This test was done with the Autopilot gyro nulling loop closed and the output of the nulling amplifier recorded. No unusual transients appeared on the recording and the output appeared normal. Figure 10 shows another recording taken on airborne power.

2.5.2.7 The simulated Lot C 1-G test is shown in Figure 22. In this test the gyro loop was closed and the nulling amplifier output was recorded.

2.5 TEST RESULTS: (Continued)

2.5.2.8 On 12 March 1959, the Arma MGS and Convair Autopilot were run as a system. One G problems were run with the computer cut-off signals going to the programmer. The DC power supply was adjusted for nominal, under and over voltage levels. The performance of the MGS-Autopilot discretes circuitry was normal under all conditions.

2.5.2.9 The entire simulated load was switched on and off to simulate an extreme airborne power profile. No significant variations appeared in the recorded outputs of either Arma or Convair guidance components. The Arma MGS operation was normal at the specification limits of power supply amplitude and frequency.

2.5.2.10 Power Transfer Tests were made to determine the effect on the operational status of the MGS and Autopilot components. Phase switch-over times were unequal, and transients lasted as long as thirty milliseconds. However, total separation from the ground supply was always achieved before the airborne inverter was switched in.

The servo package recovered operational status within several milliseconds and therefore posed no problems.

Changeover tests were performed with the programmer at zero ready to receive a launch command. At power changeover the programmer power supply voltage decreased which resulted in programmer logic commanding a satisfactory reset to zero as the voltages returned to normal values. No undesirable voltage transients were noted in critical programmer outputs.

The effects of power changeover on the gyro package are shown in Figures 23, 24 and 25. There appear to be no problem areas except for a 0.3 volt transient spike lasting for 0.1 second appearing at the output of the signal amplifier. This should have a negligible effect on system operation.

2.5 TEST RESULTS: (Continued)

2.5.2.10 (Continued)

The first area of investigation on the Arma equipment was the effect on platform alignment. As the system power was switched from ground to airborne, the steering resolver and pendulum outputs were recorded, as in Figures 26, 27 and 28. Any change in resolver or pendulum outputs would indicate gimbal motion. There was no change in pendulum output as a result of power changeover. A 2.5 millivolt change in roll resolver output was recorded indicating a twenty second error. As the resolver output is directly proportional to line voltage, a major factor in the resolver output change is the difference between the voltage levels of the ground and airborne supplies. The voltage difference was about 1% at the time of this measurement.

Platform azimuth alignment was monitored optically using a Watts autocollimator to sight on the platform porro prism. The angular offset of the platform in azimuth due to power transfer was less than five seconds for repeated runs.

The recovery of azimuth alignment from an offset was normally observed to be accomplished within two or three seconds as a result of the ET-1 Equipment Gyro Torquing Amplifiers. At no time did recovery exceed seven seconds. On the basis of these figures, Arma states that the platform will have fully recovered from any offset due to power transfer prior to launch.

The power transfer transient was reflected in the platform and computer power supplies. There was no significant increase in ripple or noise on the DC voltages after transfer. Observed control and power supply voltages of the Arma equipment are tabulated in Figure 30 to give qualitative definition to the supply variations after changeover.

The Arma MGS servo amplifier output showed a ripple at the difference frequency of the two supplies. See Figure 29. Maximum ripple was about 1 volt peak to peak. Total voltage was within specifications. Servo response was normal judging by the recovery time from a step input. It is presumed that this "hum" pickup will not be present in the missile once the umbilical is detached.

2.5 TEST RESULTS: (Continued)

2.5.2.10 (Continued)

Computer operation was normal on airborne power when reset after transfer. Figure 30 offers a qualitative indication of the transfer effects on the computer operating voltages.

2.6 REFERENCES:

Report ES-59-SM-322 dated 18 March 1959, Results of Initial Arma/AIG Gyro Canister Compatibility Tests.

Report ES-59-SM-384 dated 25 May 1959, Summary of Arma/AIG Autopilot Compatibility Tests.

Engineering Work Book No. 7404.

3.0 SECTION II: Electrical System Compatibility Test Results.

3.1.0 INTRODUCTION:

The purpose of this phase of testing was to evaluate the electrical compatibility of the D/AIG power system with the Arma MOD - AIG Auto-pilot guidance system.

3.2.0 OBJECTIVES:

3.2.1 Obtain a load analysis for the D/AIG Missile Power System.

3.2.2 Obtain a harmonic analysis of the airborne power system.

3.2.3 Determine power system characteristics prior to transfer, during transfer, and after transfer.

3.3.0 CONCLUSIONS:

3.3.1 The nominal load on the D/AIG Missile Power System was 1620 watts. The Arma Inertial Guidance System constituted three-fourths of the nominal load.

3.3.2 The harmonic analysis of the airborne inverter indicates that the voltage harmonic content from the second to twentieth harmonic was approximately 0.033 of the fundamental.

3.3.3 Recordings taken of power system transfer indicate that the position transfer time (power interruption) exceeds the maximum specified of 15 milliseconds.

Arma total current transients at transfer are not excessive in magnitude and are generally less than 2.5 milliseconds in duration.

3.4.0 RECOMMENDATION:

It is recommended that further testing of the changeover switch be conducted on the systems level.

3.5.0 DESCRIPTION OF SPECIMENS:

There were four major electrical components used in this test.

3.5.1 Power Changeover Switch -

3.5.1 Power Changeover Switch - (Continued)

Kinetics Corp. M-160-2

Serial No. 002 CVAC 27-06106-3

3.5.2 Airborne A.C. Power-

Inverter - Bendix, Red Bank Division 32B77-5-B

Serial Number R-14

Output: 115/200 volts AC 400 cycles,

3000VA, 3 Phase, 0.8 pf.

Input: 28 volts DC 185 amps.

3.5.3 Ground A.C. Power

Variable Frequency Motor - Generator

Inet-Palmer Division of Leach Corp.

Model A1264 Serial Number 3673-1

Convair Specification No. 7-06205

| | Input | Output |
|---|---|---|
| Volts: | 390/510 | 120/208 |
| Freq: | 58/62 cyc. | 380/420 cyc. |
| Phase: | 3 | 3 |
| Amps: | 30.5 | 41.6 |
| P.F.: | 0.8 | 0.95 lead to 0.75 lag |
| KVA: | | 15 |

3.5.4 Ground-Airborne D.C. Power

Stavolt D.C. Power Supply

3.5.4 Ground-Airborne D.C. Power - (Continued)

Mc Colpin - Christie Corp. 431-400K4

Serial Number K-458

Output: 400 amps 25-29 volts DC

Input: 440v 3 Phase 60Cyc. 30 Amps.

3.5.5 D. C. Power to Arma Ground Equipment -

Rectifier, Metallic

Christie Electric Corp. MH32-100 K4

Serial Number K-1804

Output: 100 amp. 24-32v DC

Input: 460 volts 60 cyc. 3 Phase

3.6.0 TEST PROCEDURE:

3.6.1 General Procedure -

3.6.1.1 The electrical power system used followed the schematic Drawing (SK 545-7-159) furnished by the Electrical Design Group, Dept, 545-7. Additions and changes were incorporated to facilitate instrumentation and system grounding. Basically, the system conforms to the power system diagram given in Figure 31. The solid lines indicate flow of power whereas, the dashed lines indicate measurement or instrumentation coverage.

The system was so arranged as to provide Arma ground control equipment with AC ground power at all times.

The electrical wiring was of the three-phase, four wire, configuration. Two No. 0 cables were connected between each package load and inverter to simulate missile grounding. The common neutral (fourth wire) between airborne and ground AC power supplies was separated during airborne compatibility testing.

3.6.1.1 (Continued)

The test inverter and changeover switch had been used in several other tests by Systems and Components Test Laboratories.

3.6.1.2 The system loads were operated in the ready mode during electrical power tests. The airborne loads consisted of the following:

3.6.1.2.1 Arma MGS

a, Platform Package

b, Computer Package

c, Control Package

d, Analogue Signal Converter

e, Digital Signal Converter

3.6.1.2.2 AIG Autopilot:

a, Phase A transducer (simulated)

b, Gyro Package

c, Programmer Package

d, Servo Amplifier Package

e, Programmer and Servo Amplifier Monitoring Panels

3.6.1.2.3 Simulated Loads:

a, Propellant Utilization

b, Instrumentation (Model 3)

These simulated loads were lumped together and consisted of a transformer-rectifier resistive load and an inductive load.

3.6.2 Specific Procedure:

The load analysis and harmonic analysis measurements were taken at the analyzer. Both analyses were performed on airborne inverter power with the external ground wire disconnected.

3.6.2.1 The load analysis was performed using a voltmeter, ammeter and wattmeter with associated current transformers. Pictures of the phase voltage and current waveforms were taken with a Type 2614 Dumont attachment and camera and a Type 53/54C Tektronix Dual-Trace Plug-In Unit in a Type 545 Tektronic Oscilloscope.

3.6.2.2 The harmonic analysis was performed using a Model 300A Hewlett-Packard Harmonic Analyzer. The half band width selectivity was set at 145 cycles. Frequencies outside this bandwidth were attenuated by a minimum of 40db. The voltage harmonics were measured directly across the line and the current harmonics were measured across a 50 millivolt, 10 ampere shunt in the line.

3.6.2.3 Power changeovers (transfers) were performed with over, nominal, and under voltage outputs from the inverter. Recordings were obtained on a Type 5-119 CEC oscillograph. Type 7-326 Galvanometers were used for the AC traces. These galvanometers have a frequency response flat to 3000 cycles. A Weston, Model 461 current transformer and CEC Linear Amplifier, Type 1-112-C were used to isolate and amplify the instrumentation signal of each line current. This instrumentation circuit gave erroneous indications of the line currents during transfer and was therefore revised for subsequent testing. The revised circuitry utilized a 7.5 ampere, 50 millivolt shunt in each line and a Type 7-319 Galvanometer. This galvanometer has a frequency response flat to 300 cycles.

3.7.0 <u>TEST RESULTS</u>:

3.7.1 The load analysis data are given in Figure 32. The power factor was calculated from measured values of voltage, amperes, and watts. All values with the exception of watts, given in the total rows of the table are calculated on the basis of 115 volts. The system line voltages and inverter direct current and voltage are given at the right.

The loads were not steady because of heaters turning off and on in the Autopilot packages. Therefore two load analyses were run.

3.7 TEST RESULTS: (Continued)

3.7.1.1 A nominal value of system loading was 1620 watts. In comparing the loads of Run 1; Arma MGS comprised 73.5%, AIG Autopilot was 10.6% and the simulated load was 15.9% of the total load. The AIG Autopilot load had the greatest variance in phase current and power factor.

3.7.1.2 The waveforms of voltage and current are given in Figure 33. These pictures show the distortion in the waveforms and the phase angle between the phase voltage and current. The photograph on the right shows the waveforms with total system load on the airborne inverter. The photograph on the left shows the waveforms with the simulated load dropped from the total system load. The system load without the simulated load is given in the load analysis table.

3.7.1.3 The simulated load was used for nominal and extreme variations in loading on the power supply for power ystem compatibility testing.

3.7.2 The harmonic analysis data are given in Figure 34. The values of harmonic voltages given are from direct measurements. The values of harmonic currents given are calculated from the voltage drop measured across a 10 ampere, 50 millivolt shunt in each line. Here again the load on the system was not steady and two sets of data were taken.

3.7.2.1 The middle portion of the analysis table gives the harmonics in percent of the fundamental. The seventh and eleventh harmonics are the most prominent voltages, whereas the second, third, fourth, fifth, seventh, eleventh and fifteenth harmonics are the most prominent currents.

3.7.2.2 The harmonic content of the voltage is given at the bottom of the table. Interface requirements of AZM-27-075 call out that the RMS sum of the voltage harmonics from the second through the tenth shall be equal to or less than 4% of the fundamental. Also, the RMS sum of the harmonics from the second through the fortieth shall be equal to or less than 0.05 of the fundamental. The voltage harmonic content of the tested inverter clearly meets the first part of the specification. The harmonic content was only measured to the twentieth therefore a categorical statement about its harmonic content to the fortieth is impossible. Nevertheless, if the harmonic content to the twentieth is doubled the calculated R.M.S. content is 0.0495 of the fundamental. It is unlikely that the harmonic content from the twentieth through the fourtieth will be as great as the content from the second through the twentieth. Therefore it is assured that the harmonic content of the inverter meets the second part of the specification.

3.7 TEST RESULTS: (Continued)

3.7.3 Power transfer recordings are given in Figures 35 through 43. The changeover switch used in this test was not of the type that will be on the D/AIG Series. A proper changeover switch was not procured for this test. The essential difference between the two switches consists of the number of switching circuits. The switch used in the test had three sets of three AC load switching circuits. A set consists of either three Phase A, Phase B or Phase C switches. The changeover switch that will be used on the D/AIG Series has three sets of five AC load switching circuits.

The changeover switch used did not have the required number of switching circuits. Therefore, the packages of each subsystem; Arma MGS, AIG Autopilot and Simulated were connected to a single switching circuit. The effect this had on the test is probably negligible. However, the exact time of transfer for each package would be different. Also, the transfer time sequence would cause a change in the time and magnitude of the total system transfer transient.

3.7.3.1 With the system loads as in the load analysis test, several power transfers were run. Typical recordings of these changeovers are given in Figures 35 and 36. These recordings are of total system load currents and voltages. These recordings show inconsistent transfer times. This characteristic was discussed with the Electrical Design Group. Upon investigation it was learned that the electrical system wiring was improper. Each set of load switching circuits had been connected together in order to instrument the total load current at transfer. Referring to the system diagram, Figure 31, the proper circuitry is to have the distribution coincide with the changeover switch. The proper changes were incorporated. The above mentioned recordings, Figures 35 and 36 are included here to show what the total system or each package saw for power transfer testing. When the changeover circuitry was properly revised, the Autopilot packages were no longer available for test.

3.7.3.2 In order to determine the electrical characteristics at transfer for the Arma MGS equipment, further power transfer testing was conducted. The AIG Autopilot load was lumped into the simulated load. Figure 37 is a recording of Arma voltage and current at transfer. It clearly shows the presence of high frequency transients. High frequency current transients are also apparent at the transfer command time. At this time the motor driven changeover switch begins to move.

3.7 TEST RESULTS: (Continued)

3.7.3.3 The apparent DC displacement of the currents at break and make of transfer are spurious. To check on these spurious displacements, a step function was applied to the recorder circuit and it responded approximately at two cycles, damped exponentially. The recorder current instrumentation circuit which caused the spurious displacement and its revision are discussed in Paragraph 3.6.2.3.

3.7.3.4 Figures 38 through 43 are records of Arma MGS electrical characteristics at transfer using the revised current instrumentation circuitry. The response of the Type 7-319 Galvanometer is down approximately seven percent at 400 cycles. These records show progressively power transfers from external to internal and internal to external, with over, nominal, and under voltage on the inverter. The position transfer time is more clearly defined than was indicated by the high frequency response records. The position transfer time is definitely outside the maximum specified time of 15 milliseconds. Phase A current transfer time approaches 30 milliseconds.

3.7.3.5 These records also serve to indicate the current switching transients. The transients are somewhat variable because of their dependence upon the time displacement of the voltage cycle at switching and the mode or power factor of the load.

It may be observed that the voltages are small in magnitude before the completed operation of switching at make and break. A possible cause of this may be the construction of the switching contacts. The switches are of the sliding pin-socket type and their area of contact, or contact resistance will change with the time-position of the sliding contact.

3.8.0 BIBLIOGRAPHY:

Test data from which this report was prepared are recorded in Engineering Test Laboratories Data Notebook No. 7134.

## 4.0 SECTION III - ILLUSTRATIONS:

### 4.1 LIST OF ILLUSTRATIONS -

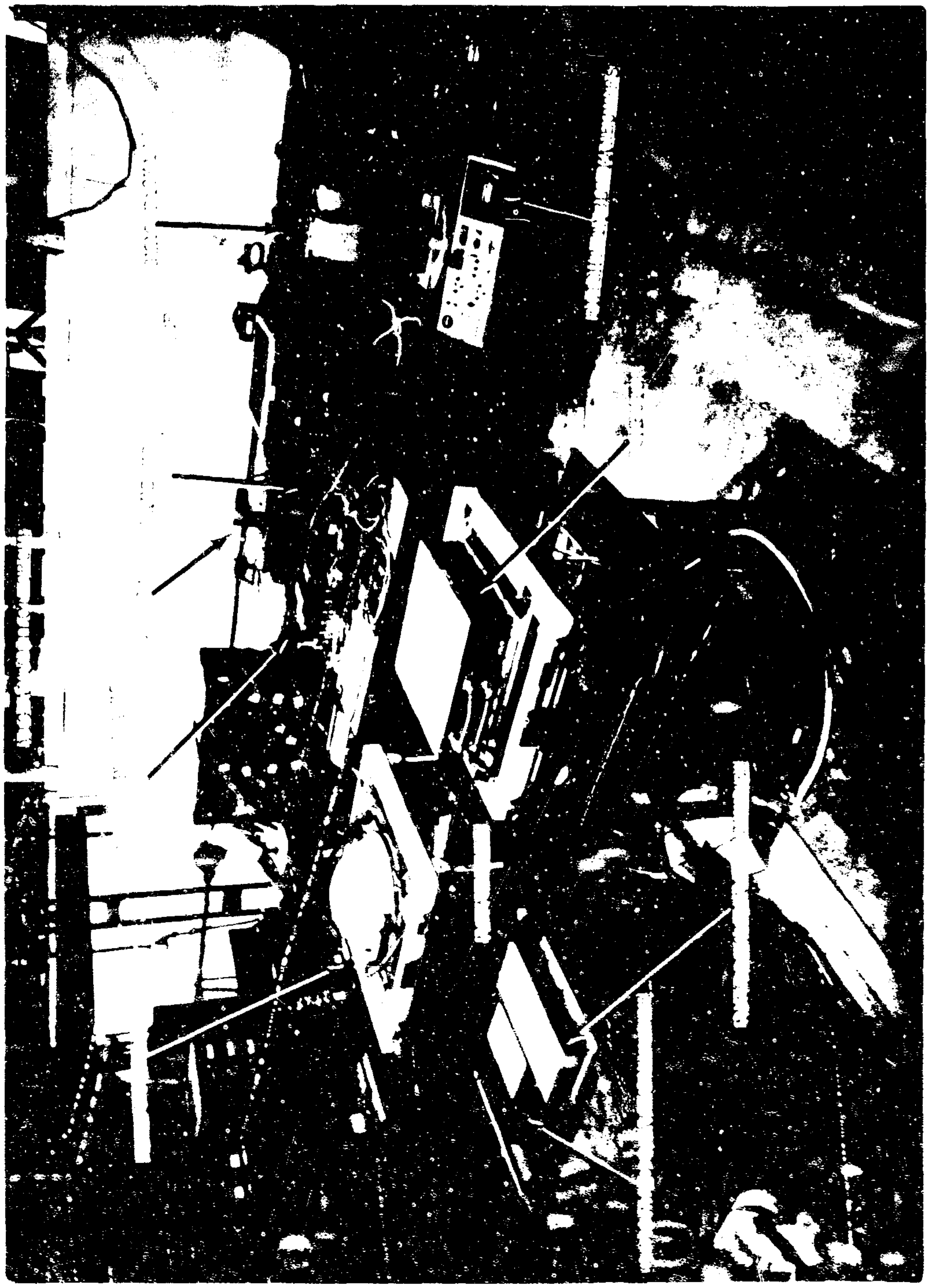

CONVAIR-ARMA COMPATIBILITY BENCH TEST AREA

FIGURE 1

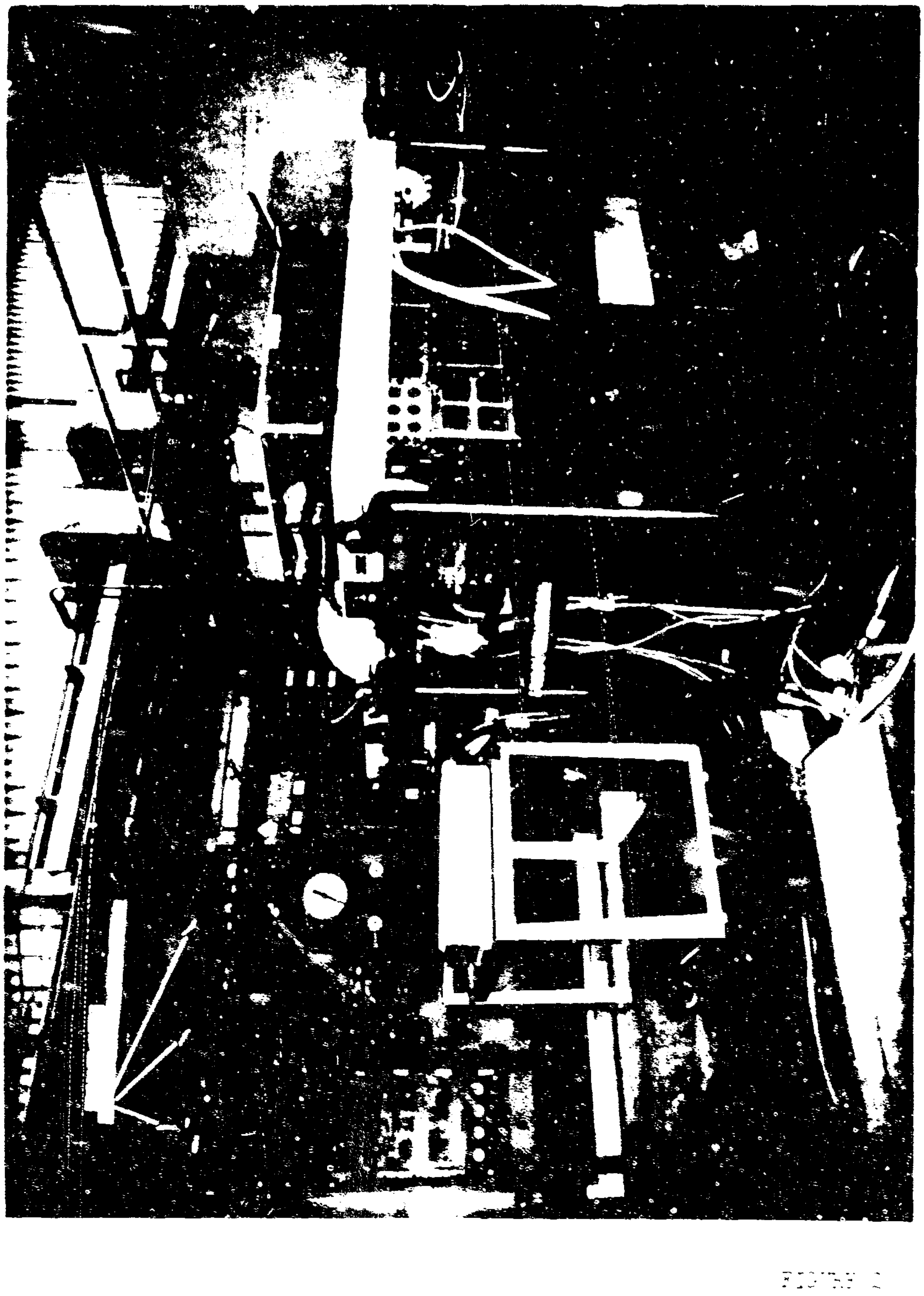

ARMA EQUIPMENT GROUP

FIGURE 2

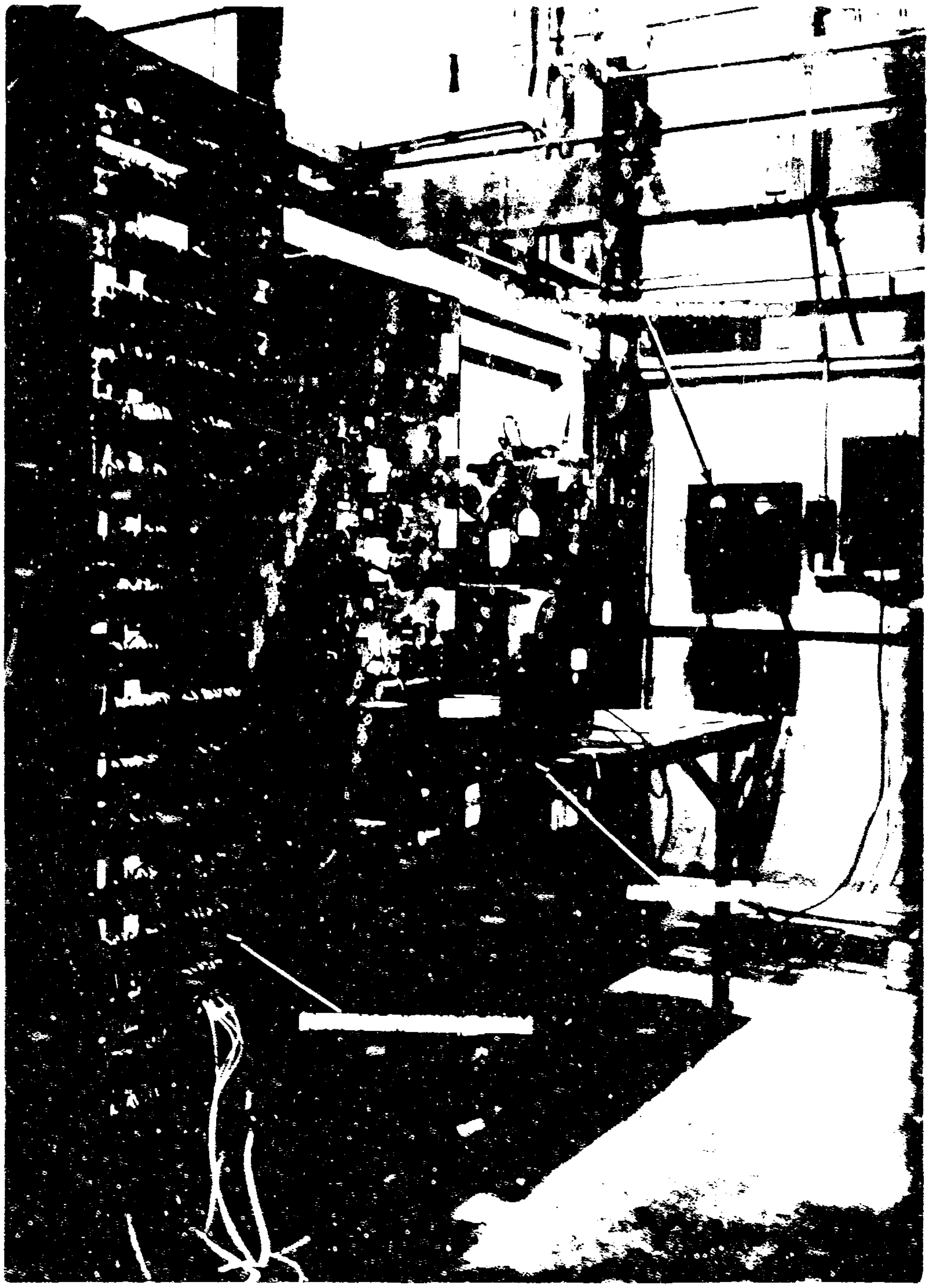

ARMA T T GROU

FIGURE 3

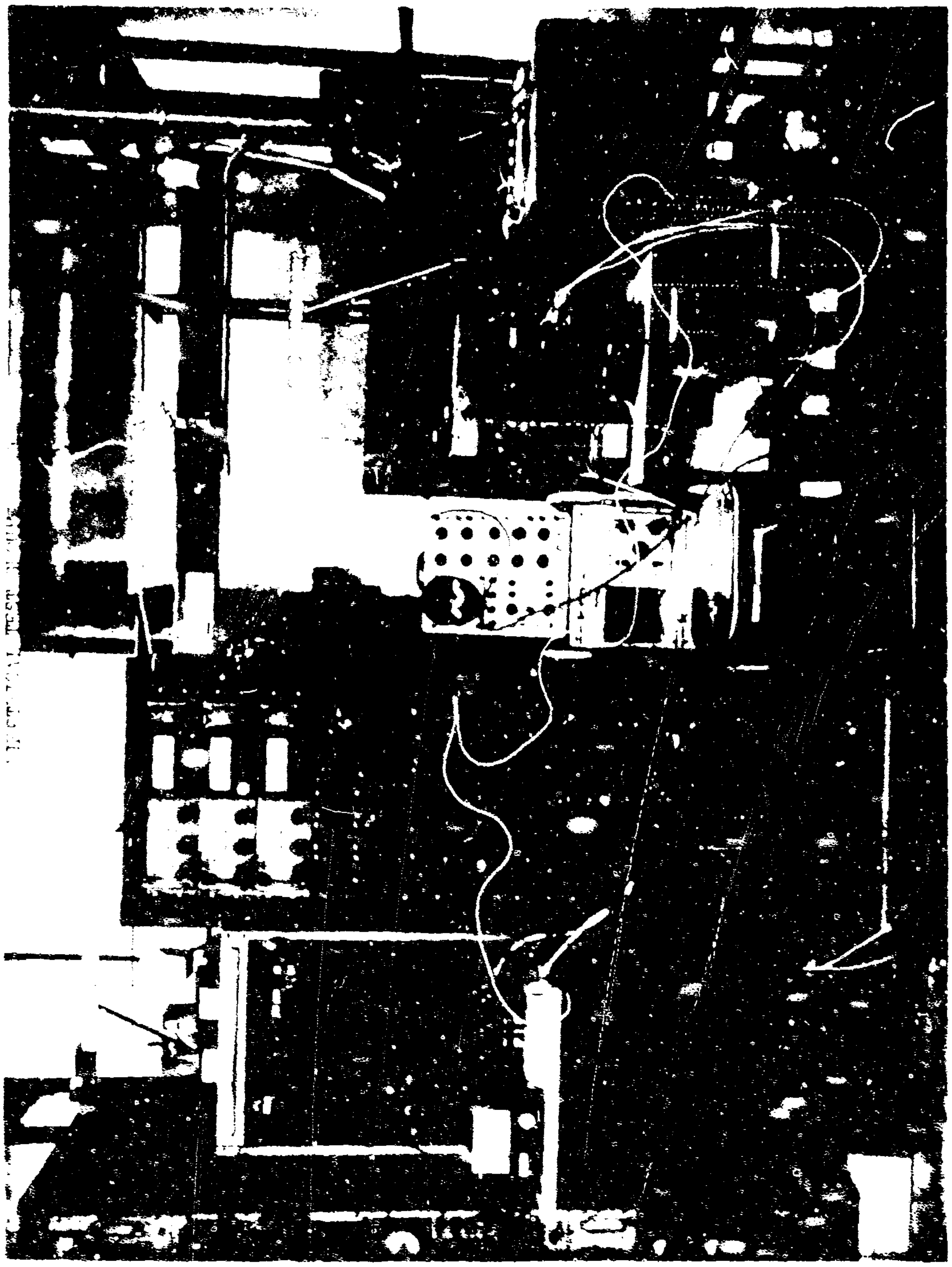

ELECTRICAL TEST GROUP

FIGURE 4

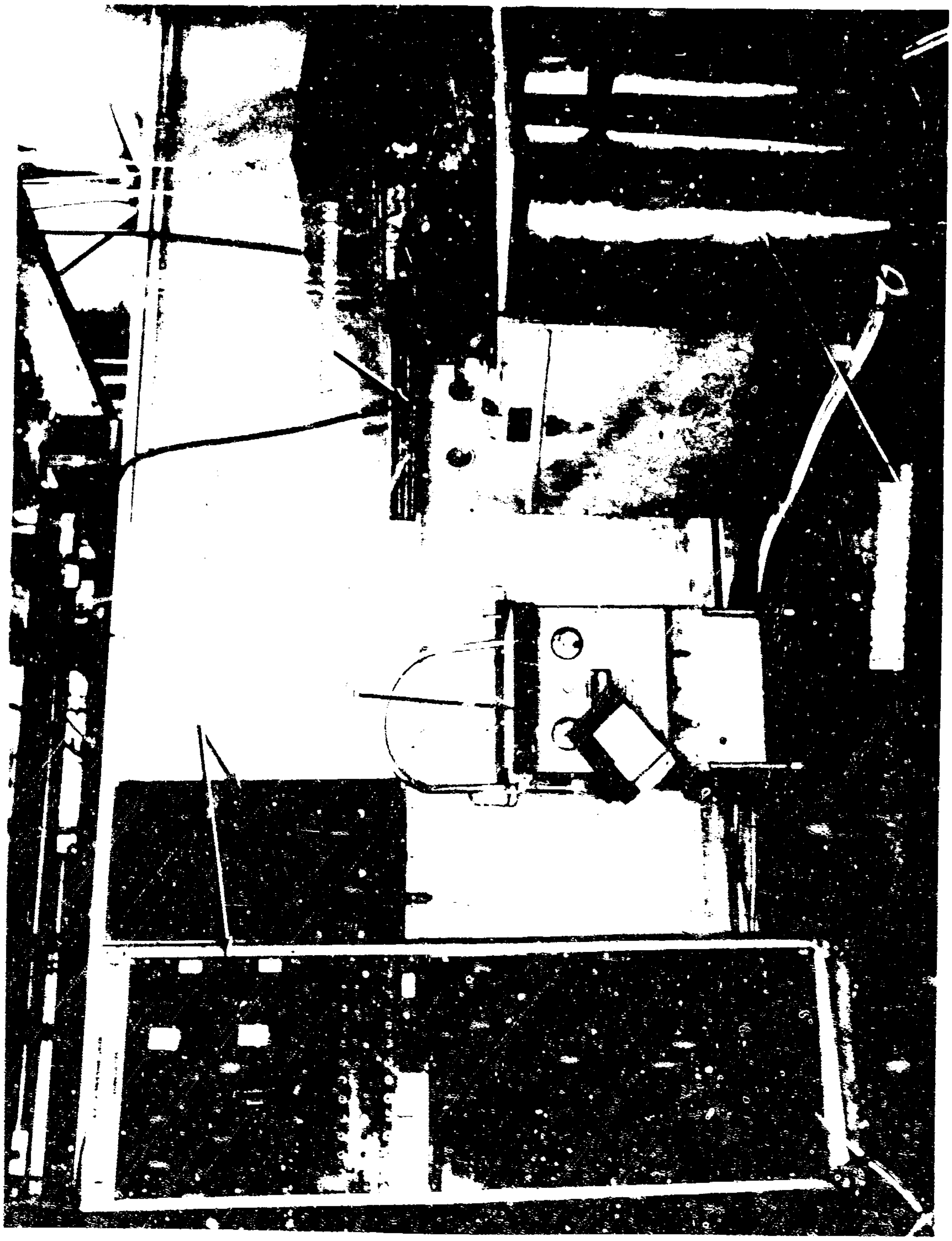

AIRBORNE POWER GROUP

FIGURE 5

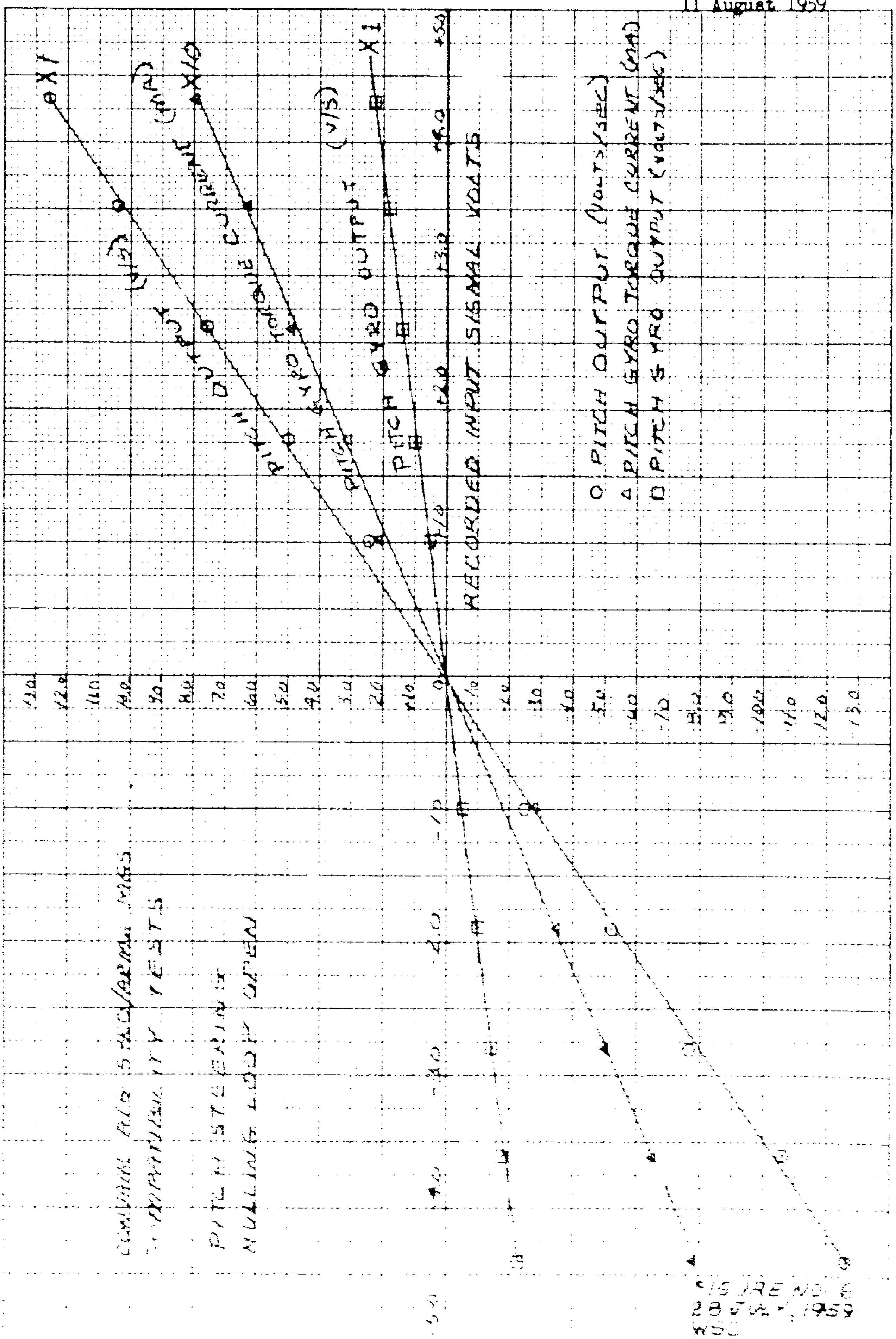
PITCH OUTPUT (VOLTS/SEC)
PITCH GYRO TORQUE CURRENT (MA)
PITCH GYRO OUTPUT (VOLTS/SEC)
RECORDED INPUT SIGNAL VOLTS
X1
X10
PITCH STEERING
NULLING LOOP OPEN

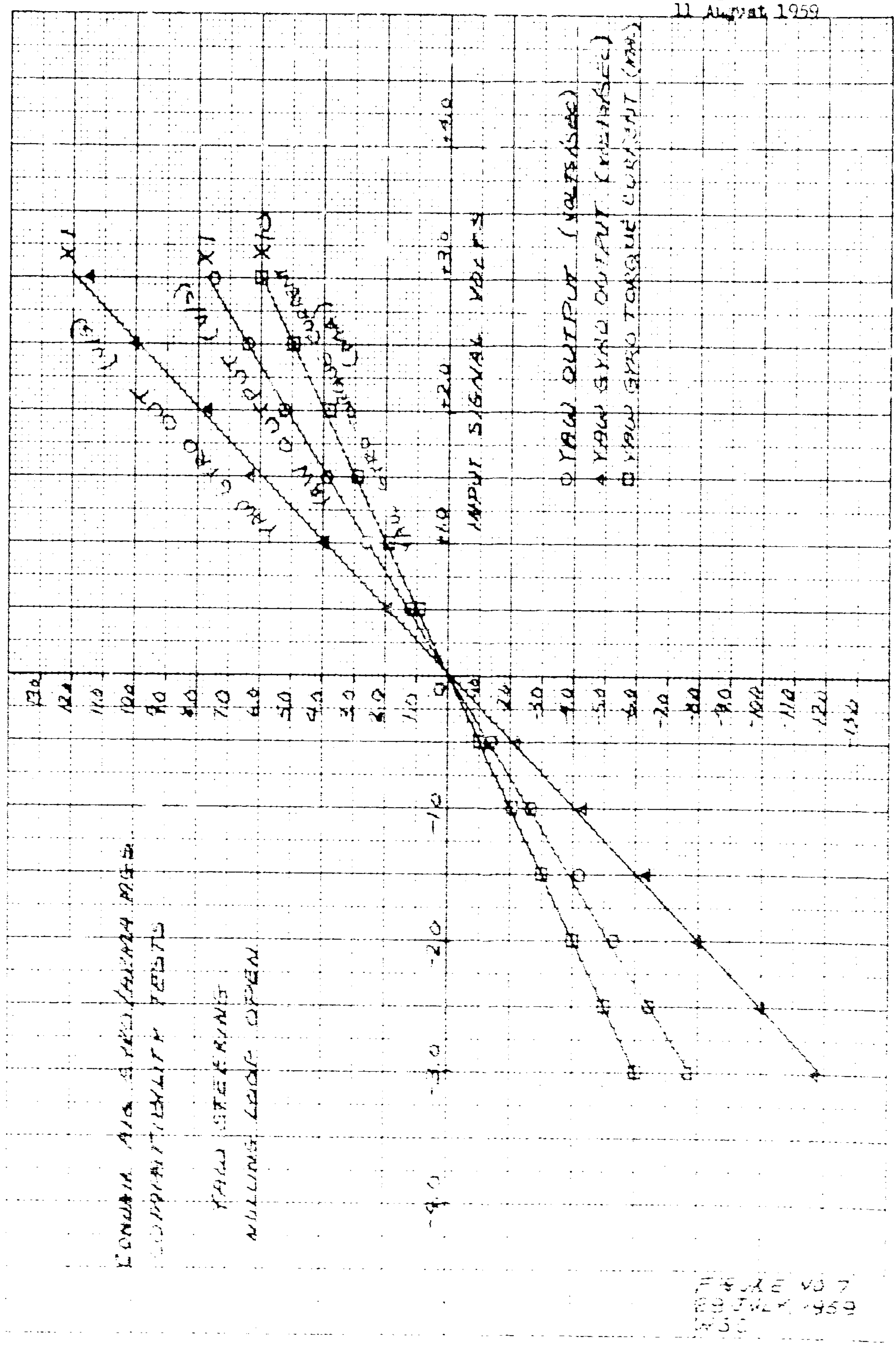
CONVAIR A1A GYRO/ARMA MGS
COMPATIBILITY TESTS
YAW STEERING
NULLING LOOP OPEN
INPUT SIGNAL VOLTS
YAW GYRO OUT
YAW OUTPUT
GYRO TORQUE CURRENT
○ YAW OUTPUT (VOLTS/SEC)
▲ YAW GYRO OUTPUT
□ YAW GYRO TORQUE CURRENT (MA)

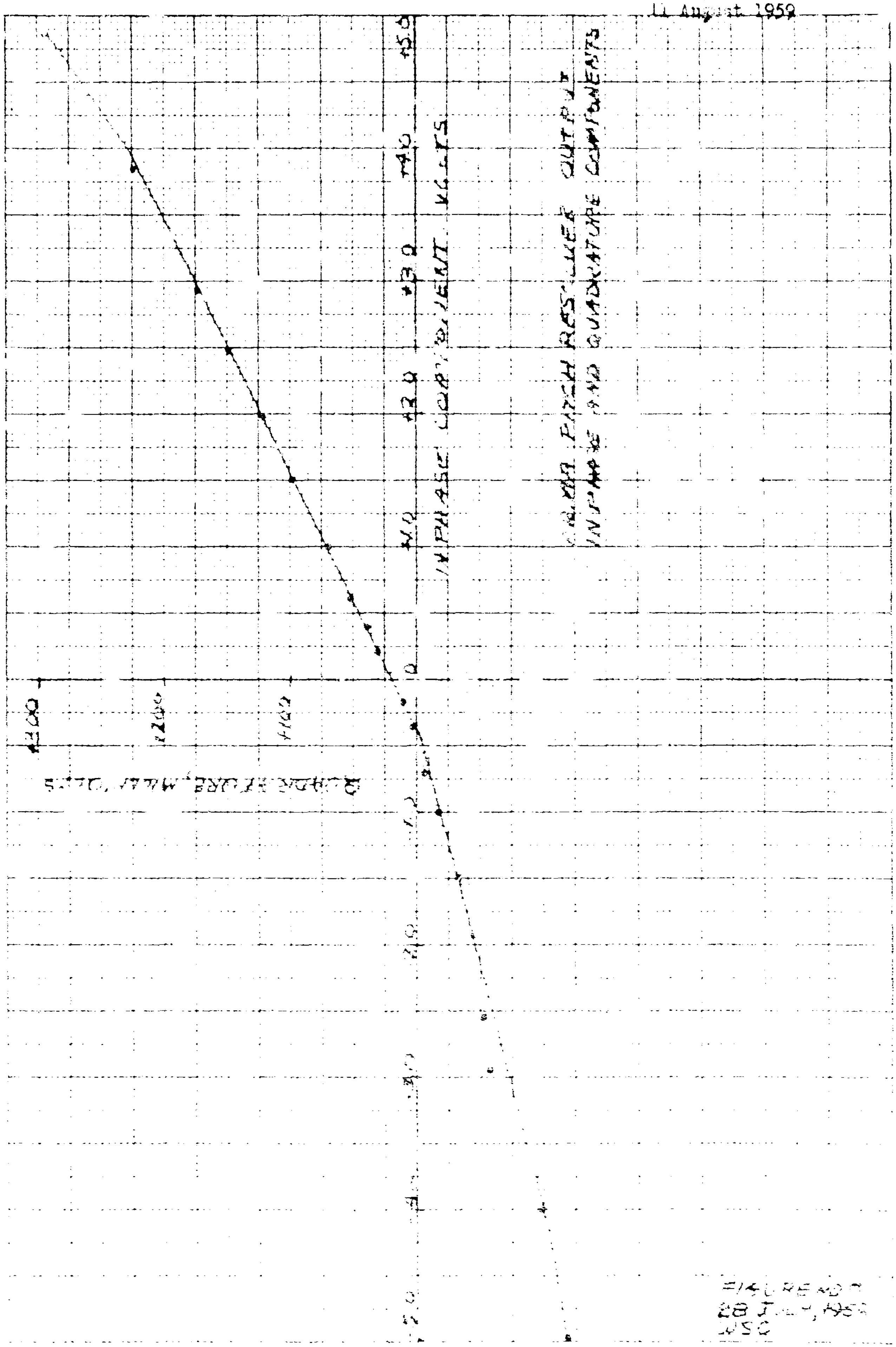
PITCH RESOLVER OUTPUT
IN PHASE AND QUADRATURE COMPONENTS
IN PHASE COMPONENT, VOLTS
QUADRATURE, MILLIVOLTS

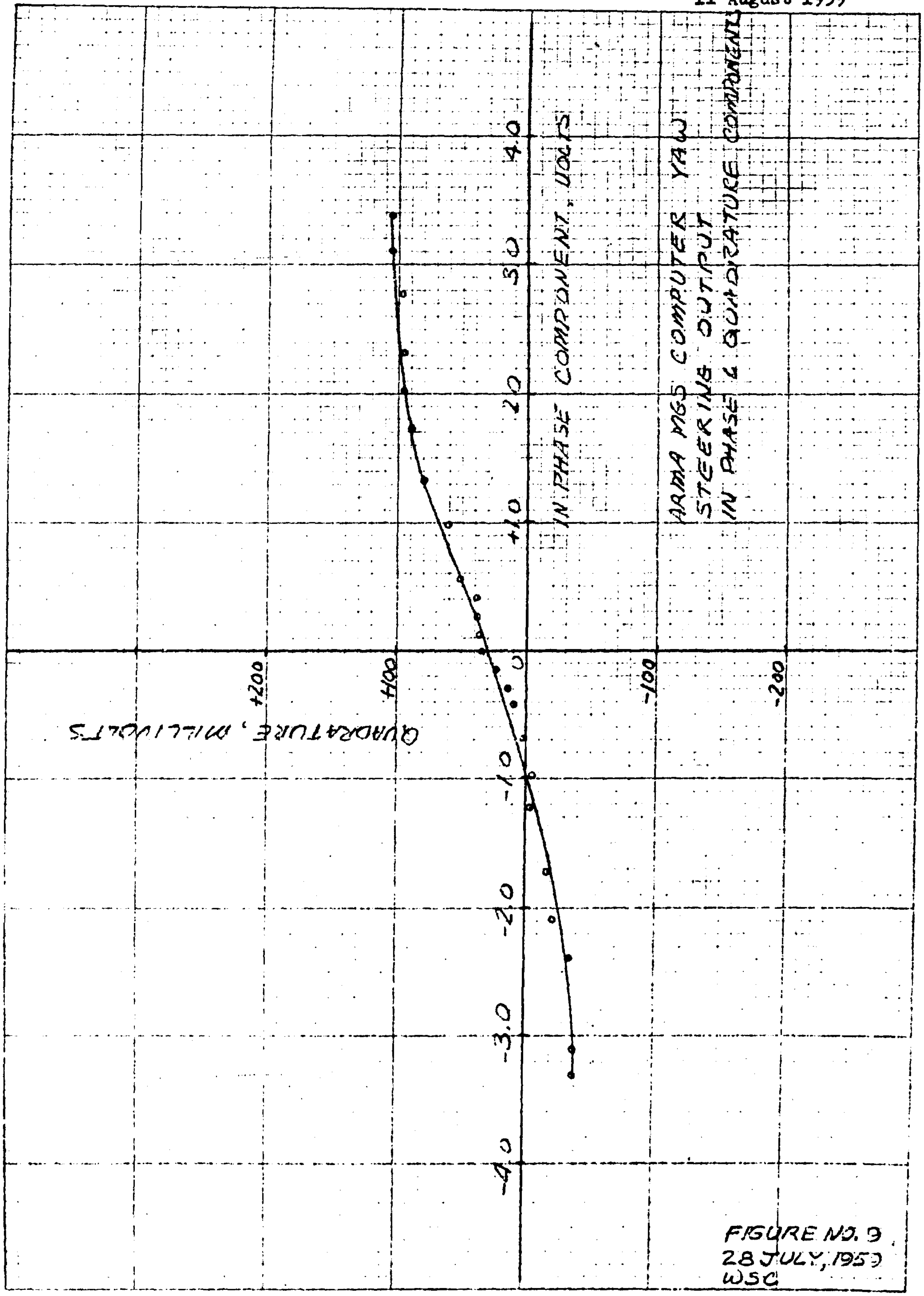


FIGURE NO. 9
28 JULY, 1959
WSC

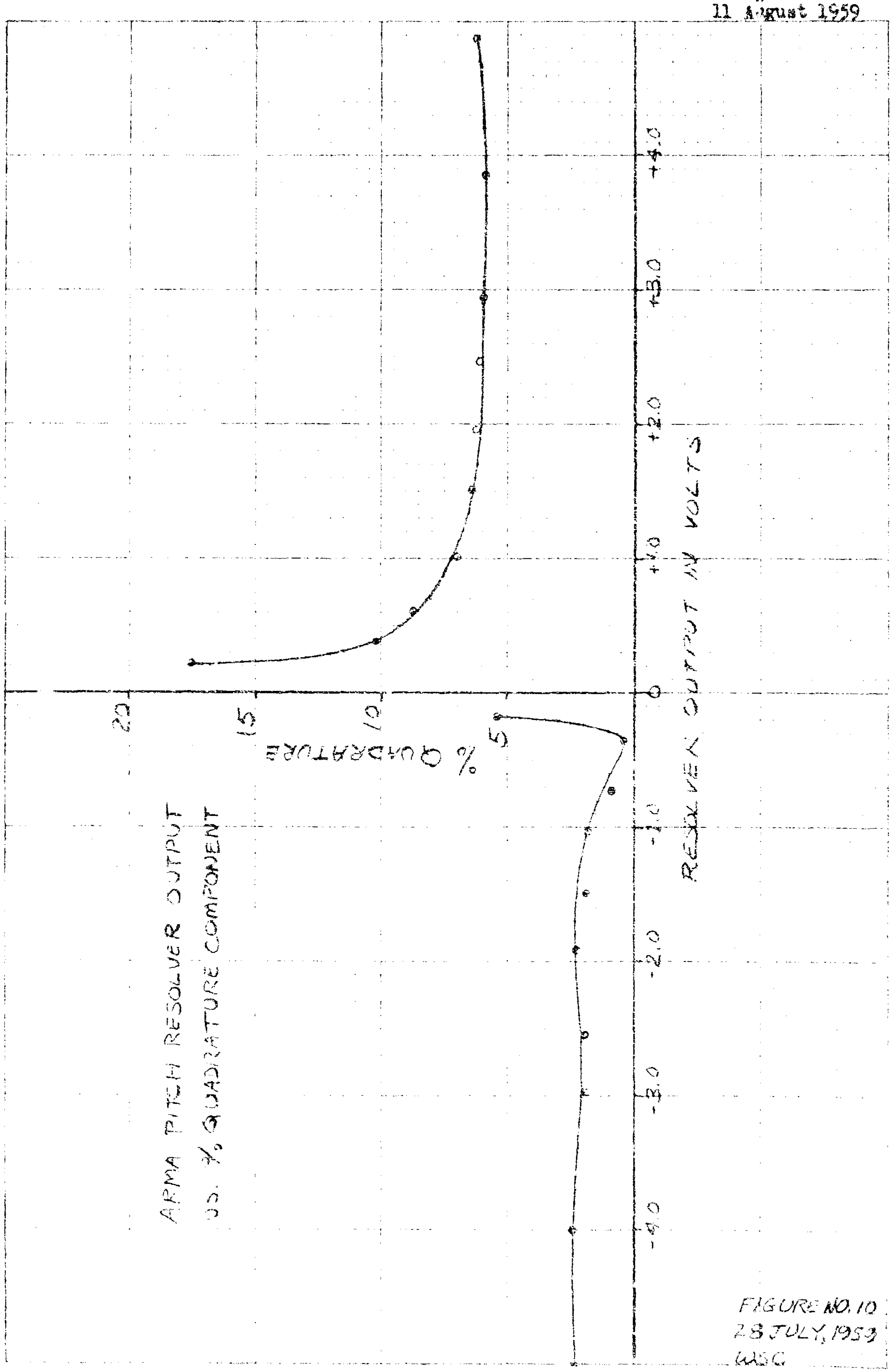
ARMA PITCH RESOLVER OUTPUT
vs. % QUADRATURE COMPONENT
% QUADRATURE
20
15
10
5
RESOLVER OUTPUT IN VOLTS
+4.0
+3.0
+2.0
+1.0
0
-1.0
-2.0
-3.0
-4.0
FIGURE NO. 10
28 JULY, 1959
WSC

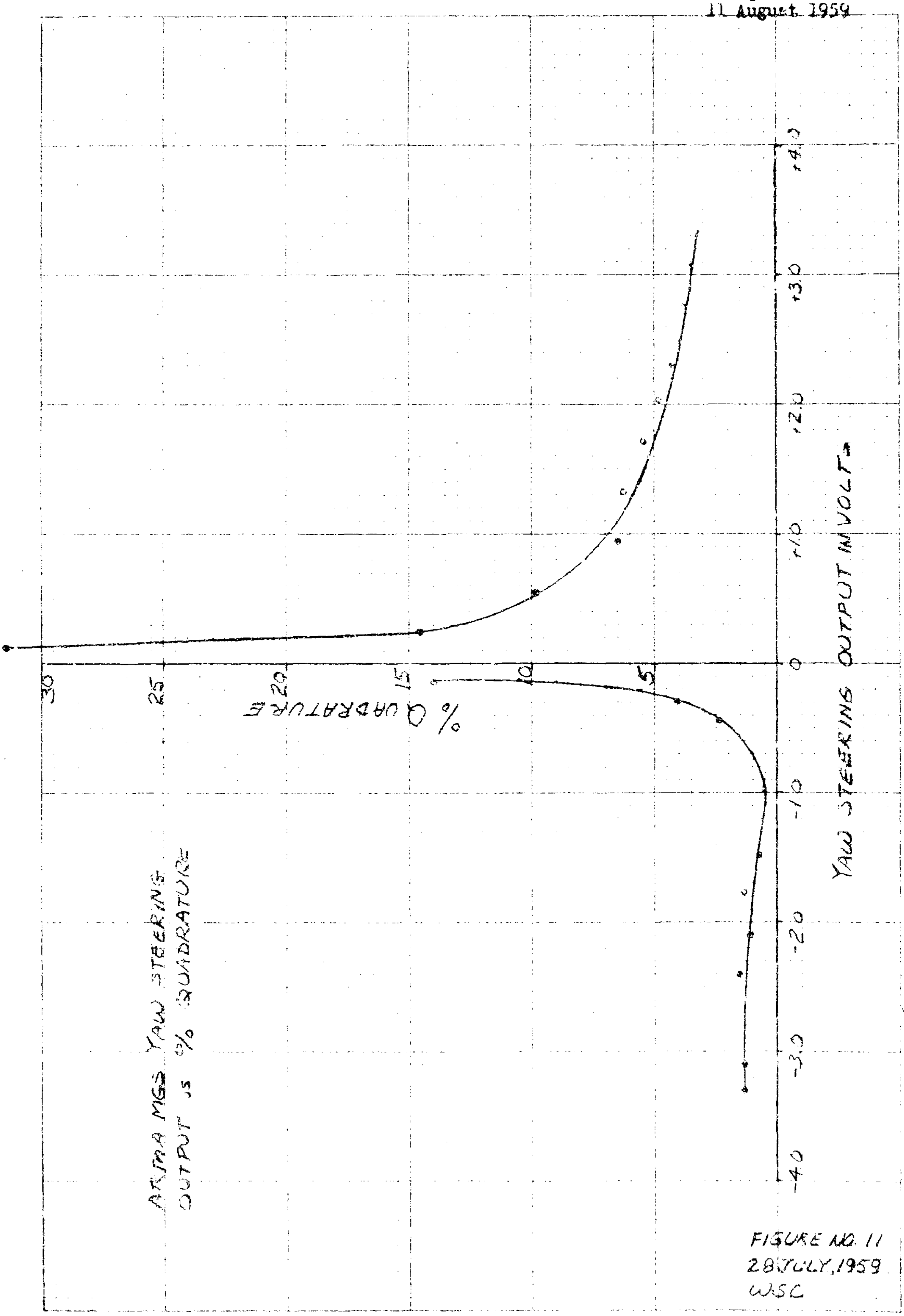


FIGURE NO. 11
28 JULY, 1959
WSC

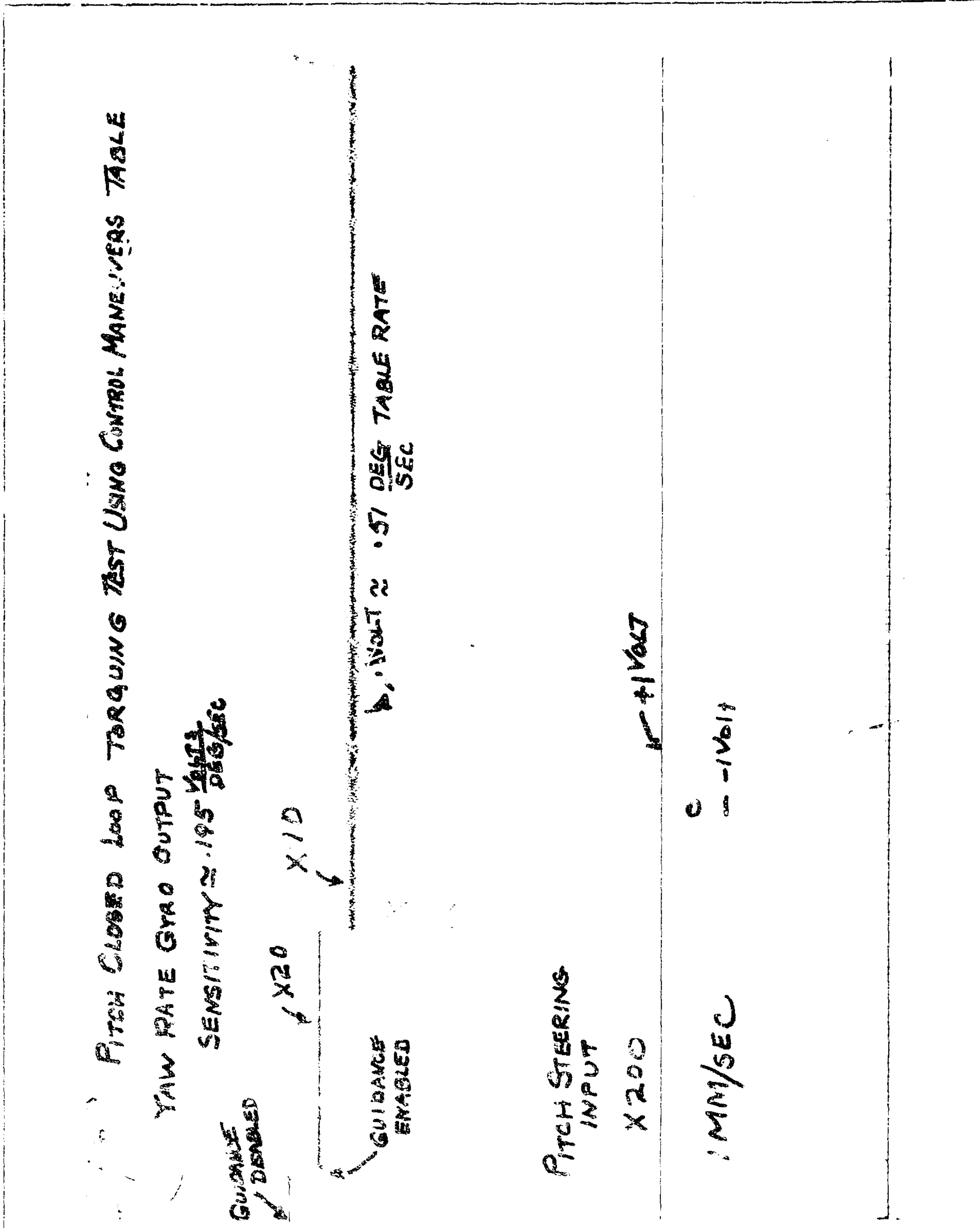
PITCH CLOSED LOOP TORQUING TEST USING CONTROL MANEUVERS TABLE
YAW RATE GYRO OUTPUT
SENSITIVITY ≈ .195 VOLTS/DEG/SEC
X20
X10
.1 VOLT ≈ .51 DEG/SEC TABLE RATE
GUIDANCE DISABLED
GUIDANCE ENABLED
PITCH STEERING INPUT
X200
+1 VOLT
-1 VOLT
1 MM/SEC

FIGURE 12

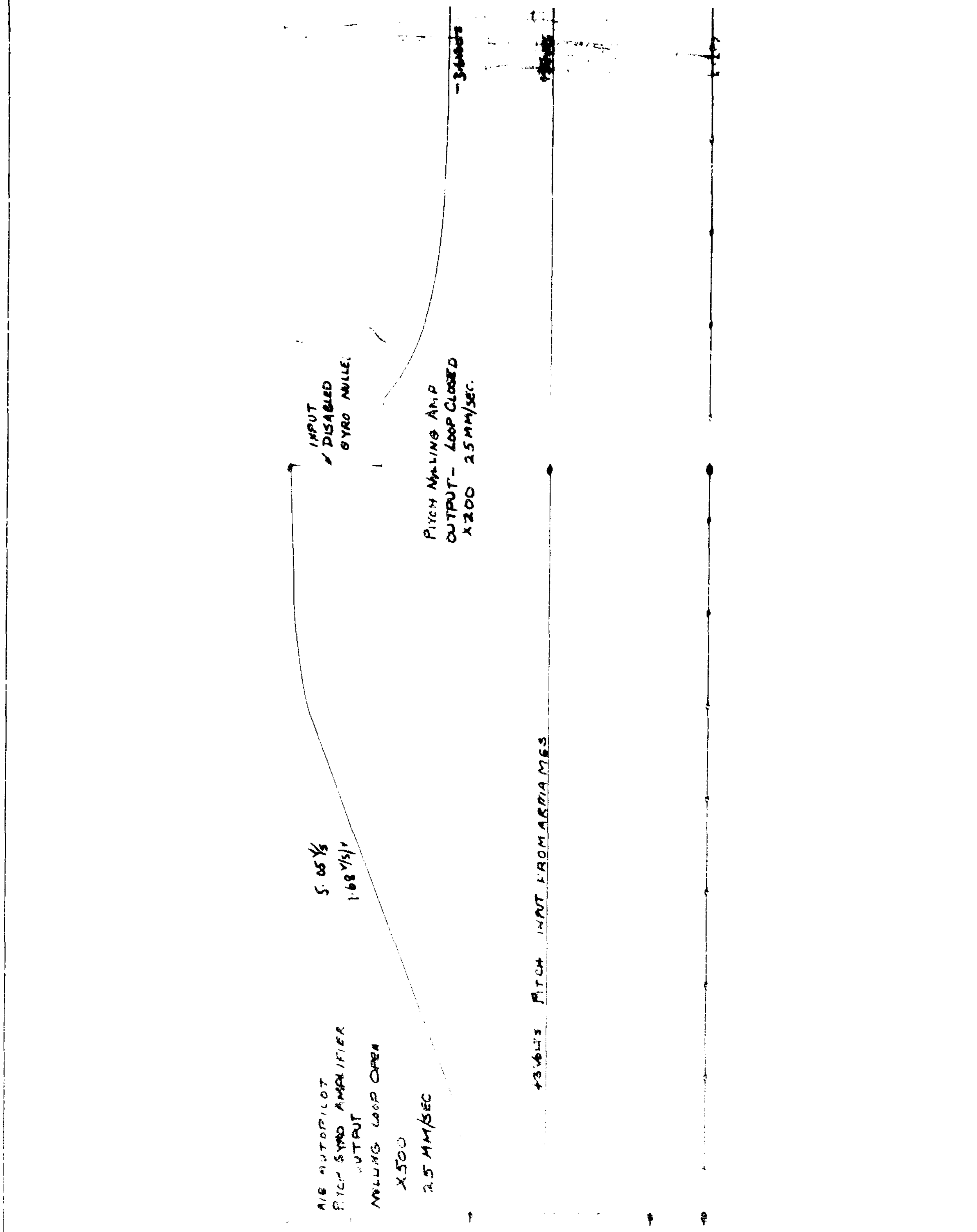
PITCH NULLING AMP
OUTPUT - LOOP CLOSED
X200 25 MM/SEC.
INPUT DISABLED
GYRO NULLED
PITCH INPUT FROM ARMA MES
+3 VOLTS
X500
2.5 MM/SEC

FIGURE 13

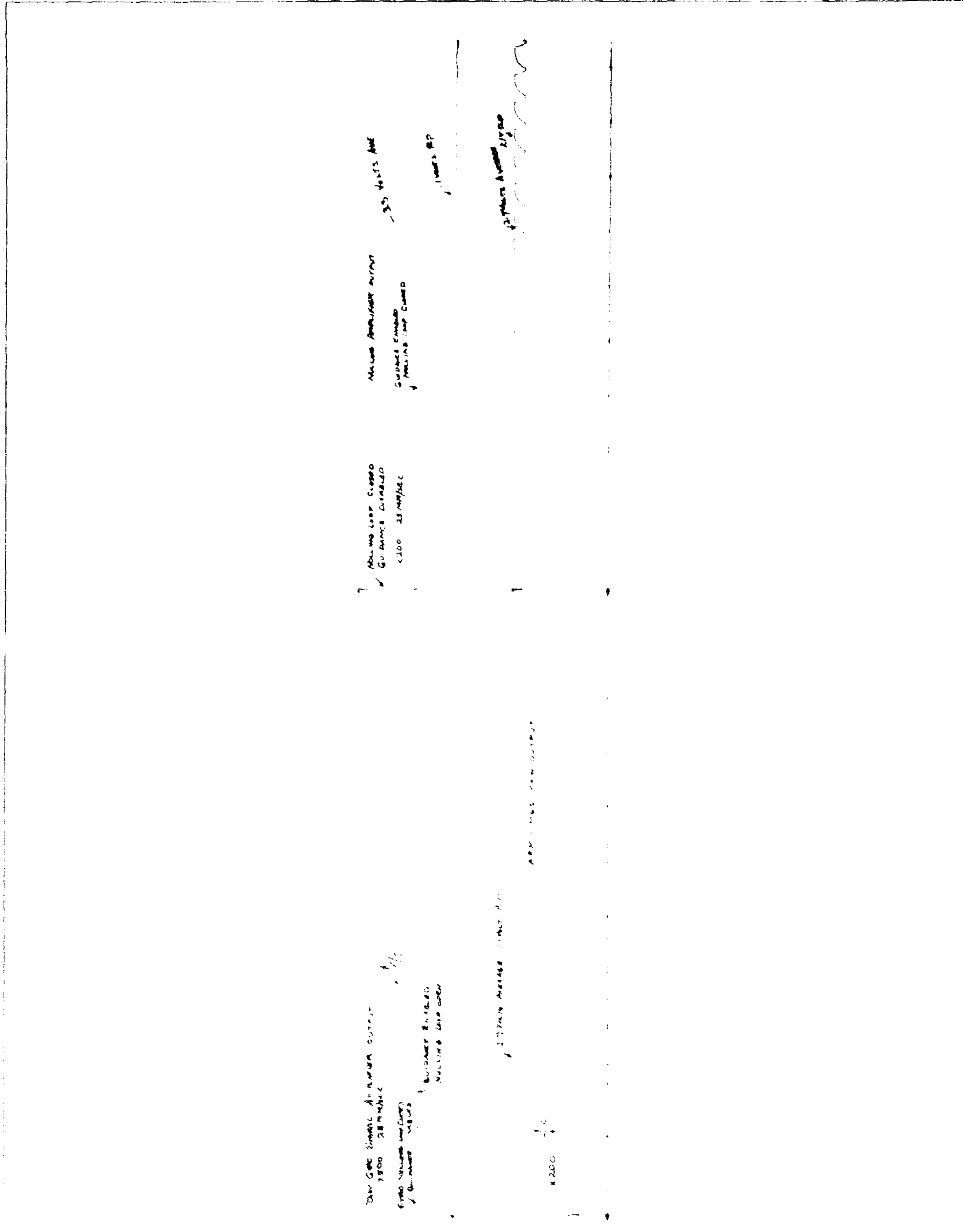

FIGURE 14

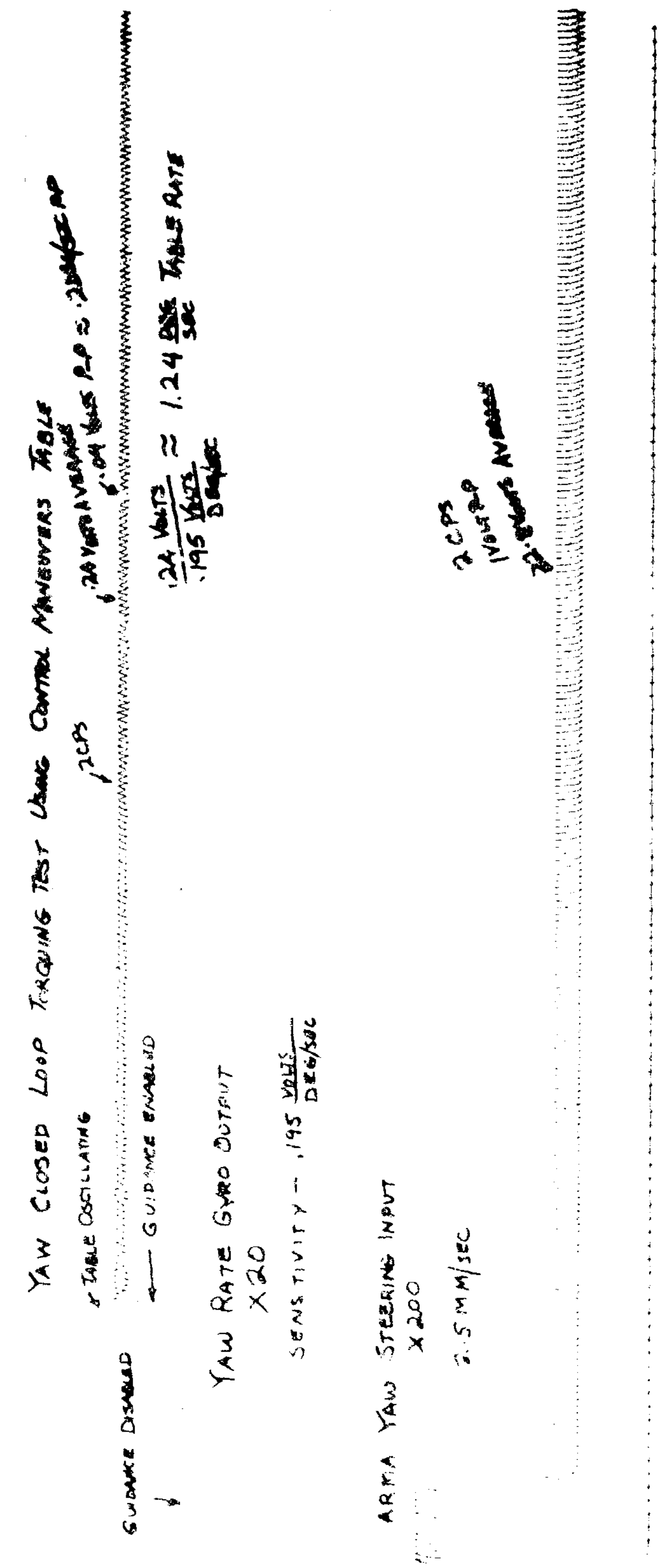
YAW CLOSED LOOP TORQUING TEST USING CONTROL MANEUVERS TABLE
TABLE OSCILLATING
GUIDANCE DISABLED
GUIDANCE ENABLED
2CPS
YAW RATE GYRO OUTPUT
X20
SENSITIVITY - .195 VOLTS/DEG/SEC
ARMA YAW STEERING INPUT
X200
2.5 MM/SEC
2 CPS

FIGURE 15

BLOCK DIAGRAM OF FLOATED RATE INTEGRATING GYRO

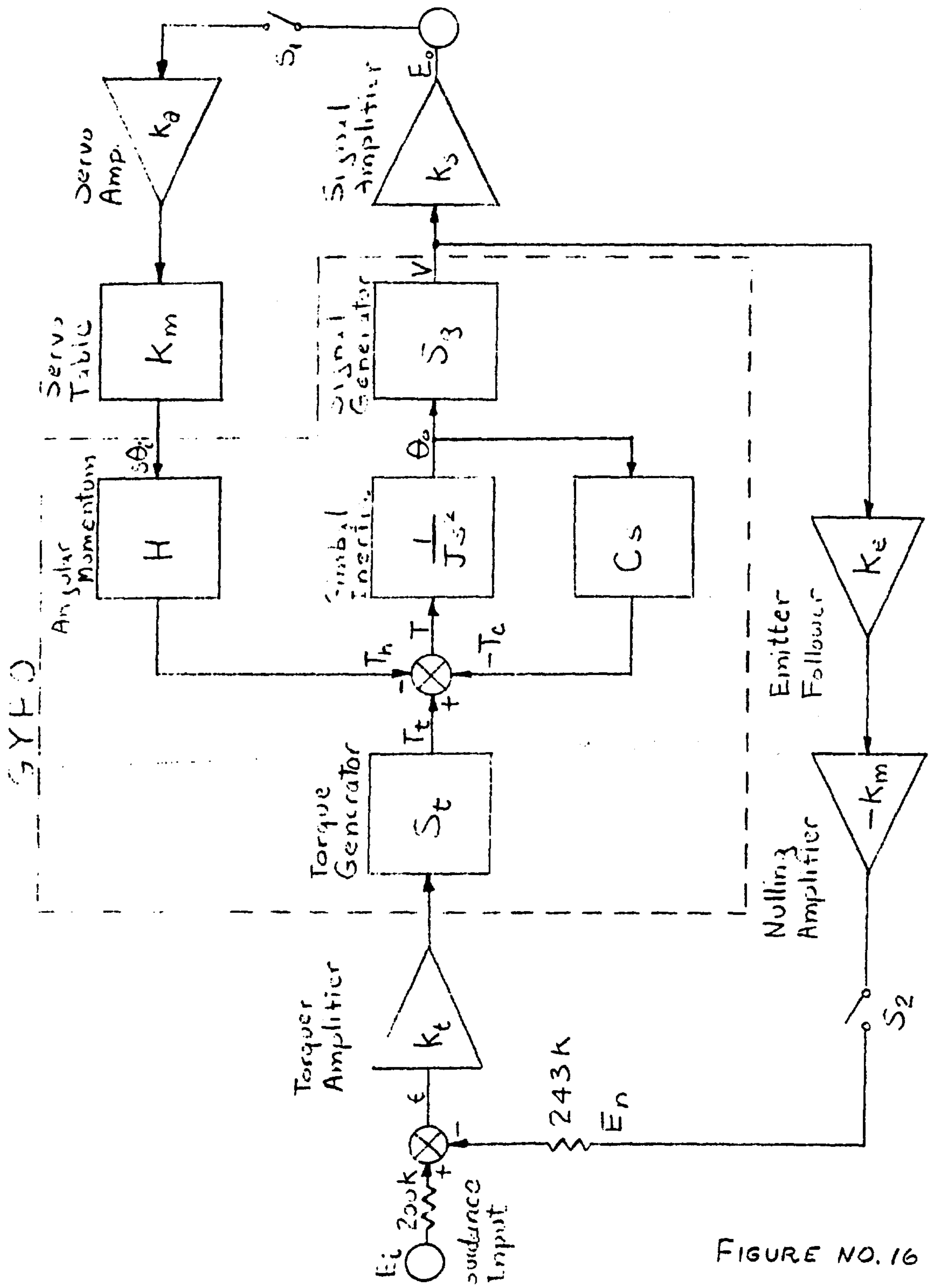


FIGURE NO. 16

| PREPARED BY | DATE | CHECKED BY | DATE | REVISED BY | DATE |
|---|---|---|---|---|---|
| J. S. Curry | 7/28/59 | | | | |

| | Torquer Rate Calibration | | Steering Input Tests | | | | | % Change Between Closed Servo Loop Torquing and Open Loop Torquing |
|---|---|---|---|---|---|---|---|---|
| | Input Voltage | Table Rate Deg/Sec | Steering Input Volts | Table Rate Deg/Sec | Closed Gyro Loop | | Open Gyro Loop | | |
| | | | | | Nulling Amp Output Volts | Null Volts 1.2 | Sig.Amp. Out Volts/Sec | Calculated Torquing Rate Volts/Sec=Deg / Volts/Deg Sec | |
| PITCH | +4.0 | 1.842 | +4.0 | 1.870 | | | | | |
| | +3.0 | 1.384 | +3.0 | 1.434 | -3.6 | 3.0 | 5.05 | 1.440 | 0.43% |
| | +2.0 | 0.921 | +2.0 | 0.937 | -2.4 | 2.0 | 3.375 | 0.965 | 3.0% |
| | +1.0 | 0.463 | +1.0 | 0.458 | -1.2 | 1.0 | 1.67 | 0.477 | 4.15% |
| | -1.0 | 0.451 | -1.0 | 0.476 | +1.2 | 1.0 | 1.64 | 0.470 | 1.27% |
| | -2.0 | 0.916 | -2.0 | 0.927 | +2.4 | 2.0 | 3.350 | 0.957 | 3.24% |
| | -3.0 | 1.362 | -3.0 | 1.384 | +3.6 | 3.0 | 5.0 | 1.430 | 3.32% |
| | -4.0 | 1.80 | -4.0 | 1.822 | +4.85 | 4.05 | 6.7 | 1.910 | 4.82% |
| YAW | +3.0 | 1.285 | +3.0 | 1.12 | 3.8 | 3.15 | 4.0 | 1.145 | 2.16% |
| | +2.0 | 0.854 | +2.0 | 0.820 | 2.3 | 1.92 | 3.0 | 0.86 | 4.88% |
| | +1.0 | 0.428 | +1.0 | 0.410 | 1.2 | 1.0 | 1.44 | 0.412 | 0.5% |
| | +0.5 | 0.216 | +0.5 | 0.205 | 0.6 | 0.5 | 0.72 | 0.205 | 0% |
| | -0.5 | 0.215 | -0.5 | 0.210 | 0.63 | 0.525 | 0.73 | 0.208 | 0.96% |
| | -1.0 | 0.430 | -1.0 | 0.411 | 1.2 | 1.0 | 1.5 | 0.428 | 4.14% |
| | -2.0 | 0.865 | -2.0 | 0.832 | 2.3 | 1.92 | 2.95 | 0.842 | 1.32% |
| | -3.0 | 1.310 | -3.0 | 1.19 | 3.5 | 2.92 | 4.25 | 1.210 | 1.68% |

FIGURE 17

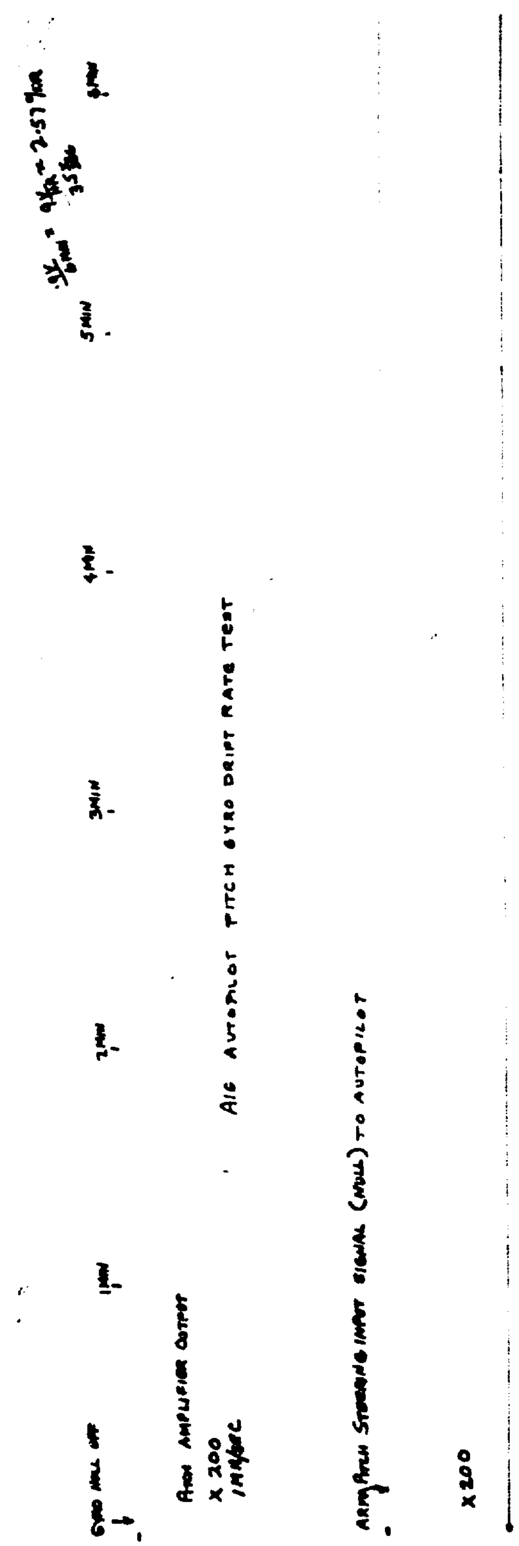
AIG AUTOPILOT PITCH GYRO DRIFT RATE TEST
GYRO NULL OFF
1 MIN
2 MIN
3 MIN
4 MIN
5 MIN
6 MIN
X 200
TO AUTOPILOT

FIGURE 18

THIS
PAGE
IS
MISSING
IN
ORIGINAL
DOCUMENT

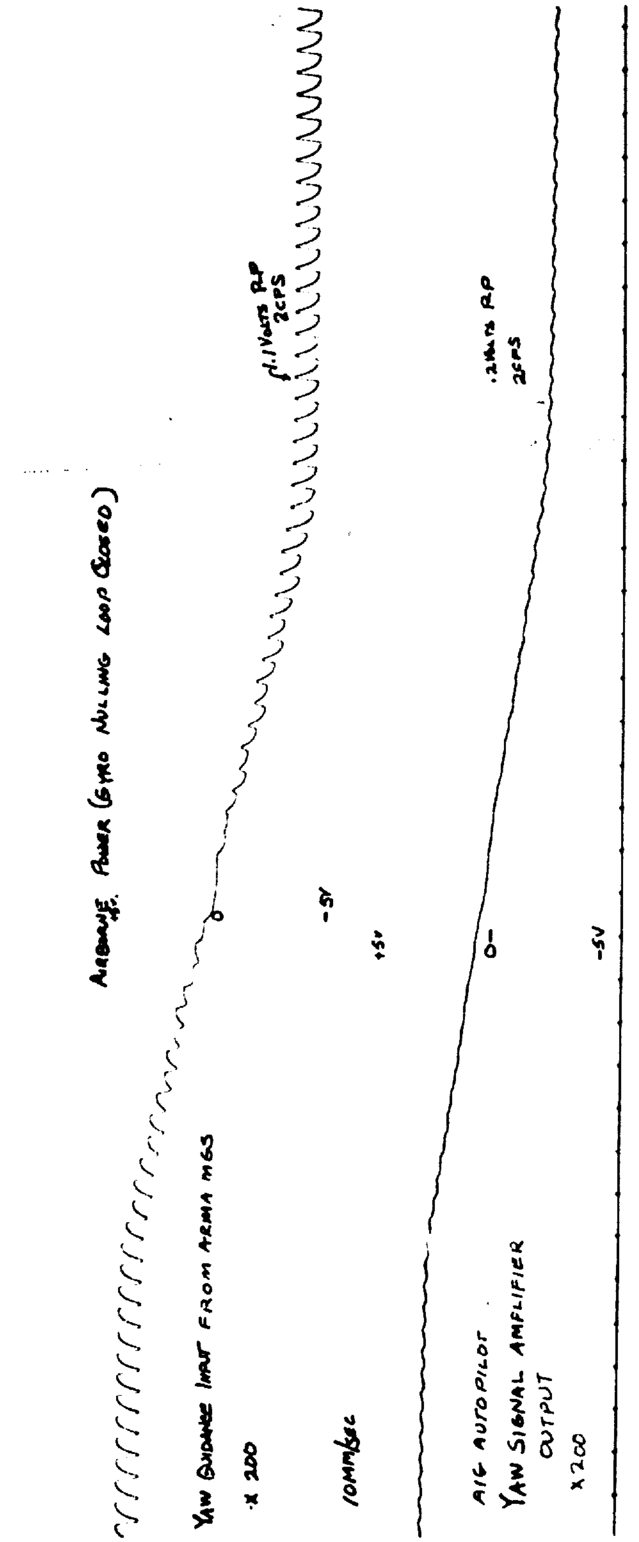
AIRBORNE A.C. POWER (GYRO NULLING LOOP CLOSED)
1.1 VOLTS P-P
2CPS
YAW GUIDANCE INPUT FROM ARMA MGS
x 200
0
-5V
+5V
10MM/SEC
A1G AUTOPILOT
YAW SIGNAL AMPLIFIER
OUTPUT
x 200
.2 VOLTS P-P
2CPS
0
-5V

FIGURE 20

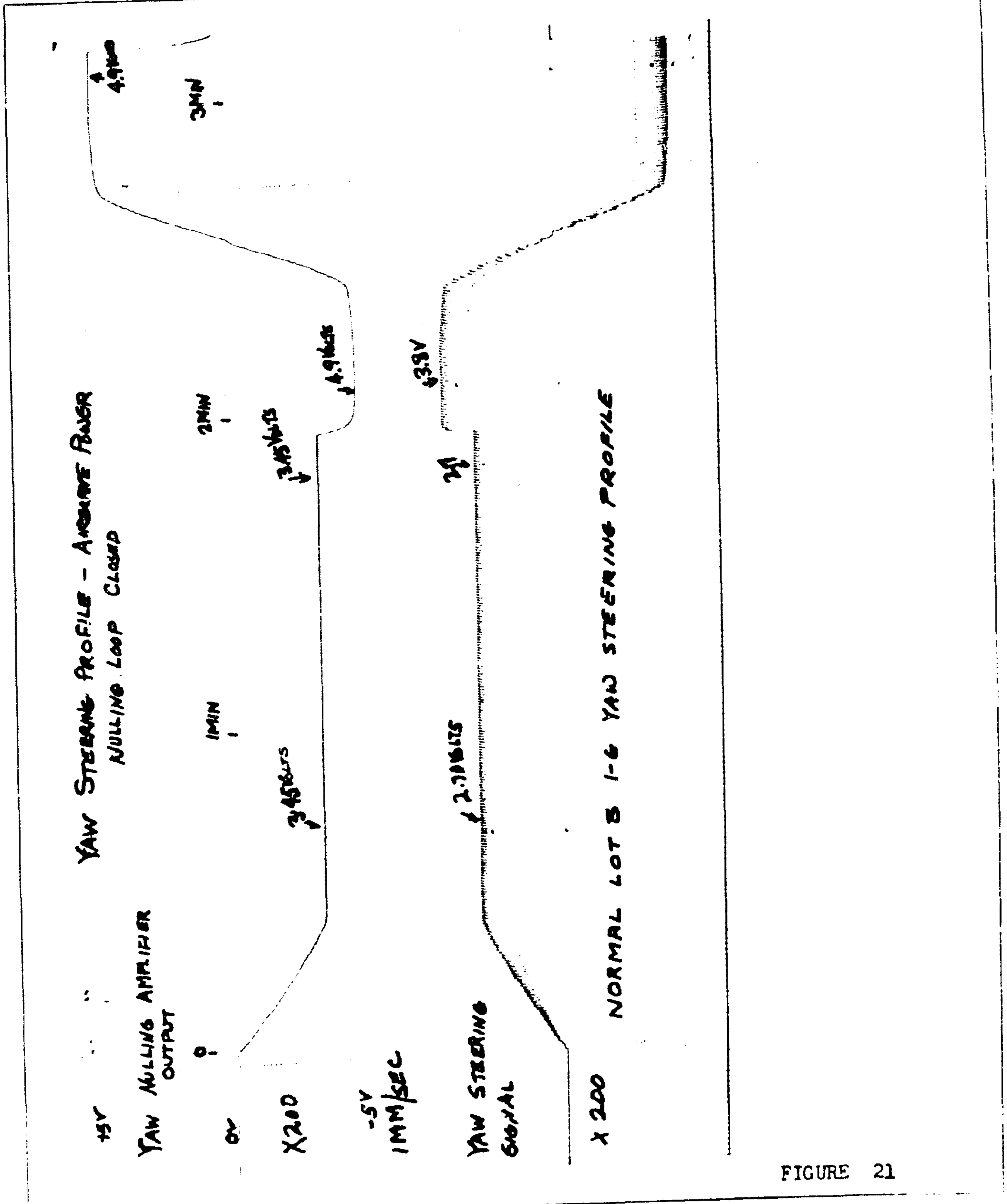
YAW STEERING PROFILE - AMBIENT POWER
NULLING LOOP CLOSED
NORMAL LOT B 1-6 YAW STEERING PROFILE
+5V
YAW NULLING AMPLIFIER OUTPUT
0V
X200
-5V
1MM/SEC
YAW STEERING SIGNAL
X 200
1MIN
2MIN
3MIN

FIGURE 21

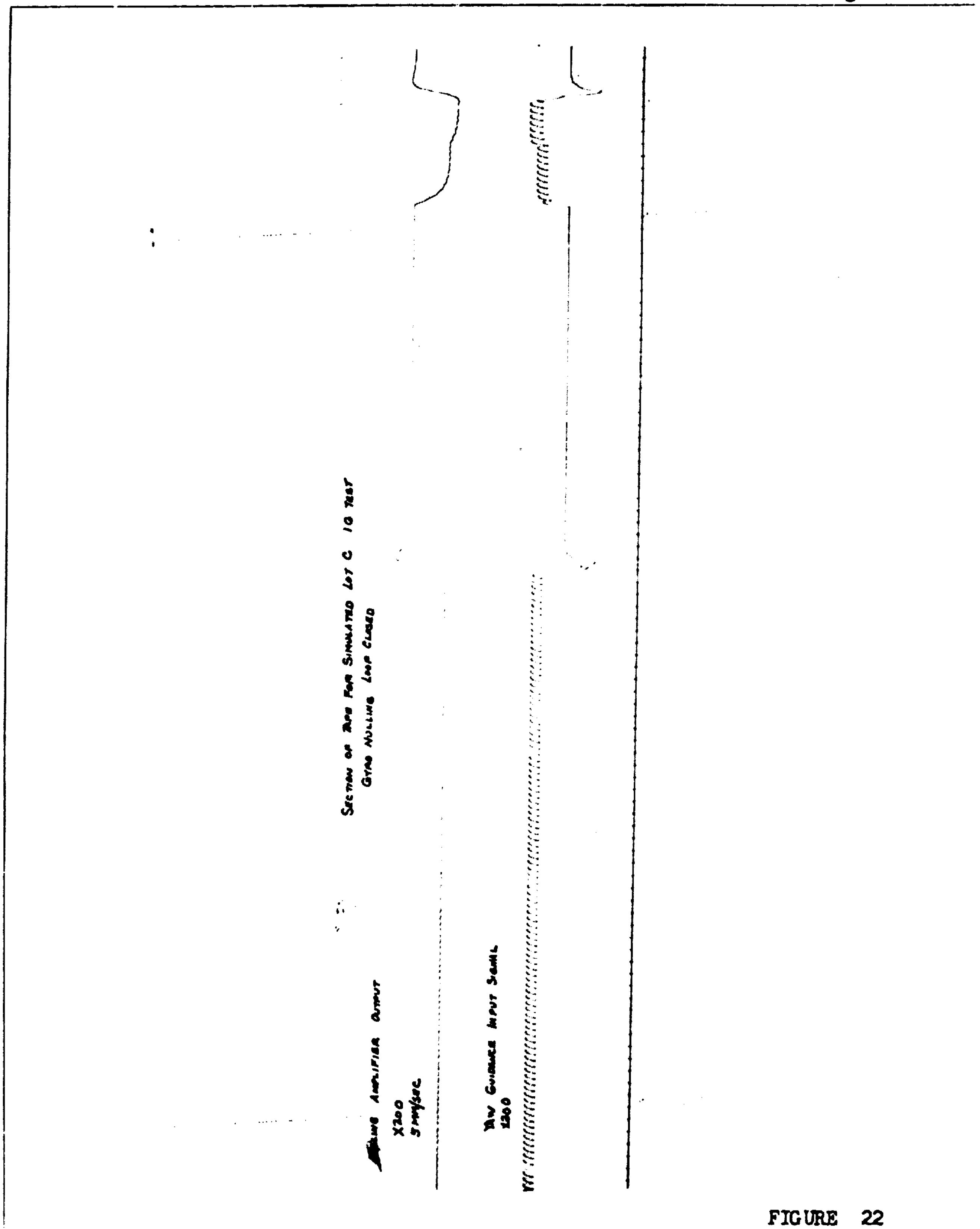
Section of Tape For Simulated Lot C IG Test
Gyro Nulling Loop Closed
Amplifier Output
X200
5 mm/sec
Yaw Guidance Input Signal
1200

FIGURE 22

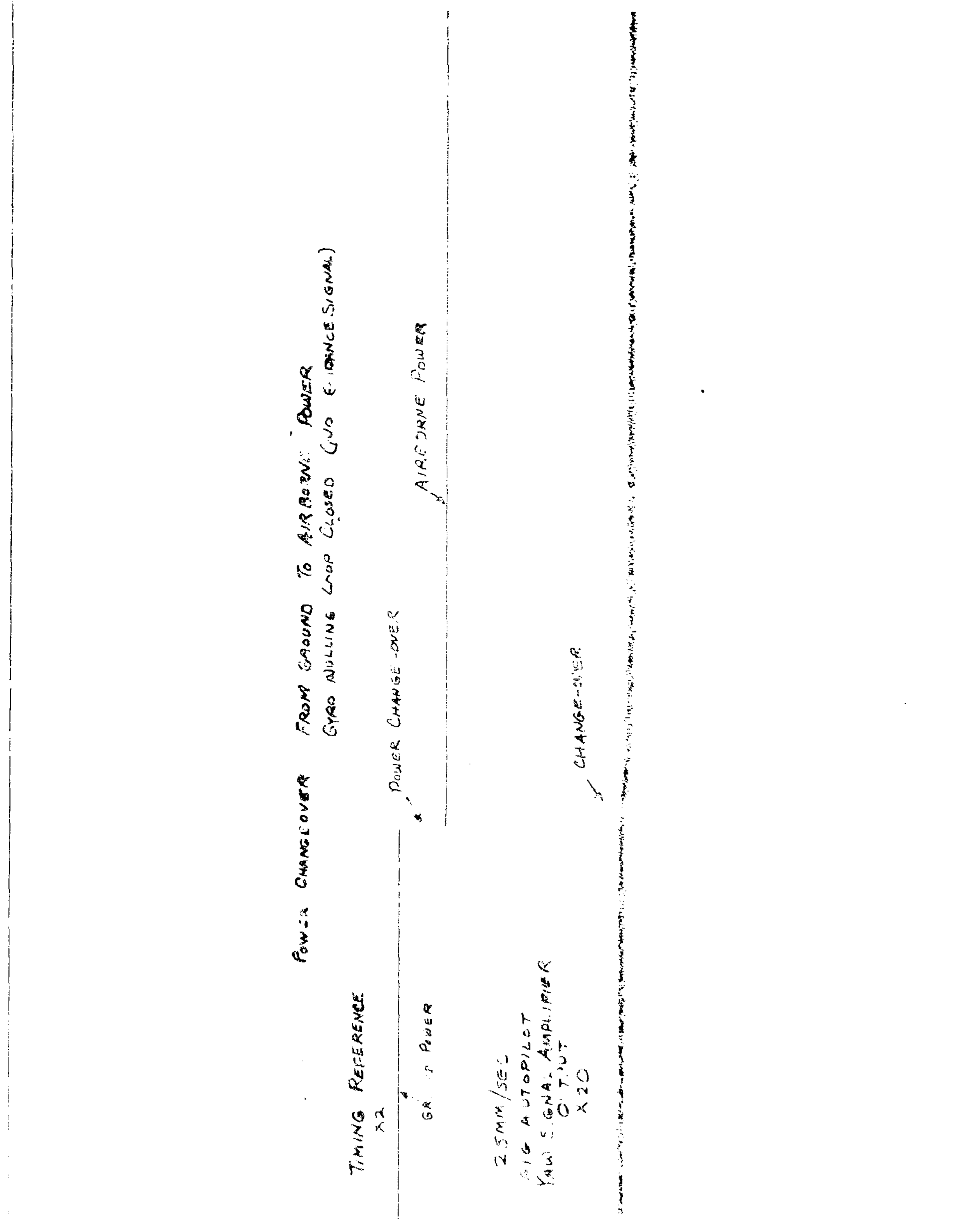
POWER CHANGEOVER FROM GROUND TO AIRBORNE POWER
GYRO NULLING LOOP CLOSED
AIRBORNE POWER
POWER CHANGE-OVER
CHANGE-OVER
TIMING REFERENCE
X2
POWER
25MM/SEC
AUTOPILOT
AMPLIFIER
X20

FIGURE 23

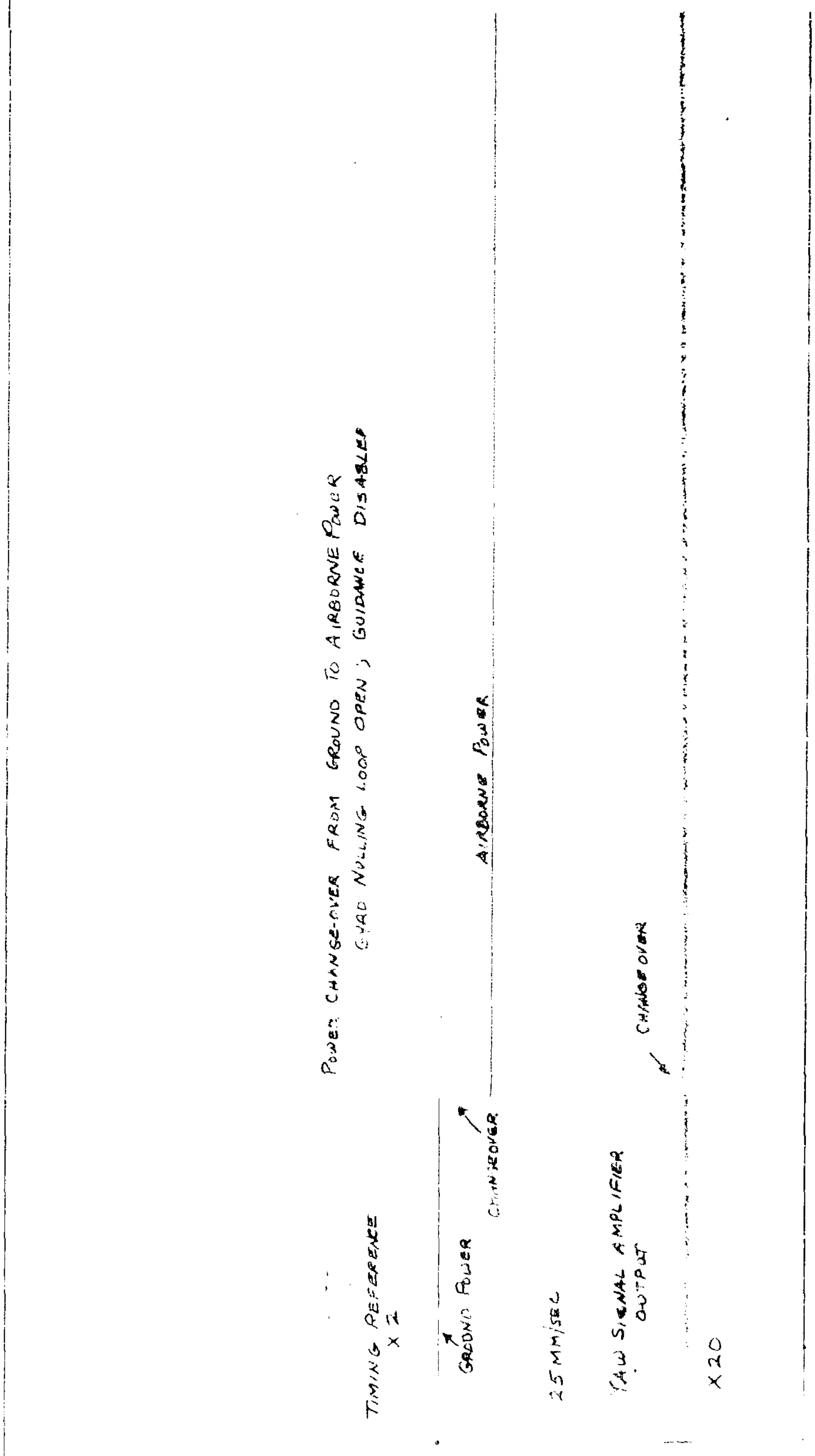
POWER CHANGE-OVER FROM GROUND TO AIRBORNE POWER
GYRO NULLING LOOP OPEN; GUIDANCE DISABLED
AIRBORNE POWER
CHANGE OVER
TIMING REFERENCE
X 2
GROUND POWER
CHANGEOVER
25 MM/SEC
YAW SIGNAL AMPLIFIER
OUTPUT
X 20

FIGURE 24

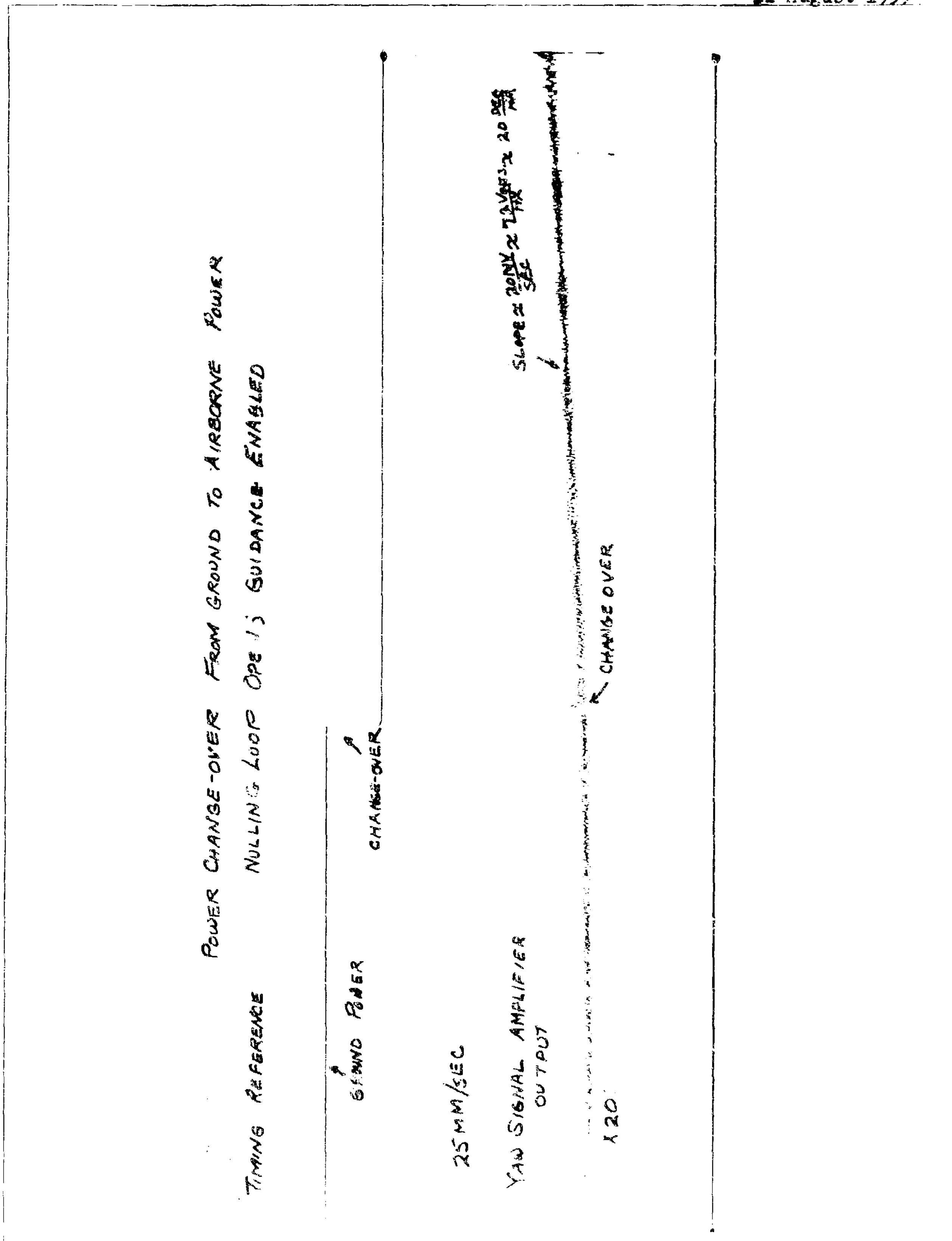
POWER CHANGE-OVER FROM GROUND TO AIRBORNE POWER
TIMING REFERENCE
NULLING LOOP
GUIDANCE ENABLED
GROUND POWER
CHANGE-OVER
25 MM/SEC
YAW SIGNAL AMPLIFIER OUTPUT
X 20
CHANGE OVER
SLOPE

FIGURE 25

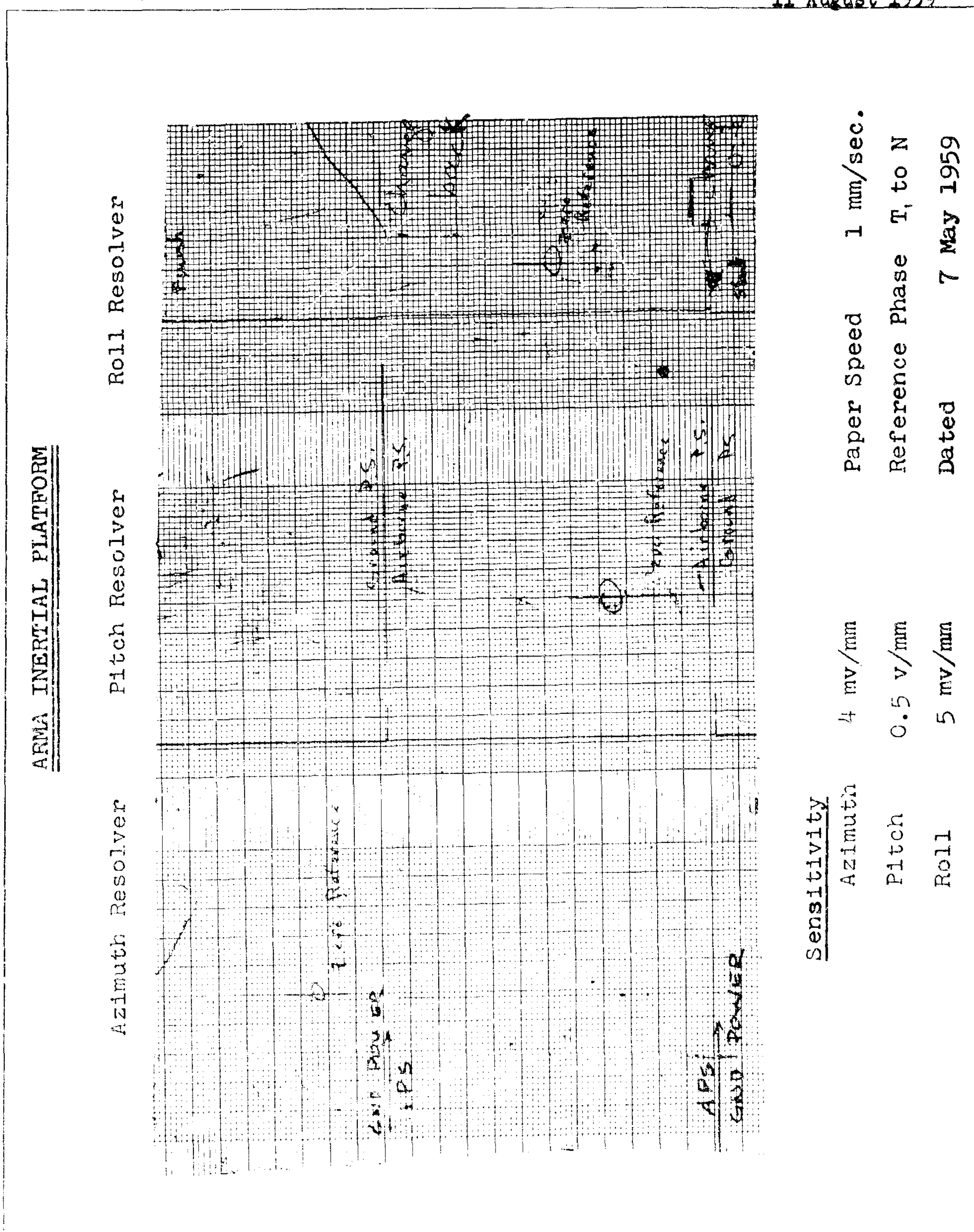
ARMA INERTIAL PLATFORM
Azimuth Resolver
Pitch Resolver
Roll Resolver
Paper Speed 1 mm/sec.
Reference Phase T, to N
Dated 7 May 1959
Sensitivity
Azimuth 4 mv/mm
Pitch 0.5 v/mm
Roll 5 mv/mm

FIGURE 26

## ARMA INERTIAL PLATFORM

Pitch Pendulum                                    Roll Pendulum

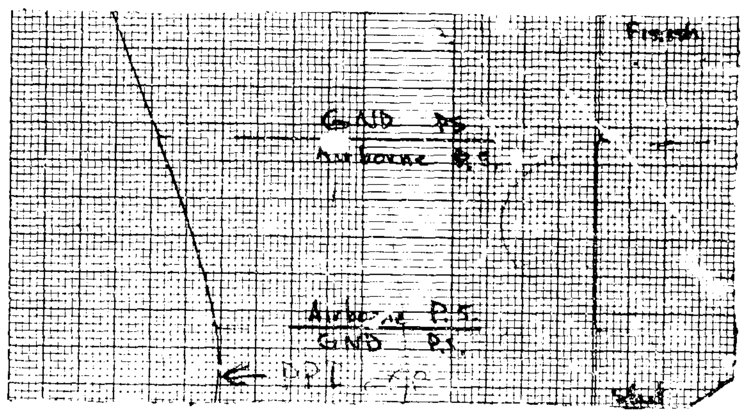


| | |
|---|---|
| Pendulum Gradient | 20 sec/mv |
| Sensitivity | 1 mv/mm |
| Paper Speed | 1 mm/sec. |
| Reference Phase | A to B |
| Earth Rotation Component about Y axis | 8 degrees/hour |

PPI Torquing Amplifier Off

FIGURE 27

## ARMA INERTIAL PLATFORM

Pitch Pendulum                Roll Pendulum

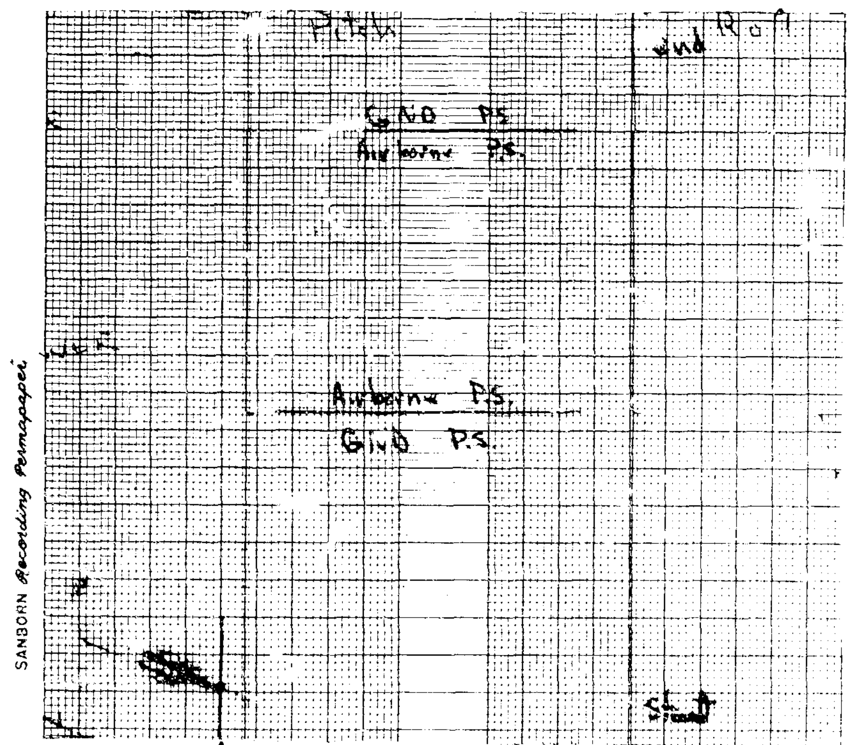


zero reference                zero reference

| | |
|---|---|
| Pendulum Gradient | 20 sec/mv |
| Sensitivity | 1 mv/mm |
| Paper Speed | 1 mm/sec |
| Reference Phase | A to B |

FIGURE 28

ARMA MGS SERVO AMPLIFIER OUTPUTS

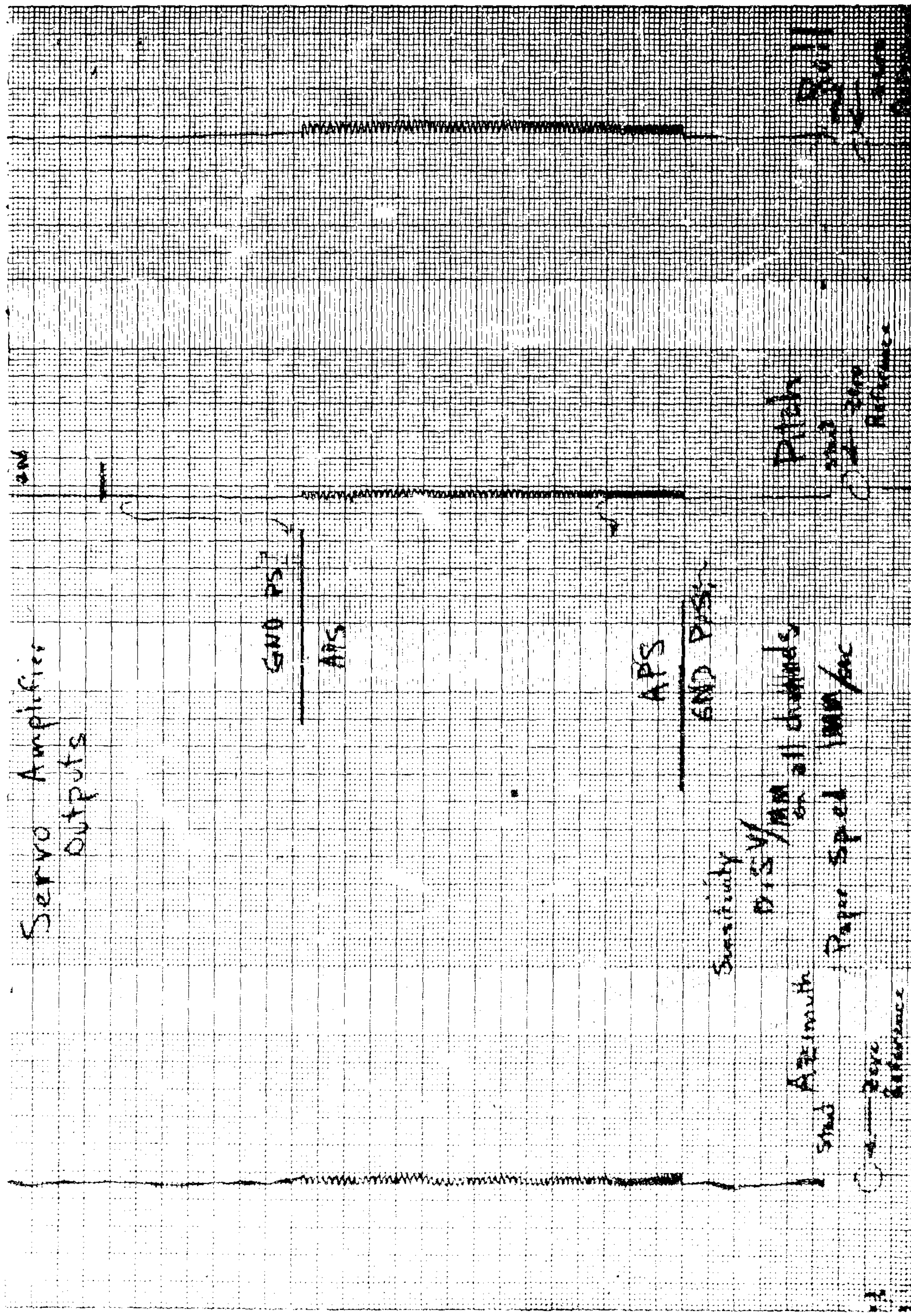


FIGURE 29

## COMPUTER POWER SUPPLY VOLTAGES

| NOMINAL VOLTAGE | OUTPUT - GROUND P.S. DC VOLTAGE | AC VOLTAGE | OUTPUT - AIRBORNE P.S. DC VOLTAGE | AC VOLTAGE |
|---|---|---|---|---|
| -50 | -49.0 | 0.3 | -49.0 | 0.7 |
| -16.5 | -15.8 | 0.2 | -15.8 | 0.19 |
| -10 | -10.1 | 0.16 | -10.4 | 0.28 |
| +3.3 | + 3.1 | 0.12 | + 3.1 | 1.[illegible] |
| +4 | + 3.9 | 0.19 | + 3.8 | 0.3 |
| +38 | +39.5 | 0.3 | +39 | 0.36 |
| +28 | +28 | 0.27 | +28 | 0.3 |

| LINE VOLTAGE | GROUND POWER SUPPLY | AIRBORNE POWER SUPPLY |
|---|---|---|
| Phase $T_1$ - N | 115 | 114.8 |
| Phase $T_2$ - N | 117 | 116.3 |
| Phase $T_3$ - N | 116.6 | 116.2 |

## CONTROL DC VOLTAGES

| NOMINAL | OUTPUT - GND PS DC VOLTS | AC VOLTS | OUTPUT APS DC VOLTS | AC VOLTS |
|---|---|---|---|---|
| Gyro Magnet Supply 4.5VDC 8VAC | 4.0 | 8.7 | 4.2 | 8.8 |
| Gyro Torquer Voltage 3.5VDC, 3.5VDC | 3.6 | 0.16 | 3.7 | 0.16 |
| Preamplifier Voltage -22.5VDC | -22 | 0.16 | -22 | 0.16 |
| Accelerometer Supply -22.5V | -22 | 5MV | -22 | 5MV |
| Amplifier Output Supply 35V Unfiltered | 23 | 11.4 | 23 | 11.2 |

| LINE VOLTAGE | GROUND POWER SUPPLY | AIRBORNE POWER SUPPLY |
|---|---|---|
| Phase $T_1$ - N | 116.3 | 114.9 |
| Phase $T_2$ - N | 117.4 | 116.2 |
| Phase $T_3$ - N | 117.4 | 116.1 |

FIGURE 30

POWER SYSTEM DIAGRAM

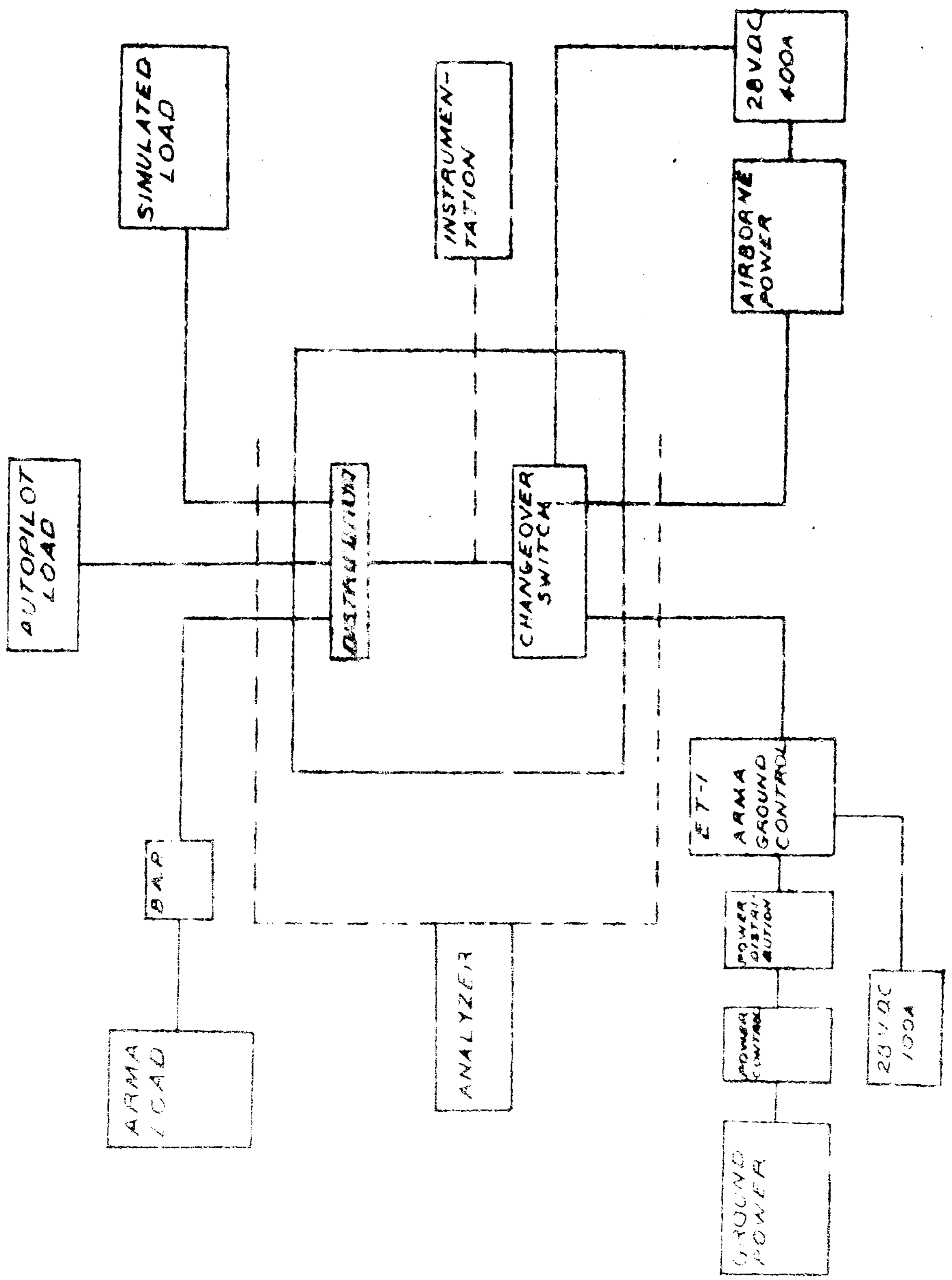


FIGURE 31

ABC 6-9-59

CONVAIR
SAN DIEGO



| RUN NO. 1 | | PHASE A V | PHASE A I | PHASE A W | PHASE A P.F. | PHASE B V | PHASE B I | PHASE B W | PHASE B P.F. |
|---|---|---|---|---|---|---|---|---|---|
| INVERTER | BEFORE | 115.6 | 5.8 | 600 | 0.896 | 116.3 | 4.84 | 500 | 0.889 |
| | AFTER | 113.9 | 5.75 | 590 | 0.90 | 115.5 | 4.7 | 500 | 0.92 |
| ARMA | | 114.5 | 3.8 | 420 | 0.966 | 115.6 | 3.6 | 400 | 0.96 |
| AUTO PILOT | | 115.0 | 1.115 | 90 | 0.703 | 115.9 | 0.813 | 37.5 | 0.399 |
| SIMULATED | | 114.5 | 0.84 | 82.5 | 0.86 | 115.4 | 0.735 | 72.5 | 0.855 |
| TOTAL: | | 115 | 5.51 | 592.5 | 0.92 | 115 | 4.75 | 510.0 | 0.894 |
| RUN NO. 2 | | | | | | | | | |
| INVERTER | BEFORE | 114.0 | 5.92 | 615 | 0.911 | 115.1 | 4.55 | 470 | 0.897 |
| | AFTER | 113.4 | 5.90 | 610 | 0.910 | 114.6 | 4.50 | 465 | 0.903 |
| ARMA | | 113.1 | 3.72 | 404 | 0.96 | 114.4 | 3.55 | 374 | 0.92 |
| AUTO PILOT | | 113.4 | 1.33 | 123.5 | 0.818 | 115.0 | 0.195 | 15.5 | 0.692 |
| SIMULATED | | 115.4 | 0.83 | 81 | 0.845 | 114.4 | 0.735 | 71.5 | 0.851 |
| TOTAL: | | 115 | 5.74 | 608.5 | 0.924 | 115 | 4.44 | 461.0 | 0.904 |
| | SYSTEM LOAD WITH SIMULATED LOAD DUMPED | | | | | | | | |
| INVERTER | | 114.5 | 4.8 | 511 | 0.93 | 115.0 | 3.86 | 420 | 0.945 |

A

COMPATIBILITY LOAD ANALYSIS

| | | PHASE C | | | | TOTAL 3 PHASE WATTS | | | | | |
|---|---|---|---|---|---|---|---|---|---|---|---|
| P.F. | | V | I | W | P.F. | WATTS | $VT_1$-$T_2$ | $VT_3$-$T_3$ | $VT_3$-$T_1$ | Vdc | Idc |
| 0.889 | | 115.9 | 5.72 | 555 | 0.837 | 1655 | 200.4 | 200.7 | 200.4 | 27.9 | 116 |
| 0.92 | | 114.6 | 5.65 | 540 | 0.836 | 1630 | | | | | |
| 0.96 | | 115.1 | 3.8 | 390 | 0.892 | 1210 | | | | | |
| 0.399 | | 115.0 | 1.375 | 47.5 | 0.302 | 175 | | | | | |
| 0.855 | | 114.9 | 1.175 | 106 | 0.785 | 261 | | | | | |
| 0.894 | | 115 | 6.05 | 543.5 | 0.784 | 1646 | | | | | |
| 0.897 | | 114.6 | 5.82 | 550 | 0.825 | 1635 | 200.8 | 201.4 | 200.9 | 27.8 | 126 |
| 0.903 | | 114.0 | 5.8 | 545 | 0.825 | 1620 | 195.8 | 196.4 | 196 | 27.8 | 114 |
| 0.92 | | 113.8 | 3.85 | 380 | 0.870 | 1158 | | | | | |
| 0.692 | | 114.2 | 0.332 | 40 | 0.554 | 179 | | | | | |
| 0.851 | | 113.8 | 1.163 | 104.5 | 0.790 | 257 | | | | | |
| 0.904 | | 115 | 5.5 | 524.5 | 0.825 | 1594 | | | | | |
| 0.945 | | 115 | 4.4 | 440 | 0.87 | 1371 | 198 | 199 | 198.9 | 27.9 | 100 |

NOTES:

1. Measured Voltages are ±1%
2. Measured Currents are ±2%
3. Measured Watts are ±2%

FIGURE 32

B

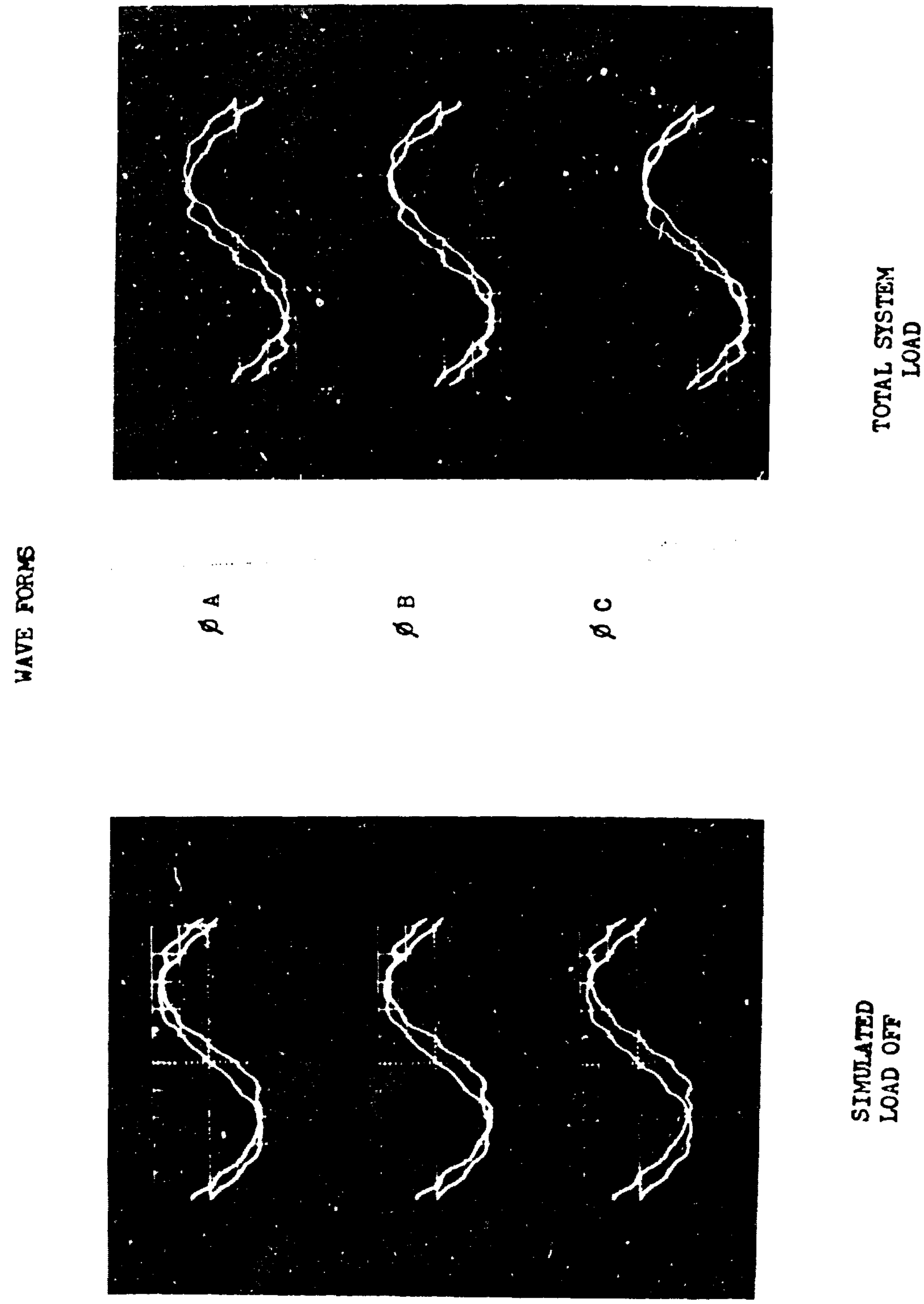


FIGURE 33

| PHASE | 1 | 2 | 3 | 4 | 5 | 6 | 7 | 8 | 9 | 10 | 11 |
|---|---|---|---|---|---|---|---|---|---|---|---|
| | 400 | 800 | 1200 | 1600 | 2000 | 2400 | 2800 | 3200 | 3600 | 4000 | 4400 |
| | | RUN NO. 1 INVERTER VOLTAGE - R.M.S. VALUES | | | | | | | | | |
| A | 110 | 0.34 | 0.38 | 0.20 | 0.50 | 0.16 | 2.50 | 0.27 | 0.48 | 0.35 | 2.50 |
| B | 107 | 0.30 | 0.60 | 0.23 | 0.63 | 0.06 | 2.0 | 0.24 | 0.54 | 0.30 | 2.0 |
| C | 109 | 0.26 | 0.22 | 0.20 | 0.60 | 0.0 | 1.9 | 0.35 | 0.04 | 0.36 | 3.0 |
| | | RUN NO. 2 INVERTER VOLTAGE | | | | | | | | | |
| A | 104 | 0.28 | 0.37 | | 0.58 | | 2.15 | | 0.30 | | 2.7 |
| B | 105 | 0.25 | 0.50 | | 0.67 | | 1.85 | | 0.33 | | 2.39 |
| C | 104 | 0.24 | 0.22 | | 0.72 | | 1.75 | | 0.10 | | 2.80 |
| | | RUN NO. 1 INVERTER CURRENT - R.M.S. VALUES | | | | | | | | | |
| A | 5.70 | 0.14 | 0.33 | 0.072 | 0.054 | 0.024 | 0.16 | 0.01 | 0.044 | 0.038 | 0.088 |
| B | 4.34 | 0.12 | 0.26 | 0.072 | 0.04 | 0.004 | 0.136 | 0.012 | 0.03 | 0.008 | 0.18 |
| C | 4.72 | 0.114 | 0.21 | 0.046 | 0.08 | 0.024 | 0.096 | 0.008 | 0.028 | 0.024 | 0.23 |
| | | RUN NO. 2 INVERTER CURRENT | | | | | | | | | |
| A | 5.40 | 0.136 | 0.30 | | 0.072 | | 0.068 | | 0.036 | | 0.116 |
| B | 4.00 | 0.12 | 0.48 | | 0.03 | | 0.124 | | 0.016 | | 0.208 |
| C | 5.20 | 0.108 | 0.20 | | 0.078 | | 0.116 | | 0.024 | | 0.23 |
| | | RUN NO. 1 INVERTER VOLTAGE - % of FUNDAMENTAL (R.M.S.) | | | | | | | | | |
| A | 100 | 0.31 | 0.346 | 0.182 | 0.455 | 0.145 | 2.27 | 0.246 | 0.437 | 0.318 | 2.27 |
| B | 100 | 0.28 | 0.56 | 0.215 | 0.589 | 0.056 | 1.87 | 0.224 | 0.505 | 0.28 | 1.87 |
| C | 100 | 0.238 | 0.202 | 0.184 | 0.55 | 0 | 1.745 | 0.321 | 0.037 | 0.33 | 2.75 |
| | | RUN NO. 2 INVERTER VOLTAGE | | | | | | | | | |
| A | 100 | 0.269 | 0.356 | | 0.558 | | 2.065 | | 0.288 | | 2.6 |
| B | 100 | 0.248 | 0.276 | | 0.638 | | 1.905 | | 0.314 | | 2.28 |
| C | 100 | 0.230 | 0.212 | | 0.692 | | 1.68 | | 0.096 | | 2.69 |
| | | RUN NO. 1 INVERTER CURRENT - % of FUNDAMENTAL (R.M.S.) | | | | | | | | | |
| A | 100 | 2.46 | 5.8 | 1.26 | 0.948 | 0.421 | 2.81 | 0.175 | 0.773 | 0.676 | 1.54 |
| B | 100 | 2.76 | 6.0 | 1.66 | 0.92 | 0.092 | 3.13 | 0.276 | 0.69 | 0.184 | 4.14 |
| C | 100 | 2.42 | 4.45 | 1.03 | 1.69 | 0.508 | 2.03 | 0.169 | 0.593 | 0.508 | 4.87 |
| | | RUN NO. 2 INVERTER CURRENT | | | | | | | | | |
| A | 100 | 2.52 | 5.56 | | 1.33 | | 1.26 | 0.666 | | 2.15 | |
| B | 100 | 3.00 | 12.0 | | 0.75 | | 3.1 | 0.4 | | 5.2 | |
| C | 100 | 2.57 | 5.76 | | 1.86 | | 2.76 | 0.571 | | 5.48 | |

HARMONIC CONTENT - VOLTAGE R.M.S.

RUN NO. 1

| | $\left[\sum_{2}^{10} V^2\right]^{\frac{1}{2}}$ | $\left[\sum_{11}^{20} V^2\right]^{\frac{1}{2}}$ | $\left[\sum_{2}^{20} V^2\right]^{\frac{1}{2}}$ |
|---|---|---|---|
| A | 0.024 V fundamental | 0.025 V Fund. | 0.035V Fund. |
| B | 0.022 V Fund. | 0.023 V Fund. | 0.031V Fund. |
| C | 0.021 V Fund. | 0.030 V Fund. | 0.035V Fund. |

COMPATIBILITY HARMONIC ANALYSIS

| HARMONIC 11 4400 | 12 4800 | 13 5200 | 14 5600 | 15 6000 | 16 6400 | 17 6800 | 18 7200 | 19 7600 | 20 8000 | R.M.S. SUM | METERED TOTAL VALUES before/after |
|---|---|---|---|---|---|---|---|---|---|---|---|
| 2.50 | 0.09 | 0.68 | 0.20 | 0.22 | 0.13 | 0.50 | 0.20 | 0.48 | 0.23 | 110.07 | 115.6/112.9 |
| 2.0 | 0.2 | 0.53 | 0.28 | 0.18 | 0.11 | 0.50 | 0.28 | 0.78 | 0.24 | 107.05 | 116.9/112.2 |
| 3.0 | 0.14 | 1.00 | 0.04 | 0.12 | 0.09 | 0.60 | 0.07 | 0.40 | 0.05 | 109.07 | 116.2/113.4 |
| | | | | | | | | | | | |
| 2.7 | | | | | | | | | | 104.06 | 113.4/112.5 |
| 2.39 | | | | | | | | | | 105.05 | 114.6/113.8 |
| 2.80 | | | | | | | | | | 104.06 | 114/113.2 |
| | | | | | | | | | | | |
| 0.088 | 0.02 | 0.088 | 0.01 | 0.01 | 0.006 | 0.006 | 0.004 | 0.028 | 0.002 | 5.70 | 6.12/5.9 |
| 0.18 | 0.02 | 0.092 | 0.016 | 0.016 | 0.006 | 0.044 | 0.006 | 0.040 | 0.004 | 4.37 | 4.55/4.5 |
| 0.23 | 0 | 0.064 | 0.004 | 0.008 | 0.004 | 0.024 | 0.004 | 0.018 | 0.002 | 4.74 | 6.0/5.8 |
| | | | | | | | | | | | |
| 0.116 | | | | | | | | | | 5.41 | 5.9/ - |
| 0.208 | | | | | | | | | | 4.04 | 4.5/- |
| 0.23 | | | | | | | | | | 5.21 | 5.3/- |
| | | | | | | | | | | | |
| 2.27 | 0.082 | 0.619 | 0.182 | 0.20 | 0.118 | 0.455 | 0.182 | 0.436 | 0.209 | | 105/102.5 |
| 1.87 | 0.187 | 0.495 | 0.261 | 0.168 | 0.103 | 0.467 | 0.262 | 0.73 | 0.224 | | 109/106.7 |
| 2.75 | 0.128 | 0.92 | 0.037 | 0.110 | 0.083 | 0.55 | 0.064 | 0.367 | 0.046 | | 106.6/104 |
| | | | | | | | | | | | |
| 2.6 | | | | | | | | | | | 109/108 |
| 2.28 | | | | | | | | | | | 109/103.2 |
| 2.69 | | | | | | | | | | | 109.5/108.9 |
| | | | | | | | | | | | |
| 1.54 | 0.351 | 1.54 | 0.175 | 0.175 | 0.105 | 0.105 | 0.07 | 0.492 | .0351 | | 107.2/103.5 |
| 4.14 | 0.46 | 2.12 | 0.368 | 0.368 | 0.138 | 1.01 | 0.138 | 0.92 | 0.092 | | 100/103.5 |
| 4.87 | 0 | 1.36 | 0.085 | 0.169 | 0.085 | [illegible] | 0.085 | 0.381 | 0.042 | | 127/123 |
| | | | | | | | | | | | |
| | | | | | | | | | | | 109/- |
| | | | | | | | | | | | 112/- |
| | | | | | | | | | | | 138/- |

NOTES:

1. Harmonic readings are ±5%

FIGURE 24

B

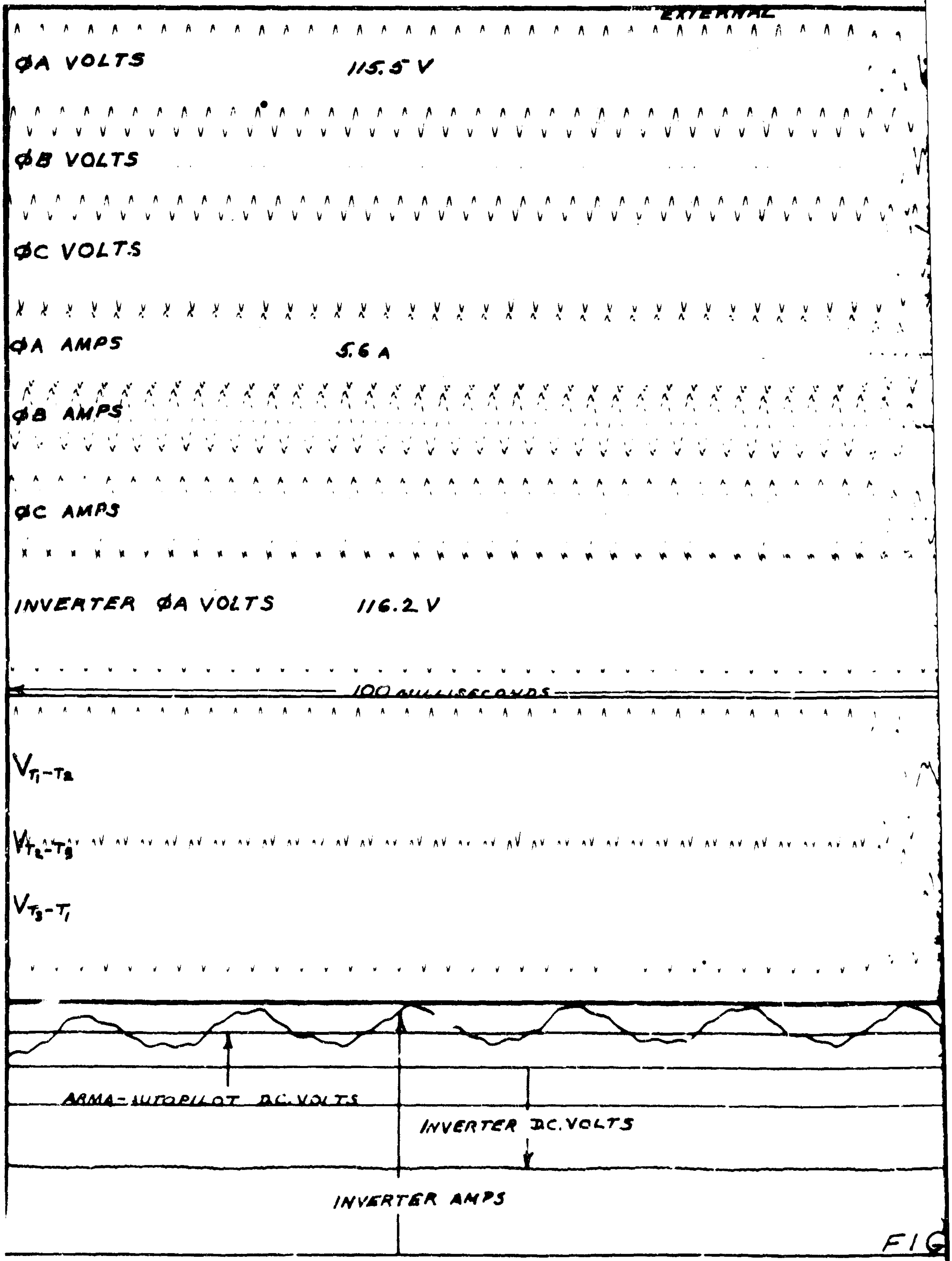
EXTERNAL
ØA VOLTS
115.5 V
ØB VOLTS
ØC VOLTS
ØA AMPS
5.6 A
ØB AMPS
ØC AMPS
INVERTER ØA VOLTS
116.2 V
100 MILLISECONDS
$V_{T_1-T_2}$
$V_{T_2-T_3}$
$V_{T_3-T_1}$
ARMA-AUTOPILOT D.C. VOLTS
INVERTER D.C. VOLTS
INVERTER AMPS

A

FIG

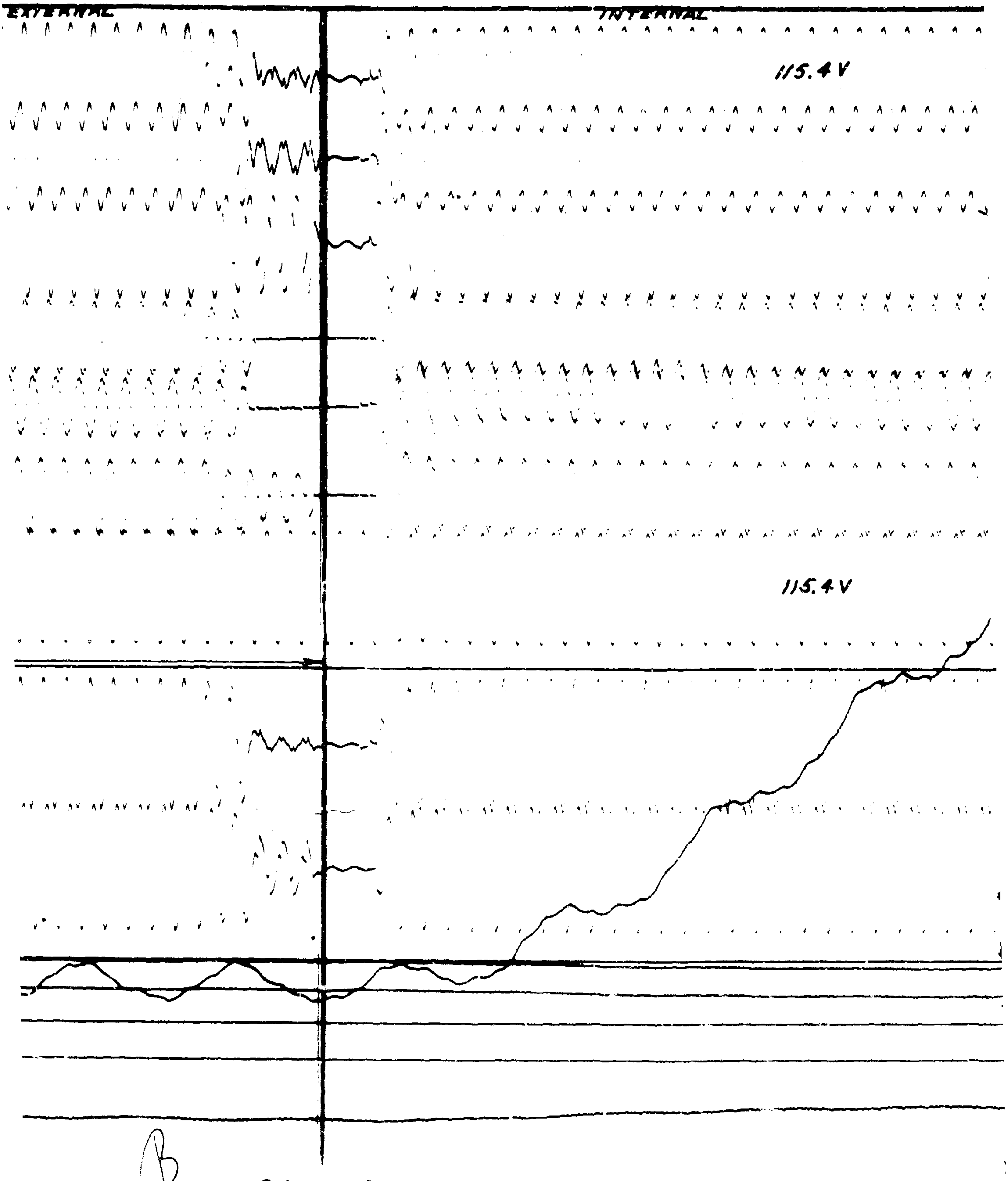


B FIGURE 35

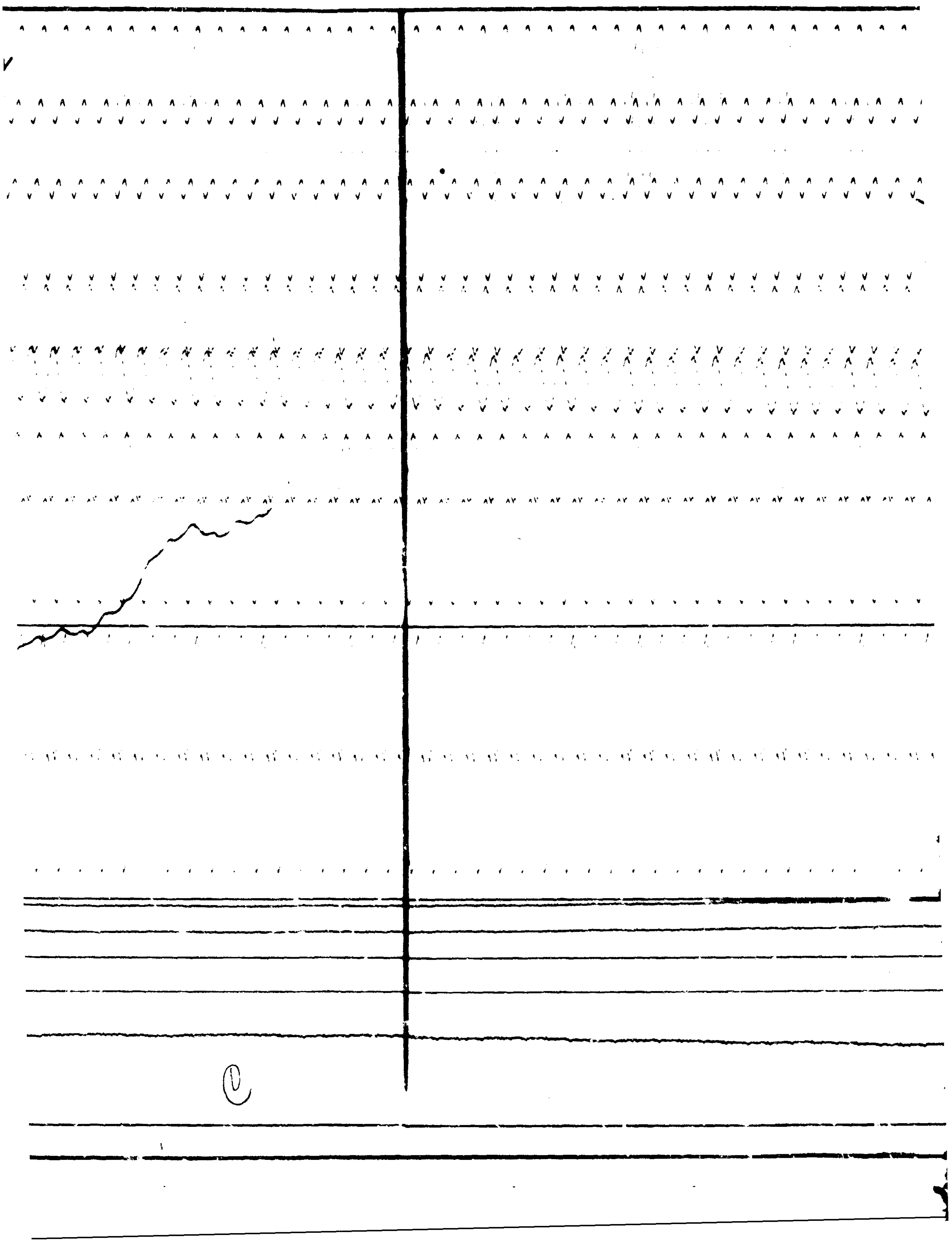

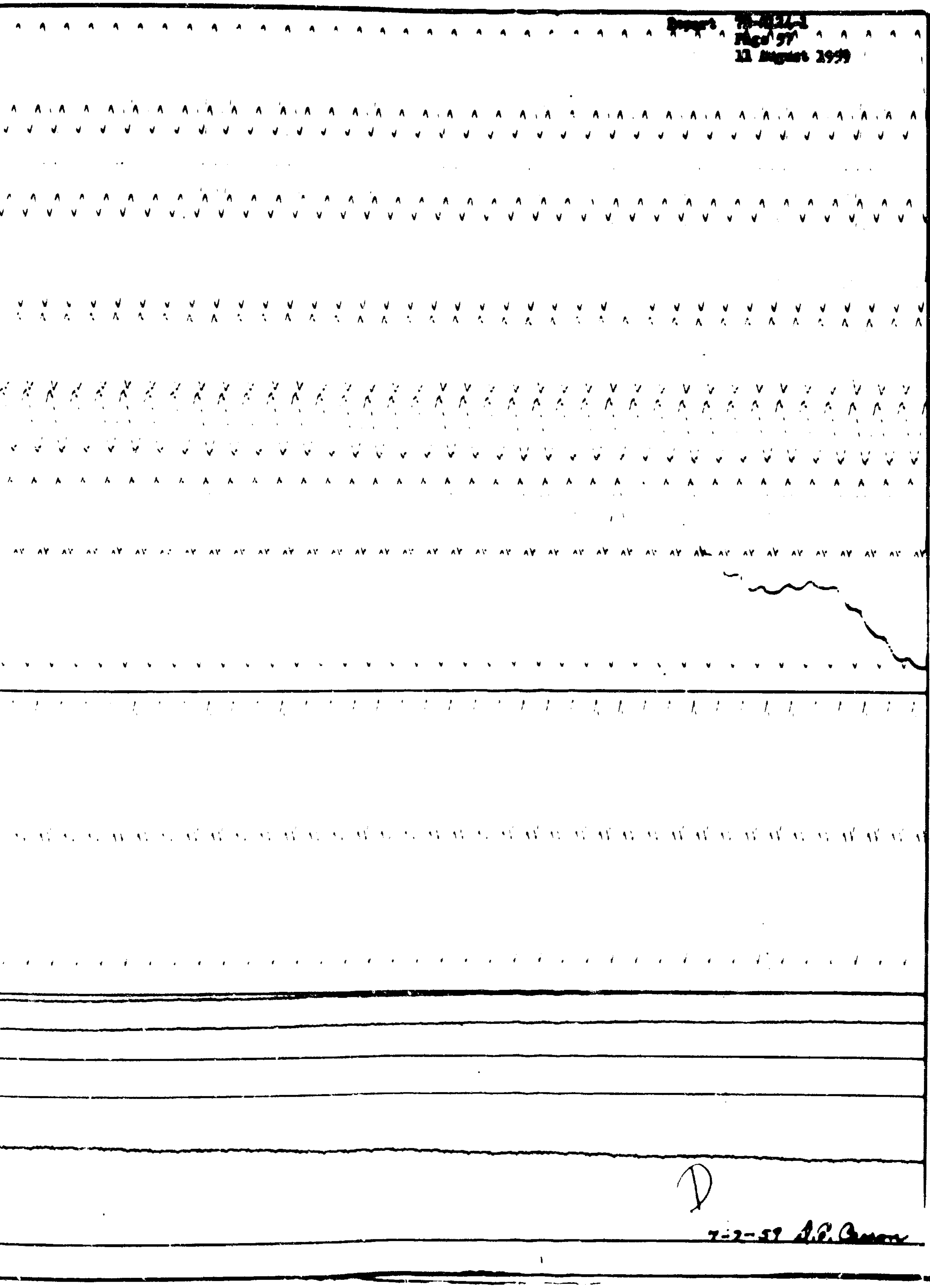
D
7-2-59

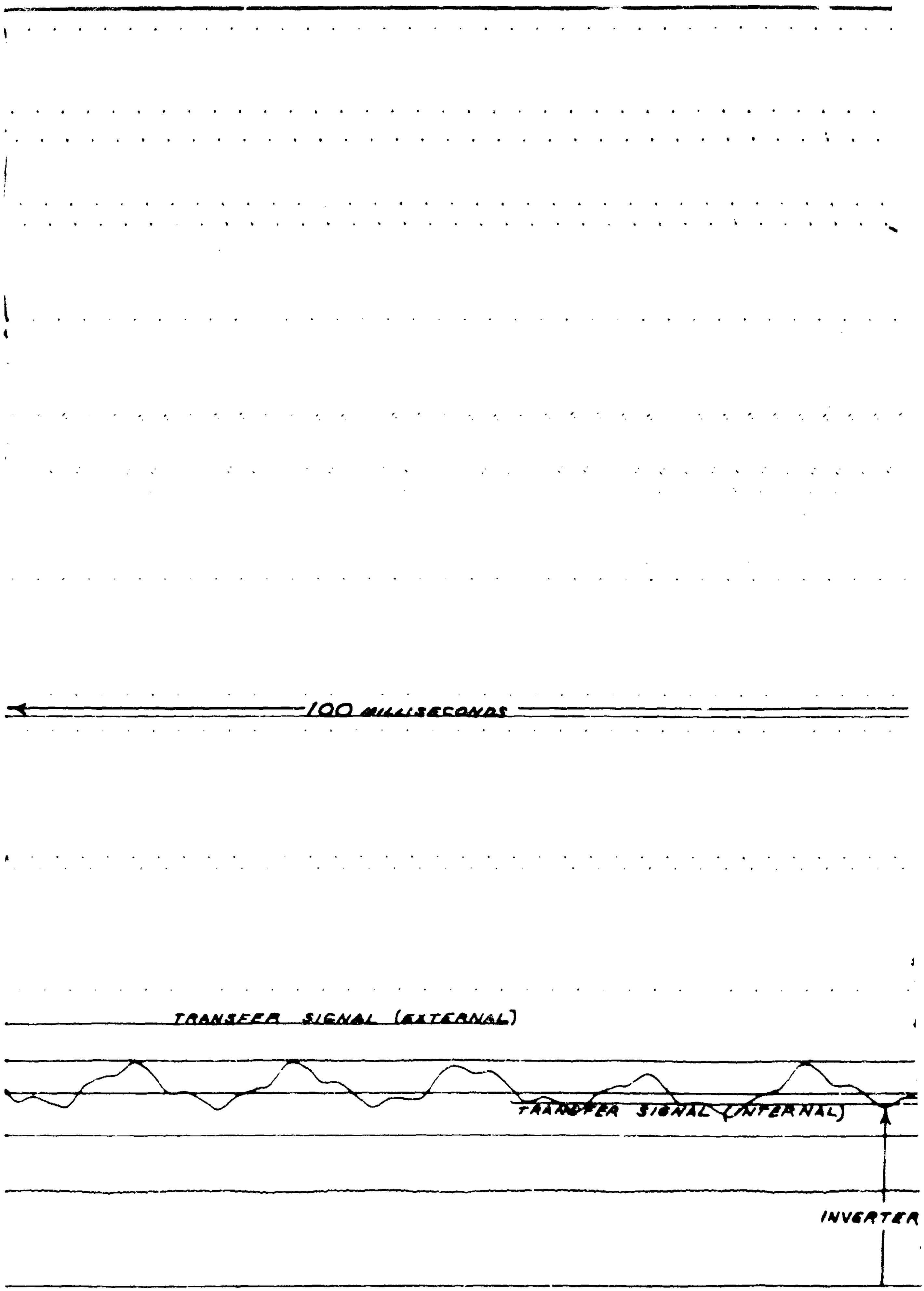
100 MILLISECONDS
TRANSFER SIGNAL (EXTERNAL)
TRANSFER SIGNAL (INTERNAL)
INVERTER

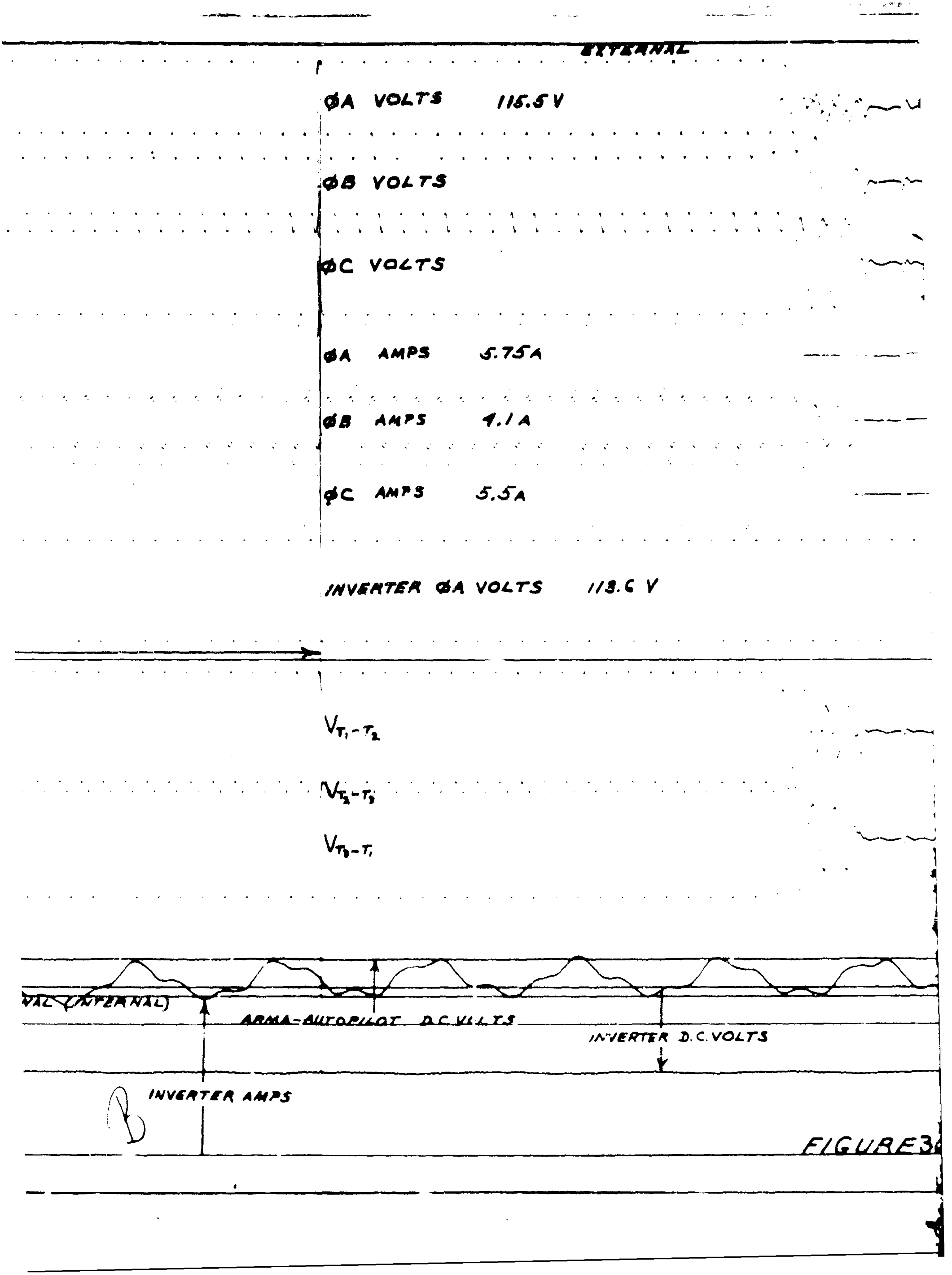
EXTERNAL
ØA VOLTS 115.5 V
ØB VOLTS
ØC VOLTS
ØA AMPS 5.75 A
ØB AMPS 4.1 A
ØC AMPS 5.5 A
INVERTER ØA VOLTS 113.6 V
$V_{T_1-T_2}$
$V_{T_2-T_3}$
$V_{T_3-T_1}$
VAL (INTERNAL)
ARMA-AUTOPILOT D.C. VOLTS
INVERTER D.C. VOLTS
INVERTER AMPS
B

FIGURE 3

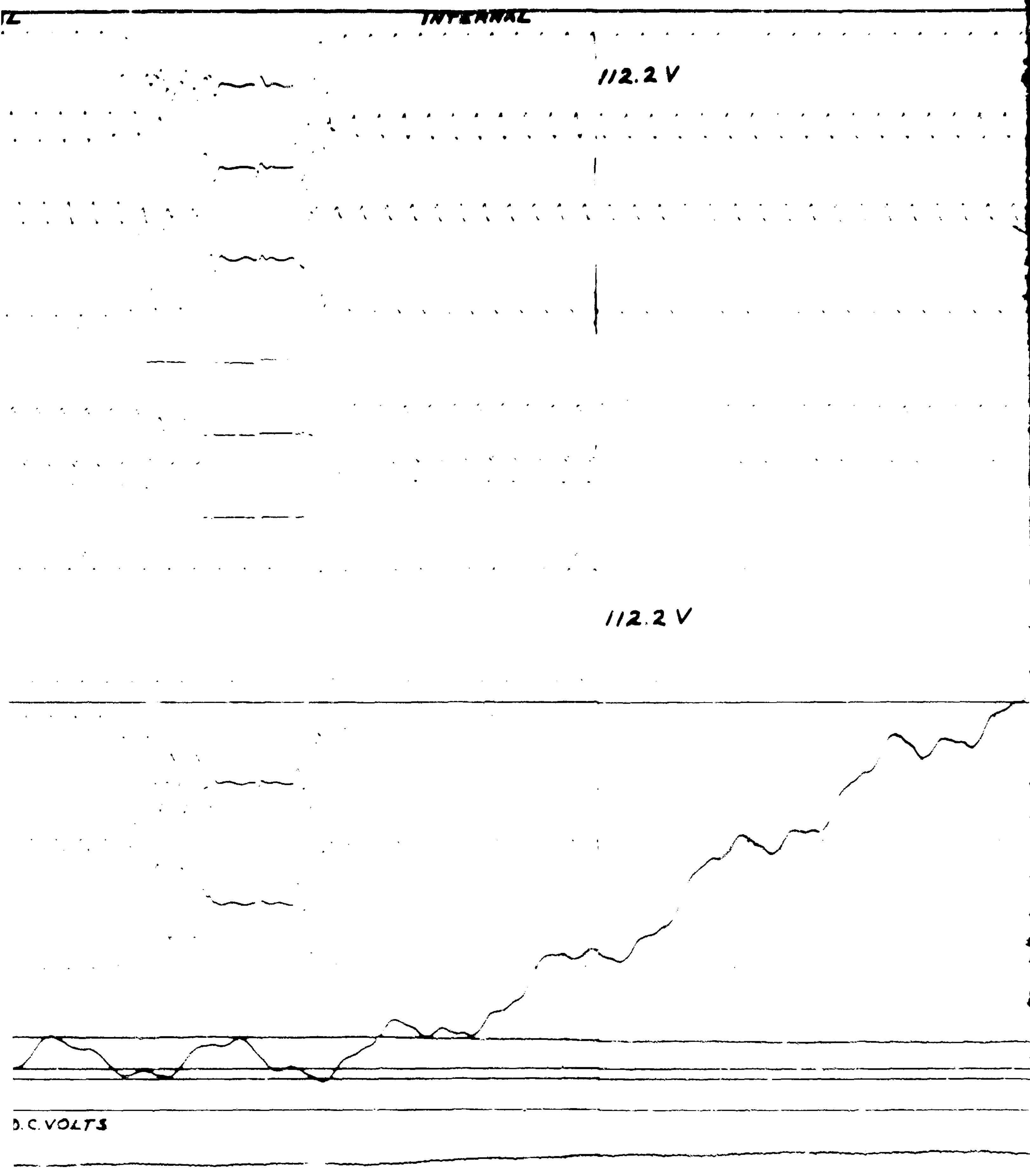


FIGURE 36

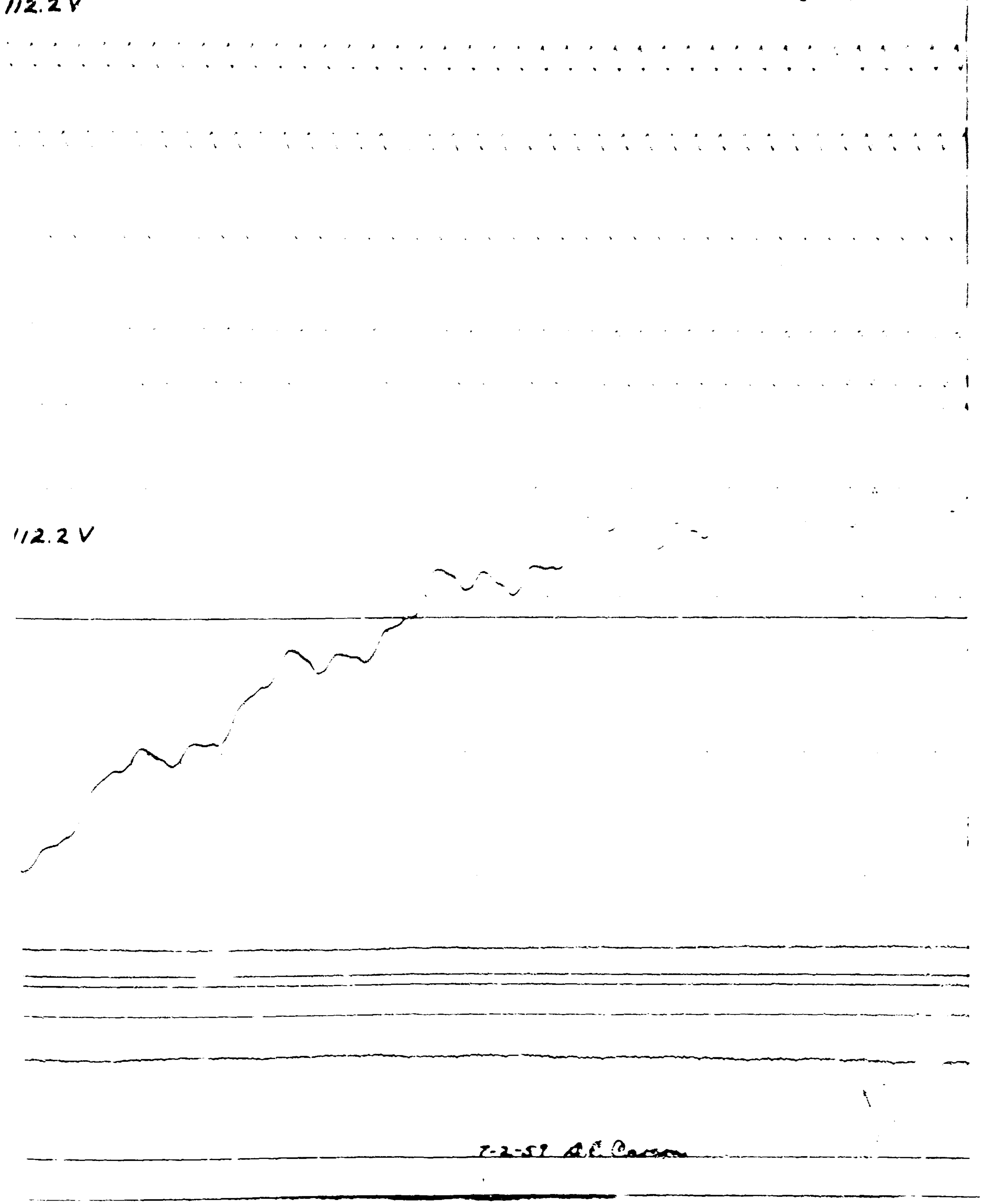
112.2 V
112.2 V
7-2-59

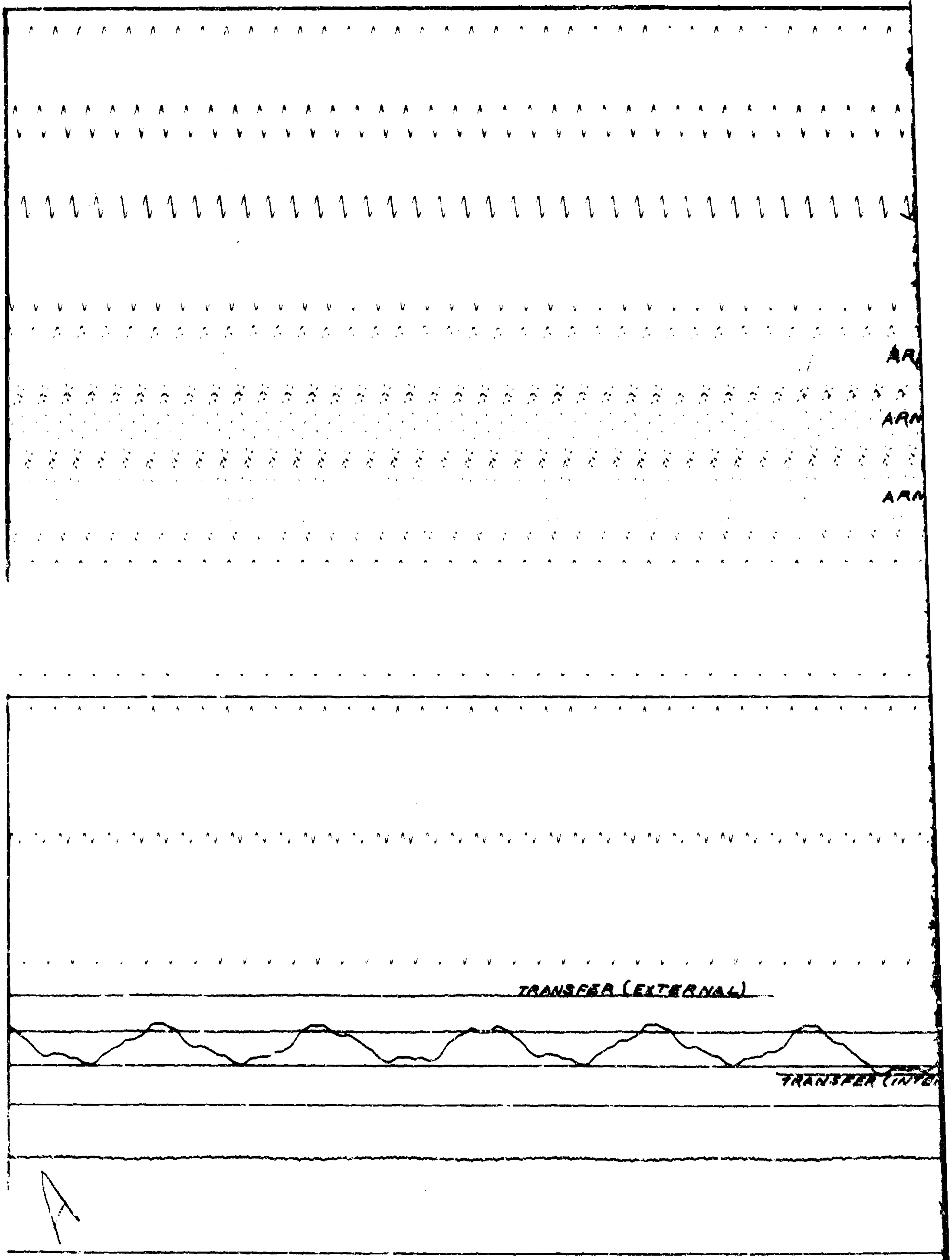
TRANSFER (EXTERNAL)

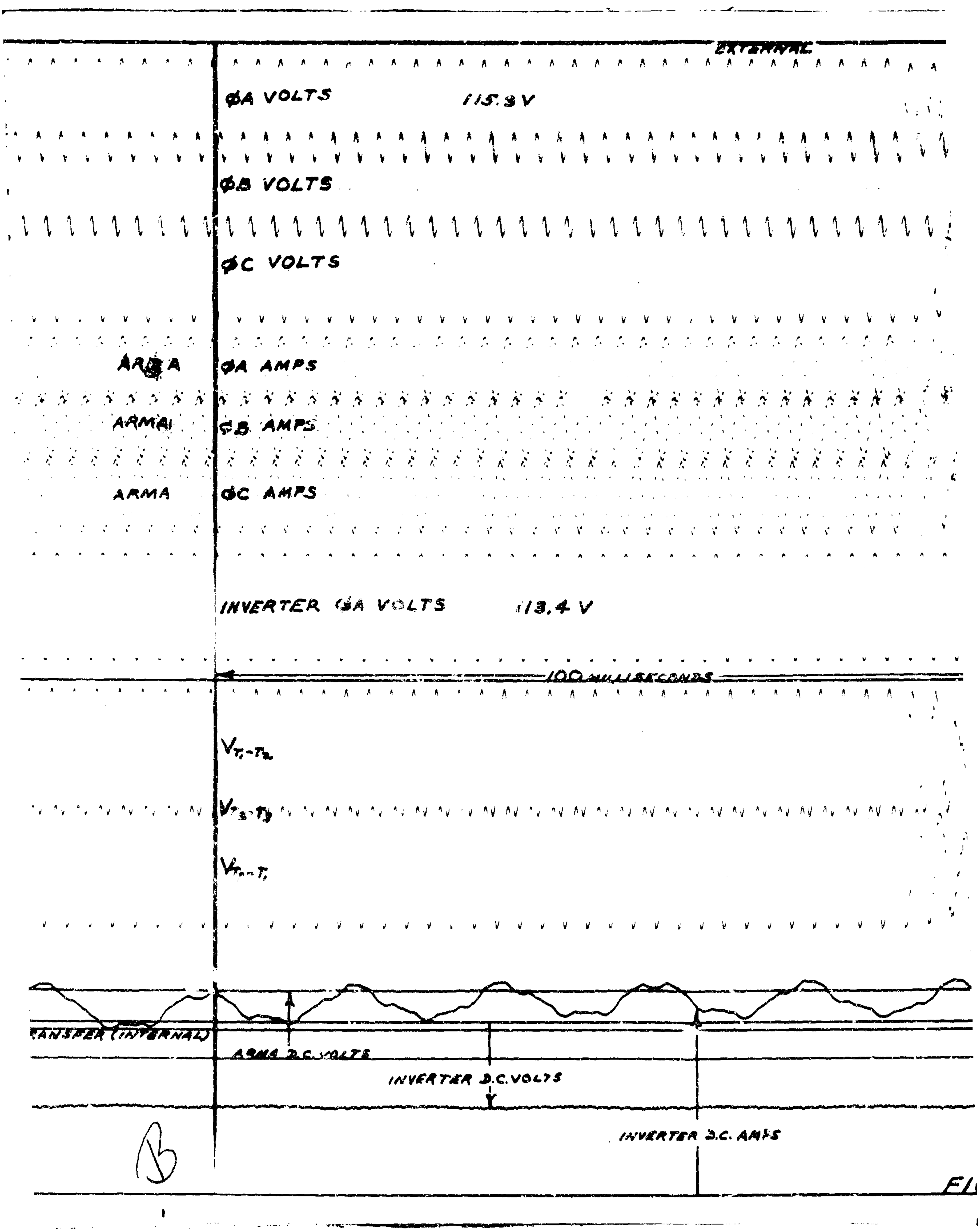
EXTERNAL
ØA VOLTS
115.3V
ØB VOLTS
ØC VOLTS
ARMA
ØA AMPS
ARMA
ØB AMPS
ARMA
ØC AMPS
INVERTER ØA VOLTS
113.4 V
100 MILLISECONDS
$V_{T_1-T_2}$
$V_{T_2-T_3}$
$V_{T_3-T_1}$
TRANSFER (INTERNAL)
ARMA D.C. VOLTS
INVERTER D.C. VOLTS
INVERTER D.C. AMPS
B
EL

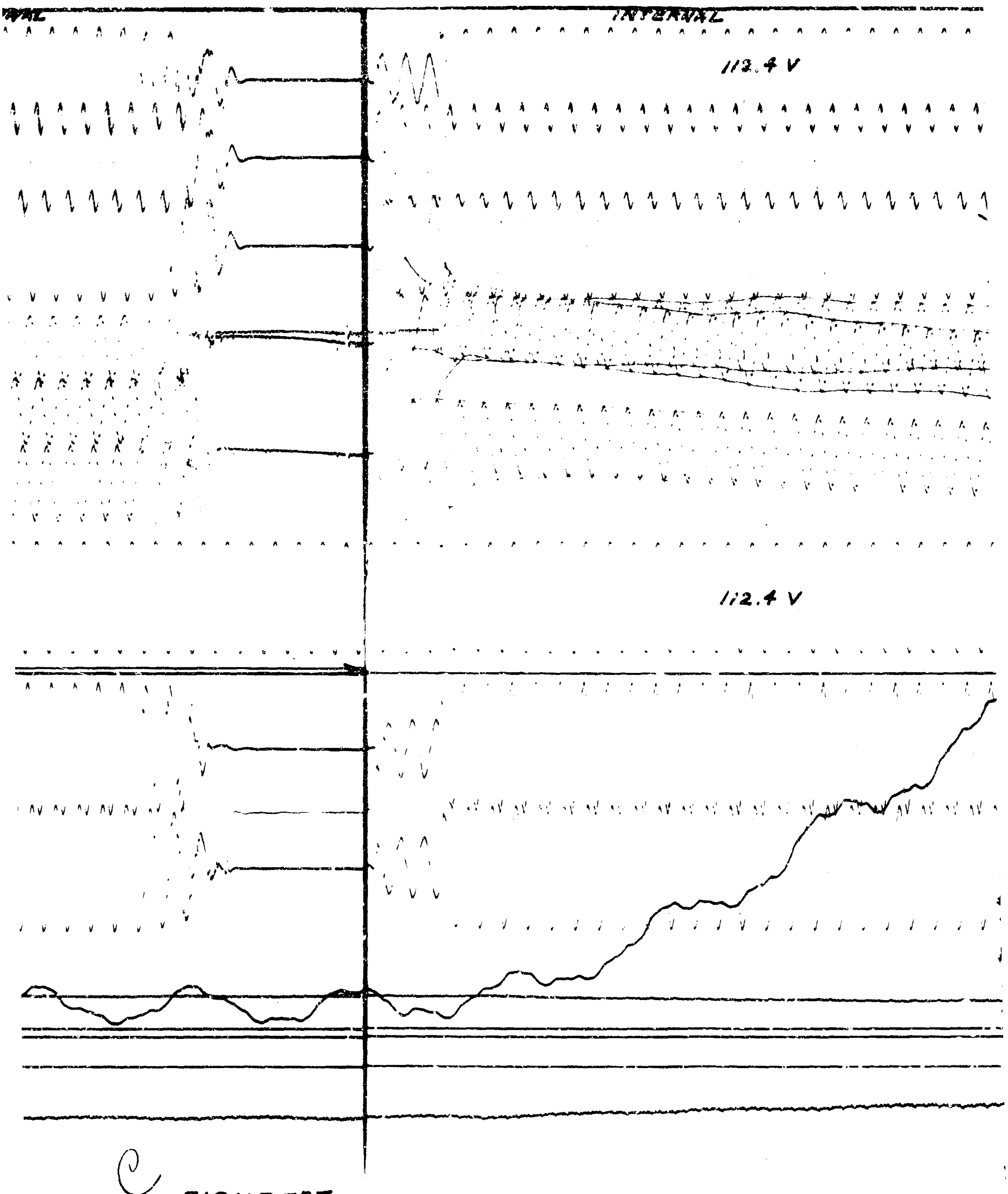


FIGURE 37

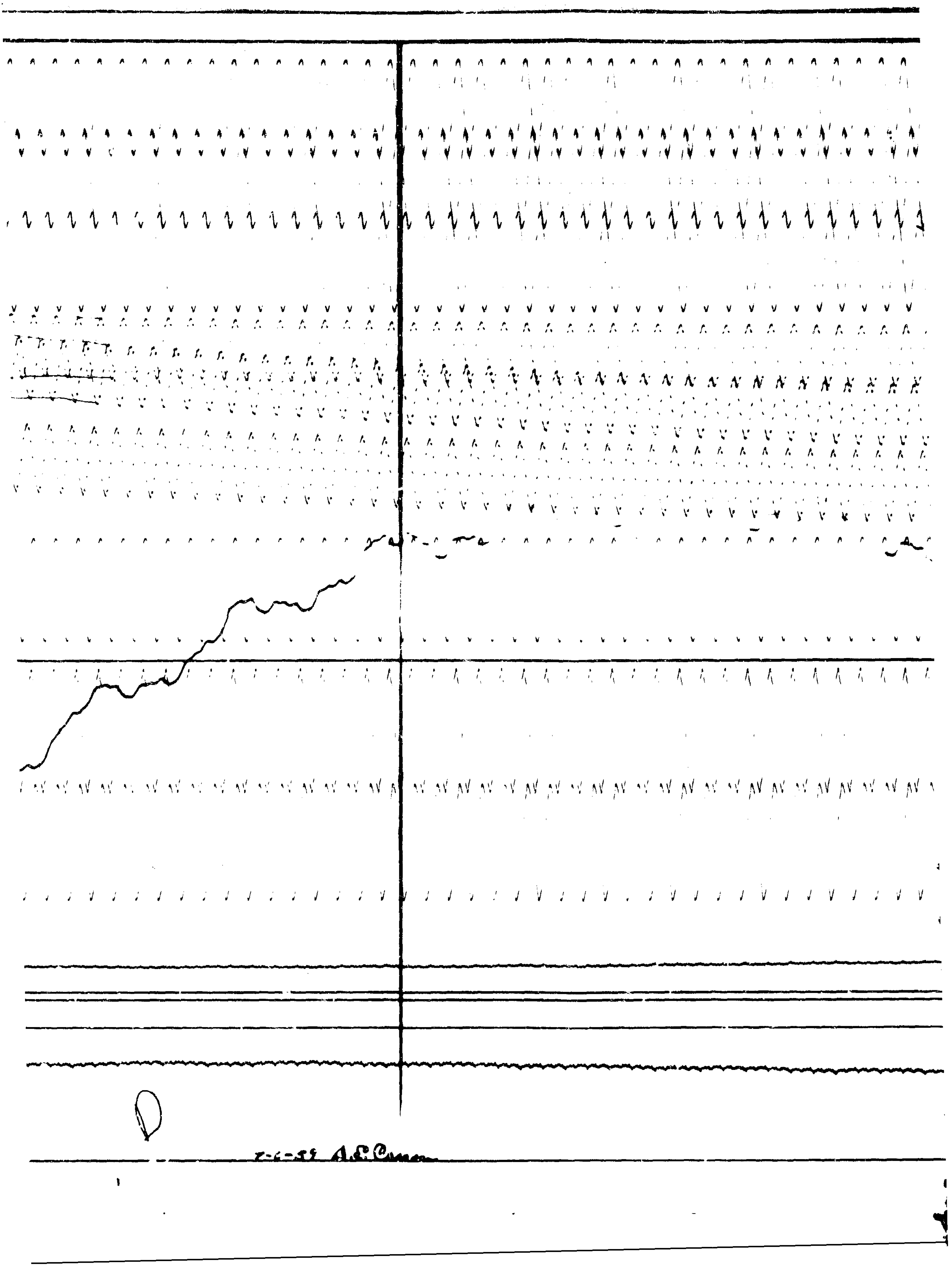

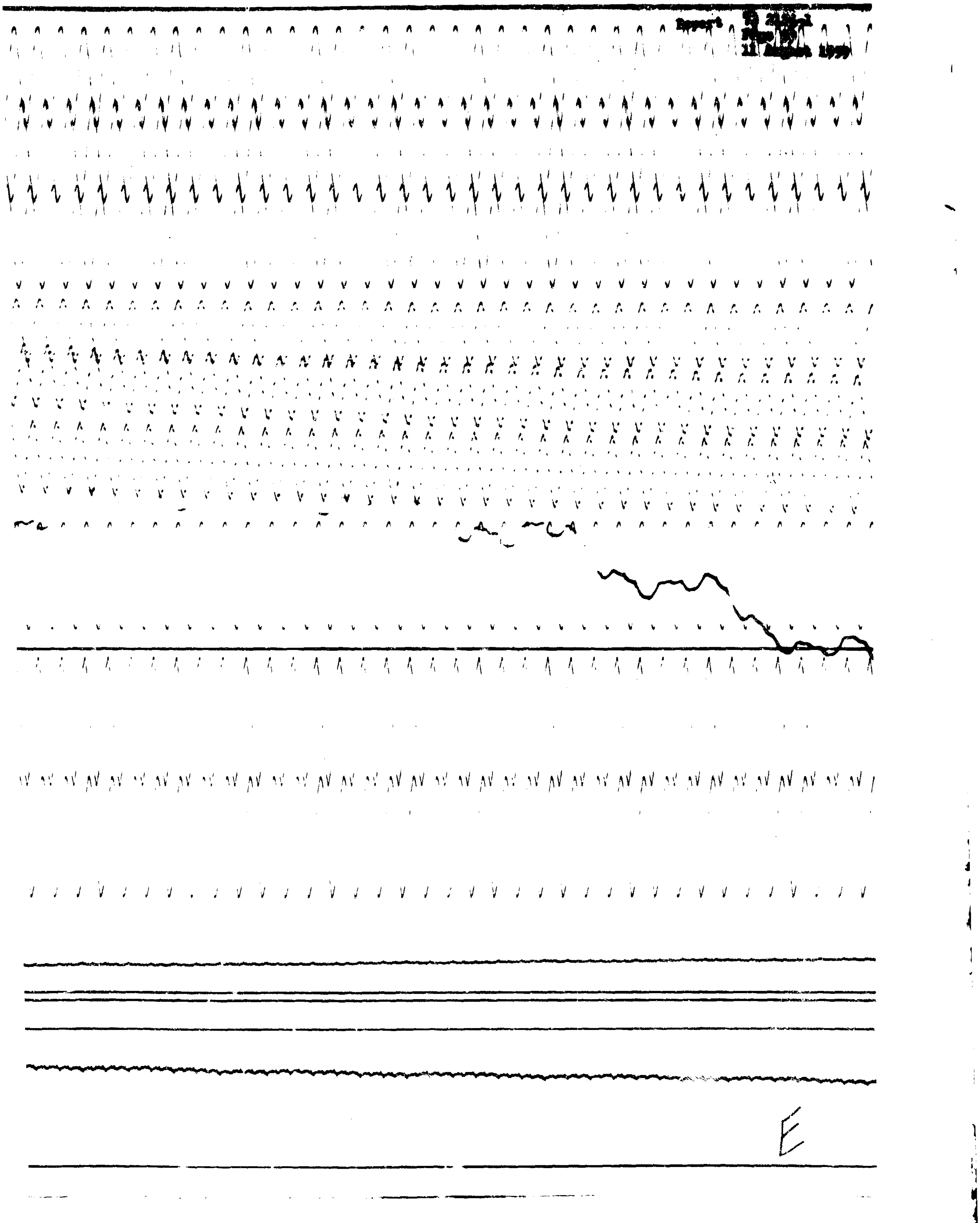
E

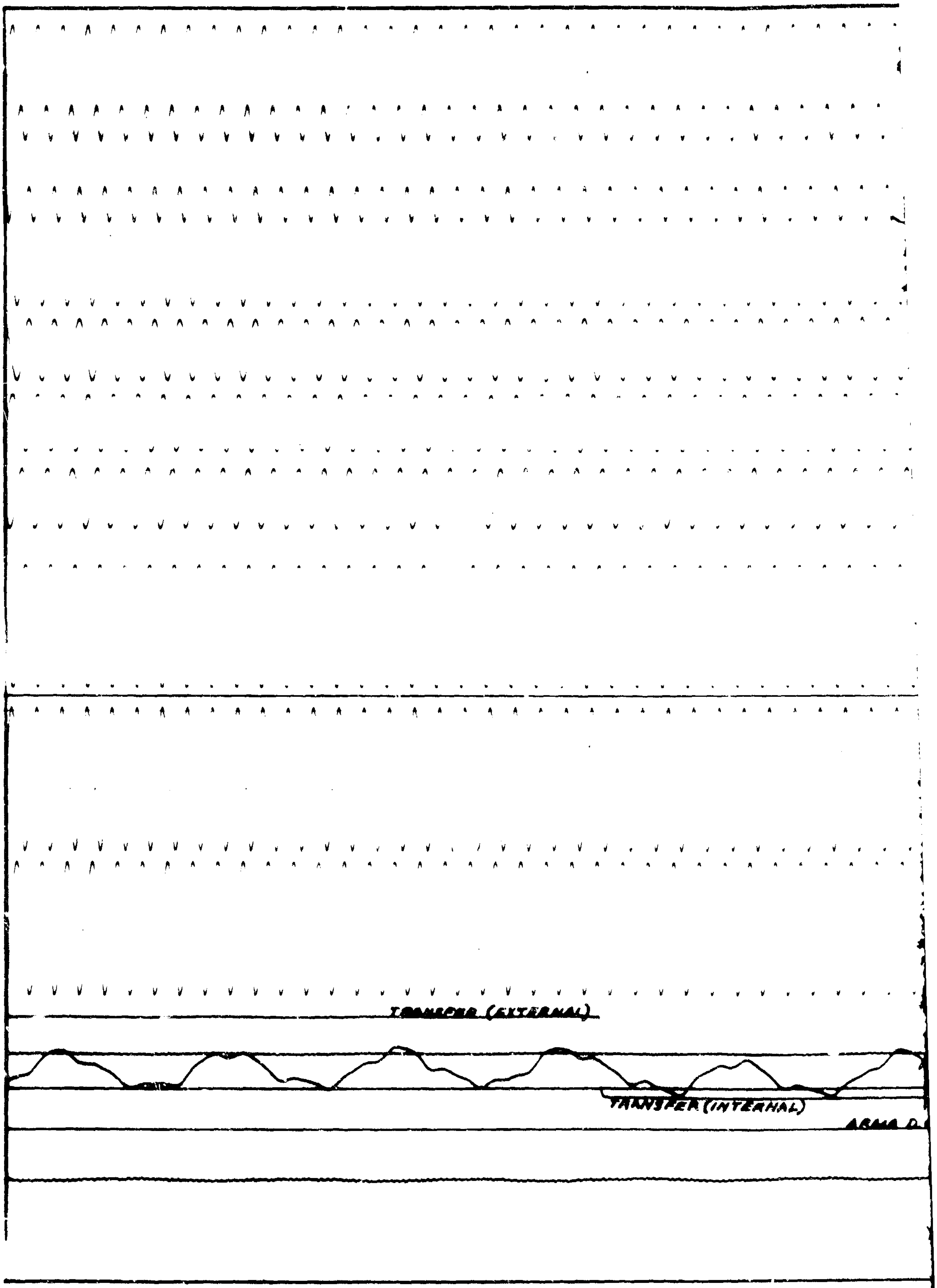


A

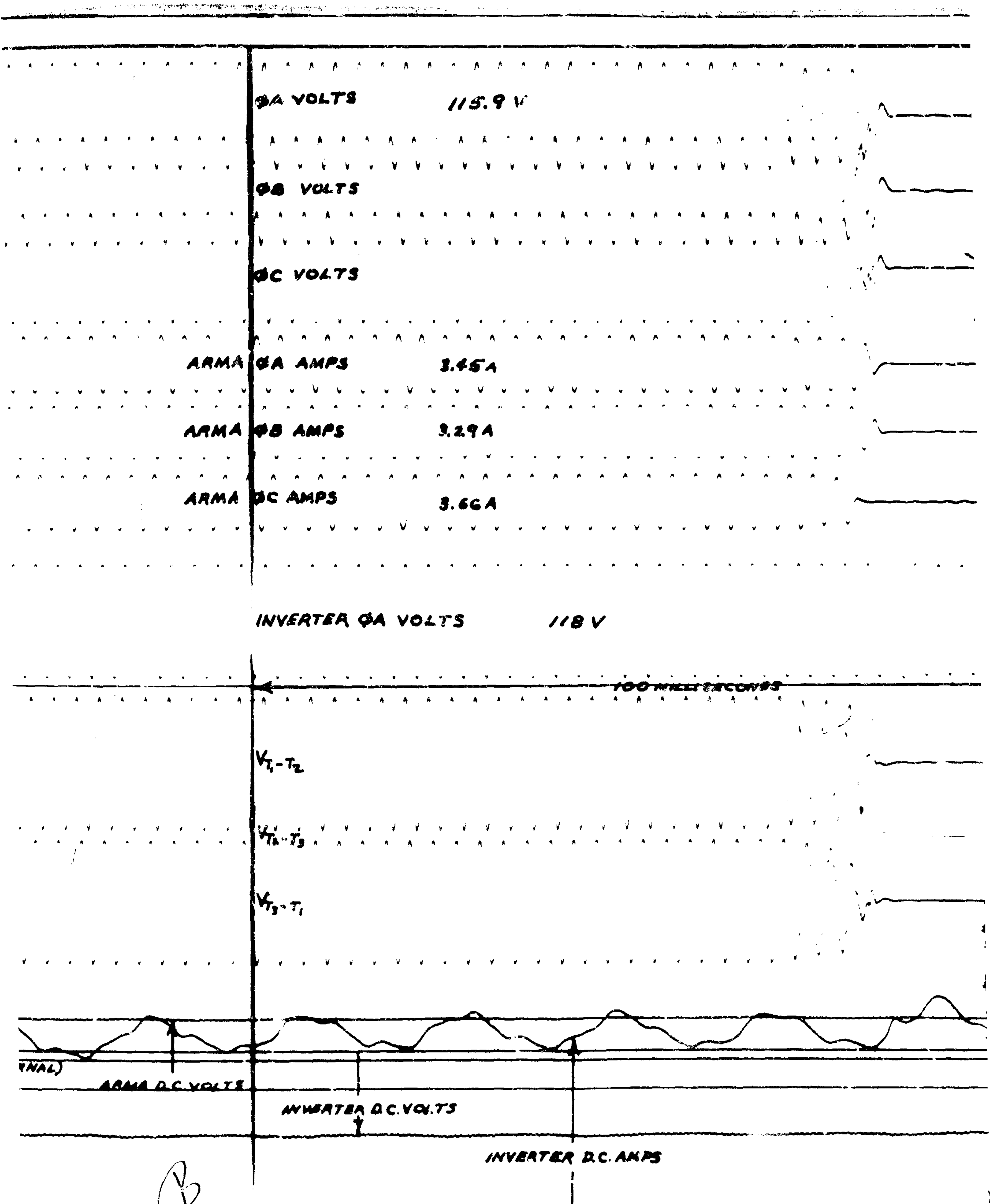

ØA VOLTS 115.9 V
ØB VOLTS
ØC VOLTS
ARMA ØA AMPS 3.45A
ARMA ØB AMPS 3.29A
ARMA ØC AMPS 3.66A
INVERTER ØA VOLTS 118 V
$V_{T_1-T_2}$
$V_{T_2-T_3}$
$V_{T_3-T_1}$
ARMA D.C. VOLTS
INVERTER D.C. VOLTS
INVERTER D.C. AMPS


FIGURE 38

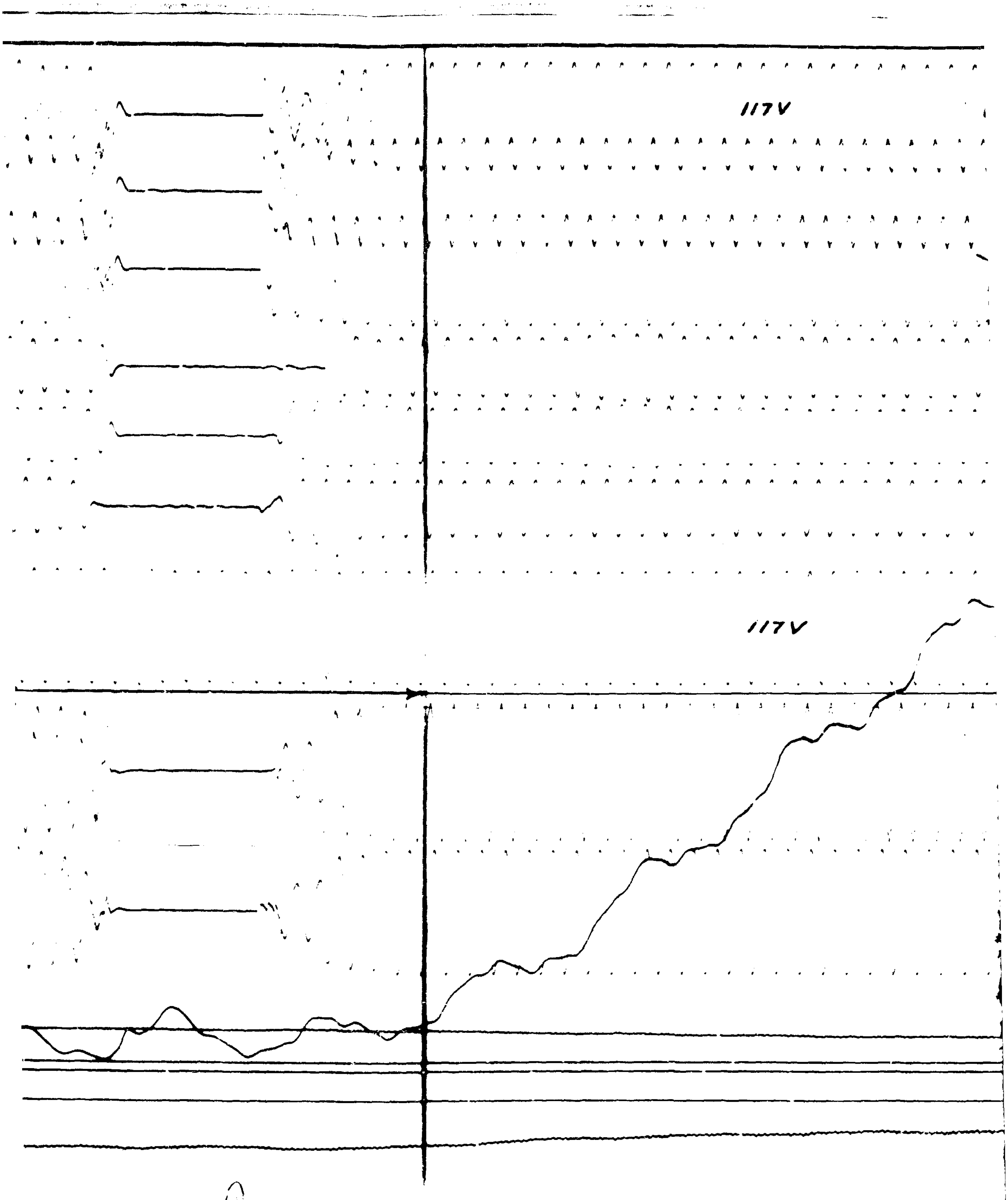


FIGURE 58

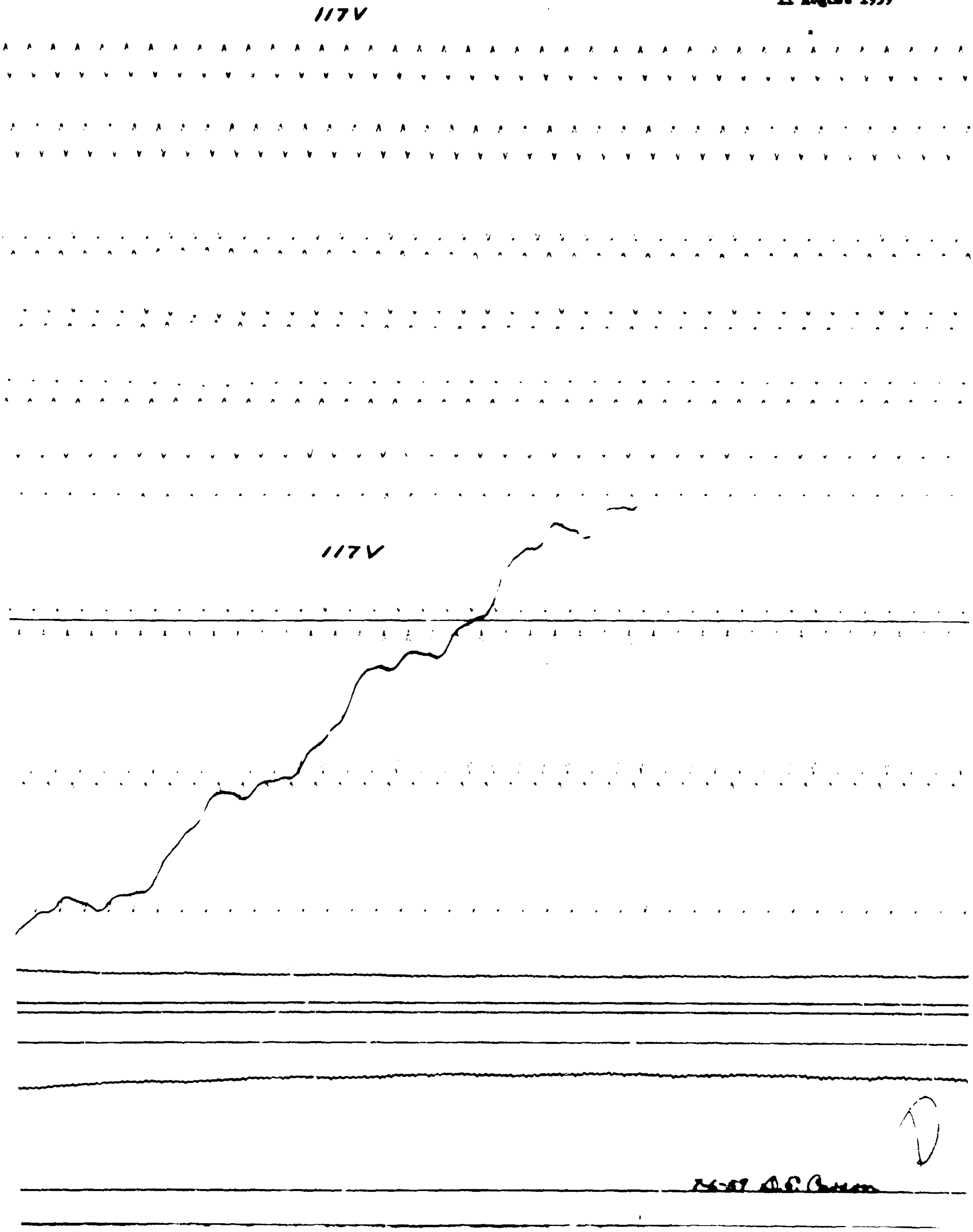
117V
117V

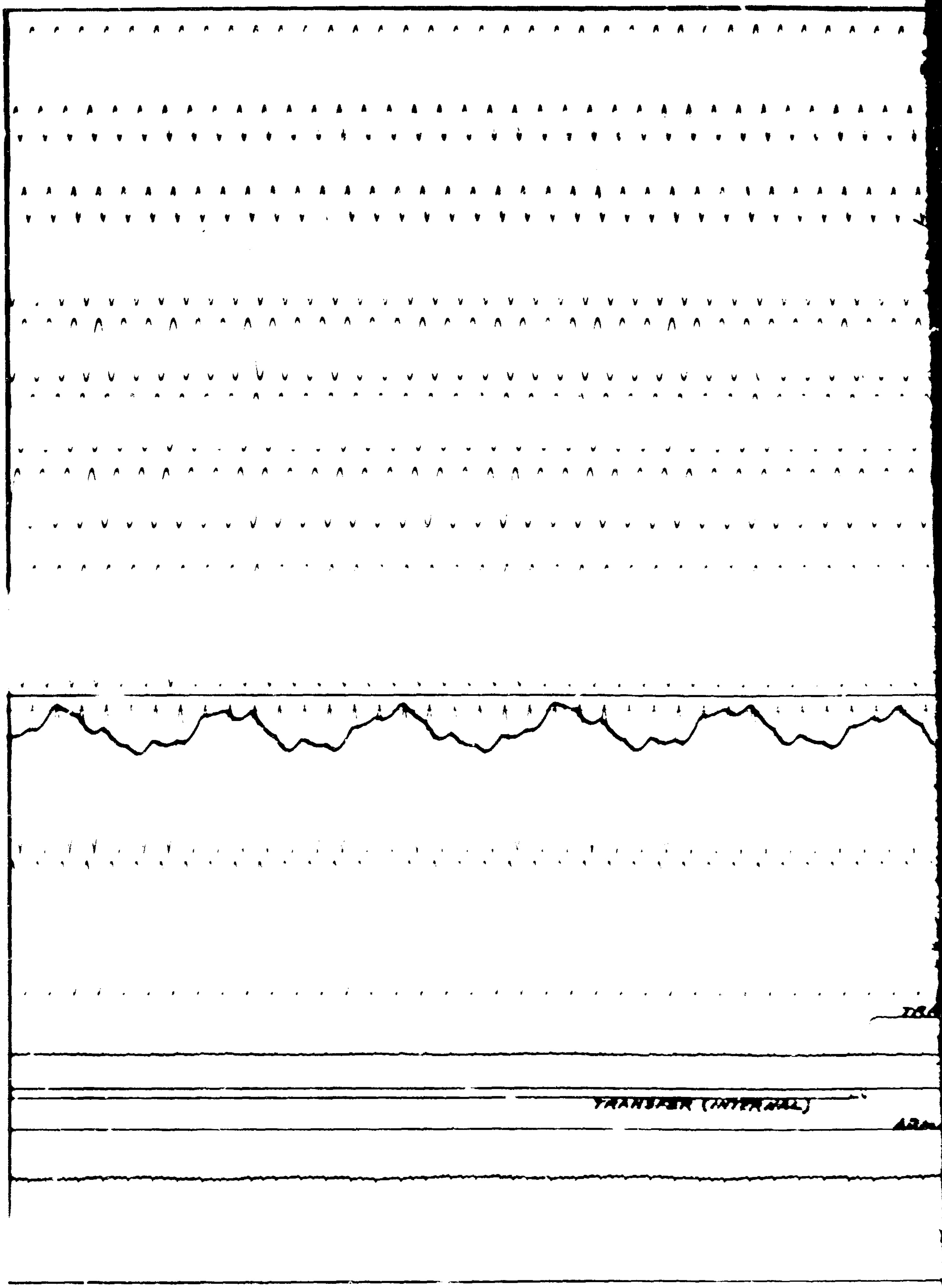
TRANSFER (INTERNAL)

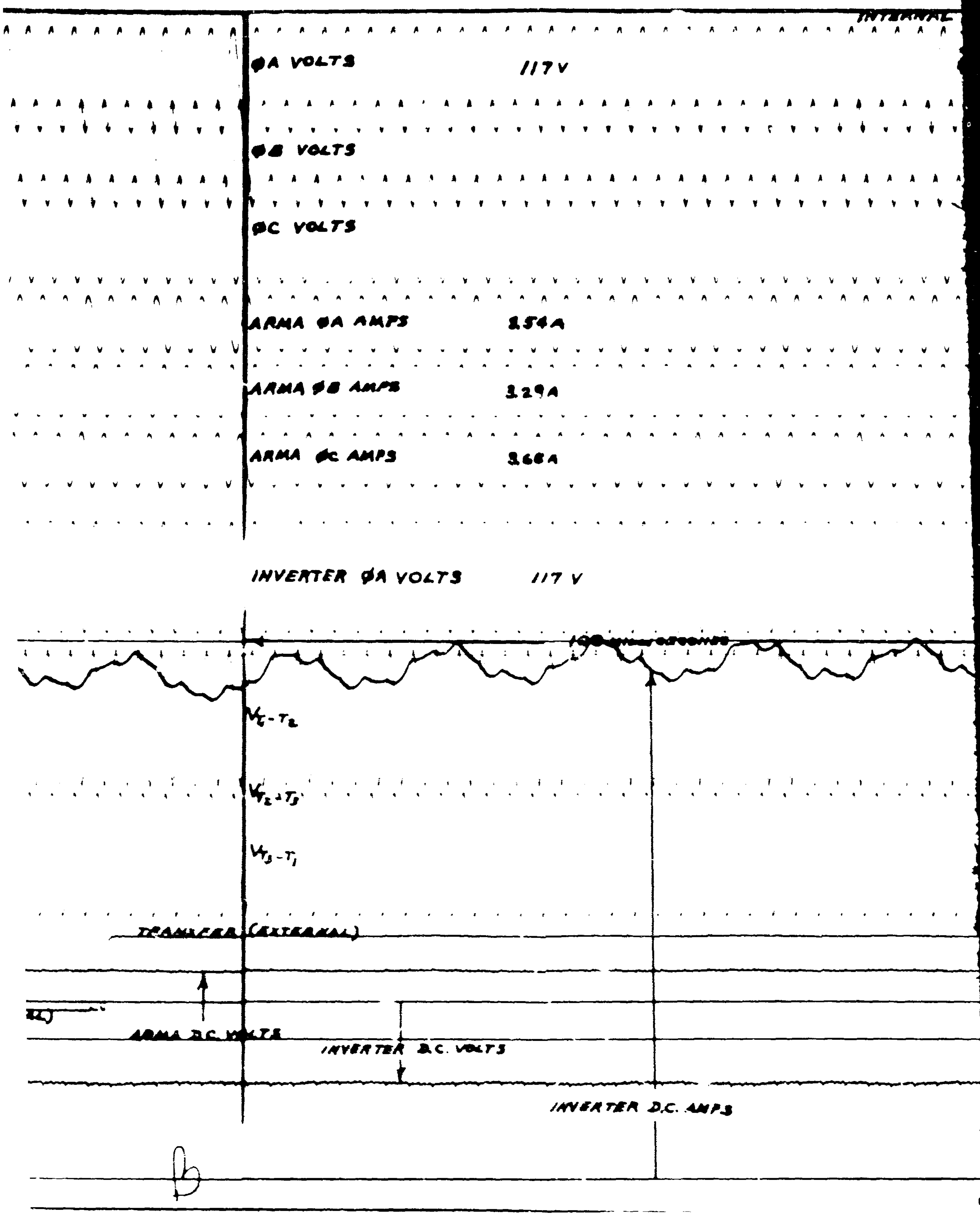

INTERNAL
ØA VOLTS
117V
ØB VOLTS
ØC VOLTS
ARMA ØA AMPS
ARMA ØB AMPS
ARMA ØC AMPS
INVERTER ØA VOLTS
117 V
$V_{T_1-T_2}$
$V_{T_2-T_3}$
$V_{T_3-T_1}$
TRANSFER (EXTERNAL)
ARMA DC VOLTS
INVERTER D.C. VOLTS
INVERTER D.C. AMPS
b

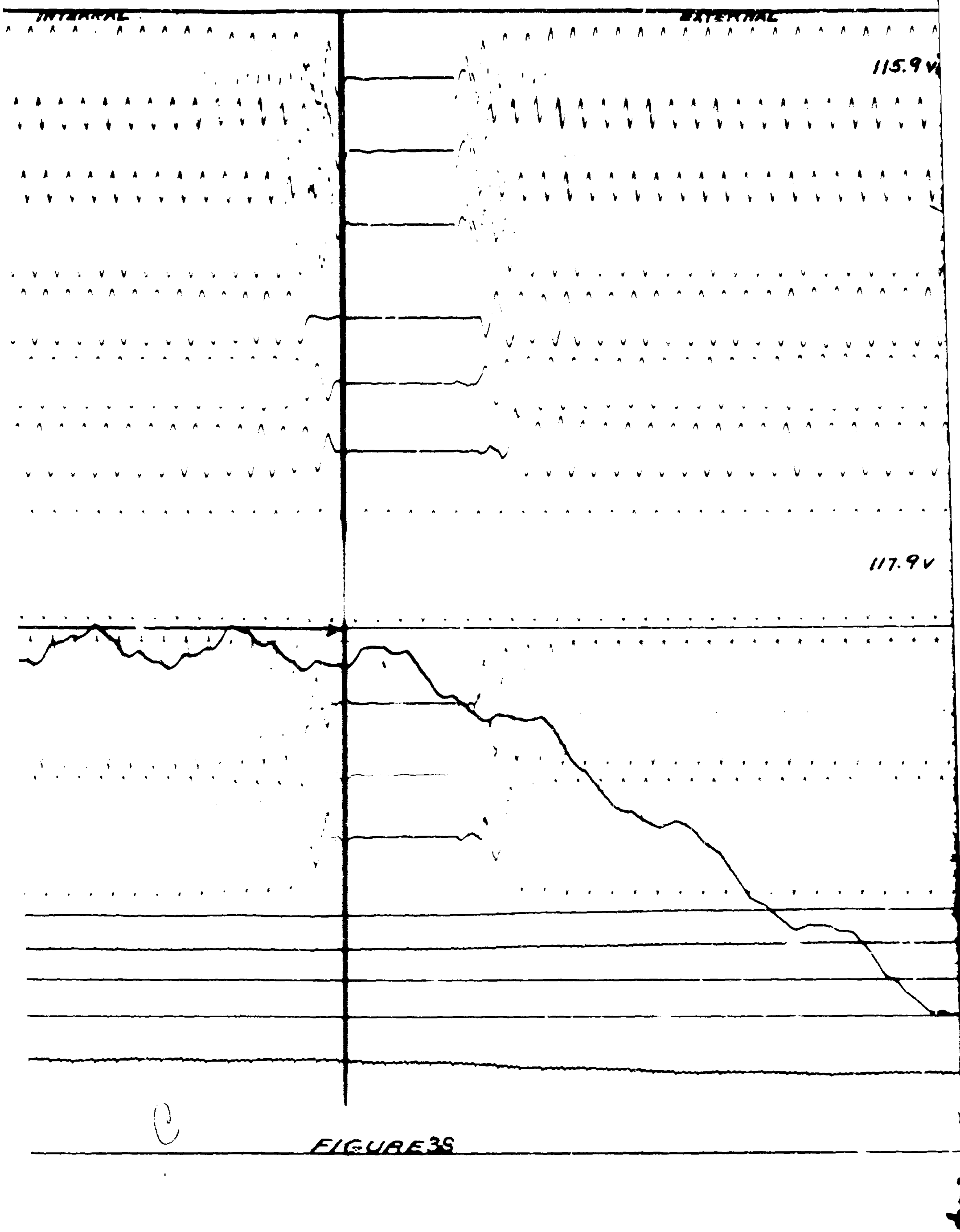


FIGURE 39

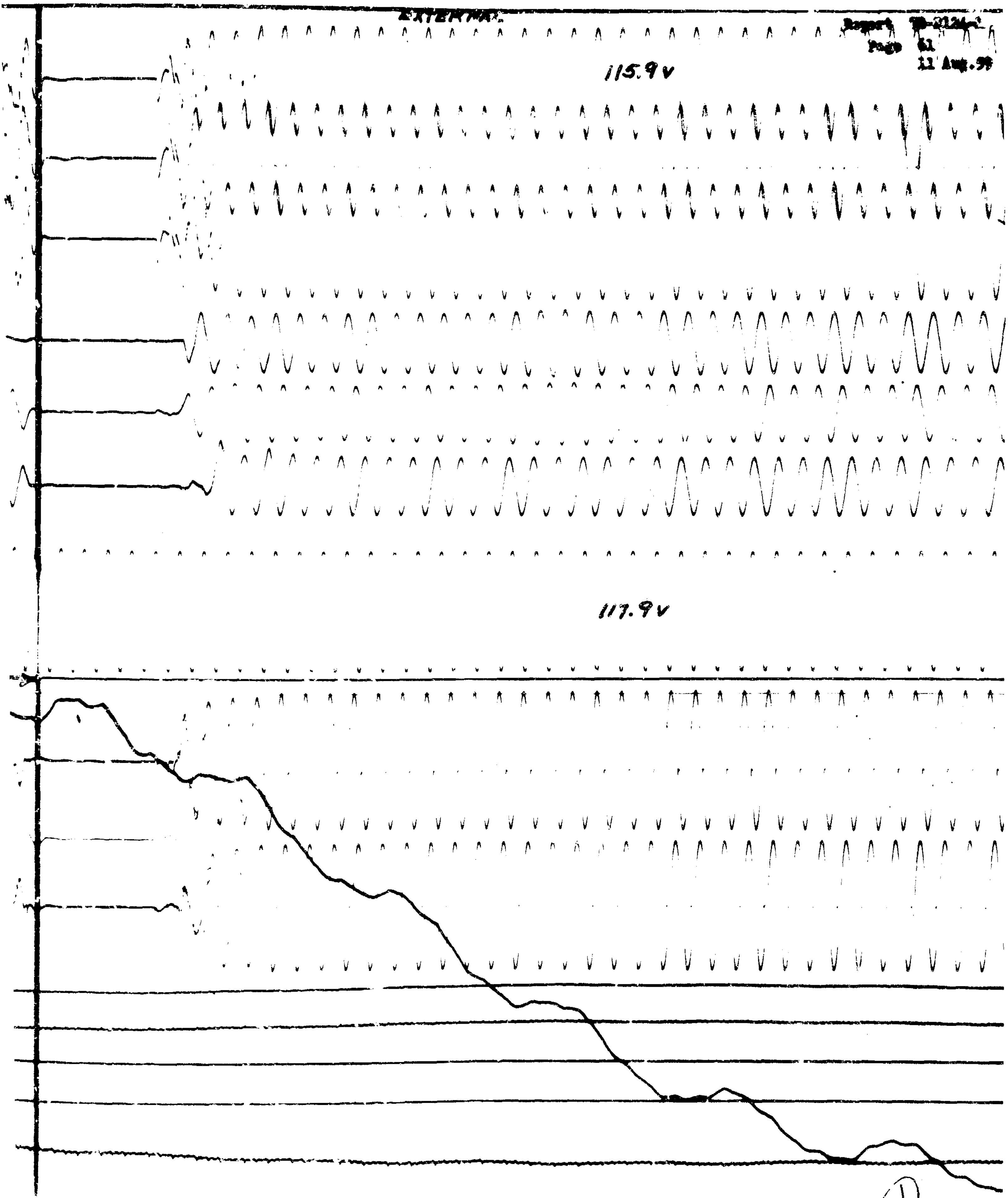


FIGURE 39

2-6-59 [illegible]

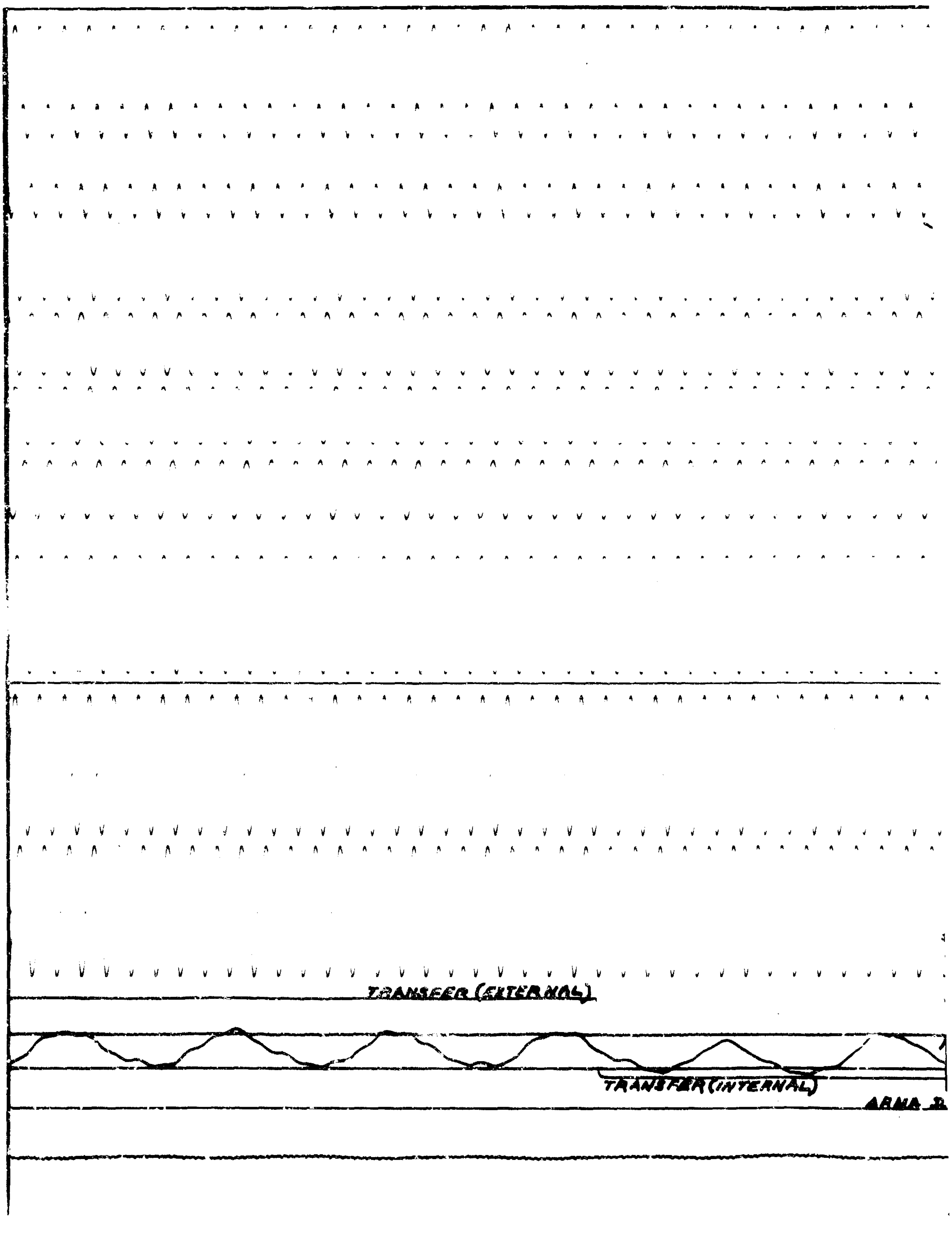

TRANSFER (EXTERNAL)
TRANSFER (INTERNAL)

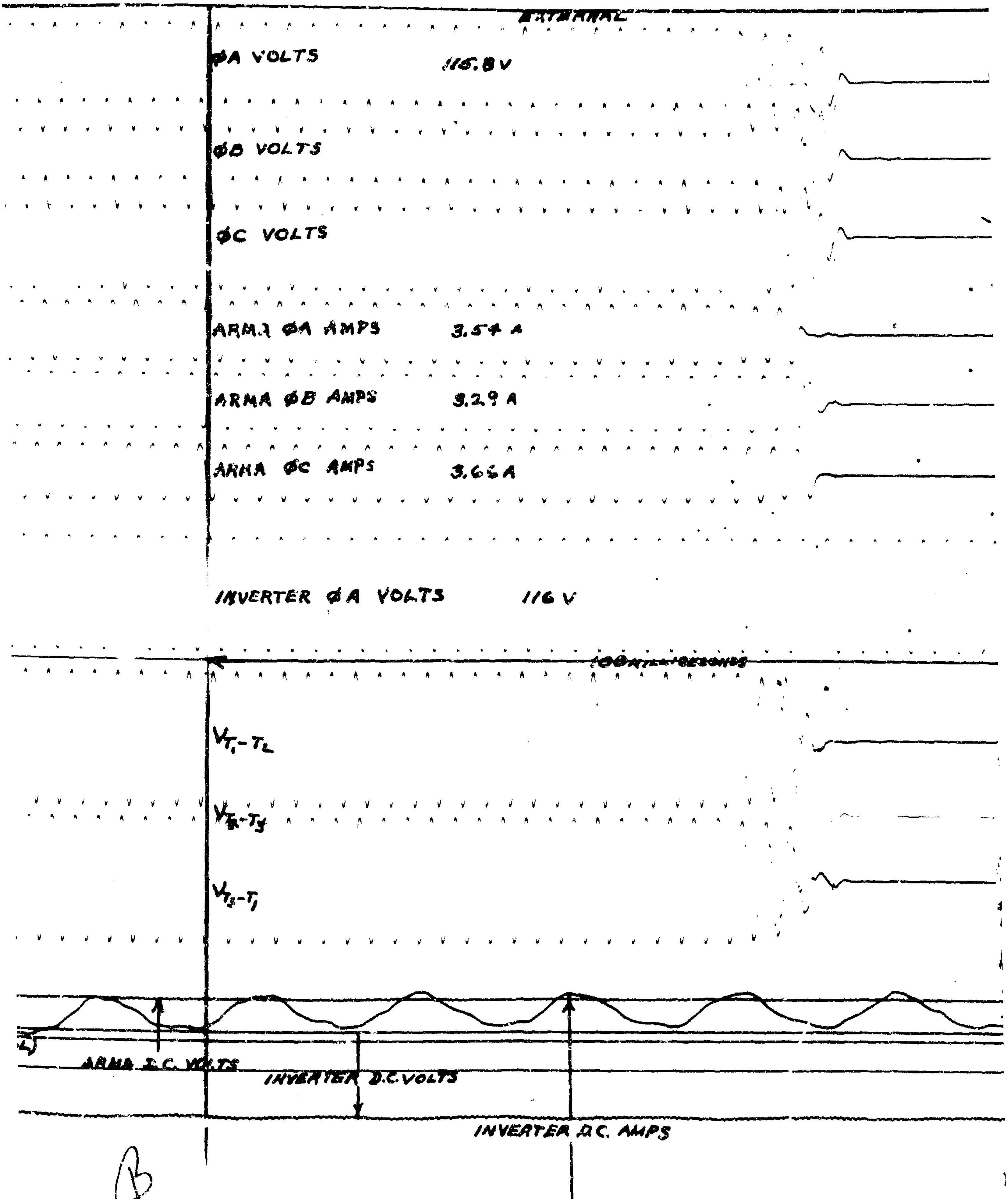
EXTERNAL
ØA VOLTS 115.8 V
ØB VOLTS
ØC VOLTS
ARMA ØA AMPS 3.54 A
ARMA ØB AMPS 3.29 A
ARMA ØC AMPS 3.66 A
INVERTER ØA VOLTS 116 V
100 MILLISECONDS
$V_{T_1-T_2}$
$V_{T_2-T_3}$
$V_{T_3-T_1}$
ARMA D.C. VOLTS
INVERTER D.C. VOLTS
INVERTER D.C. AMPS
B

FIGURE 40

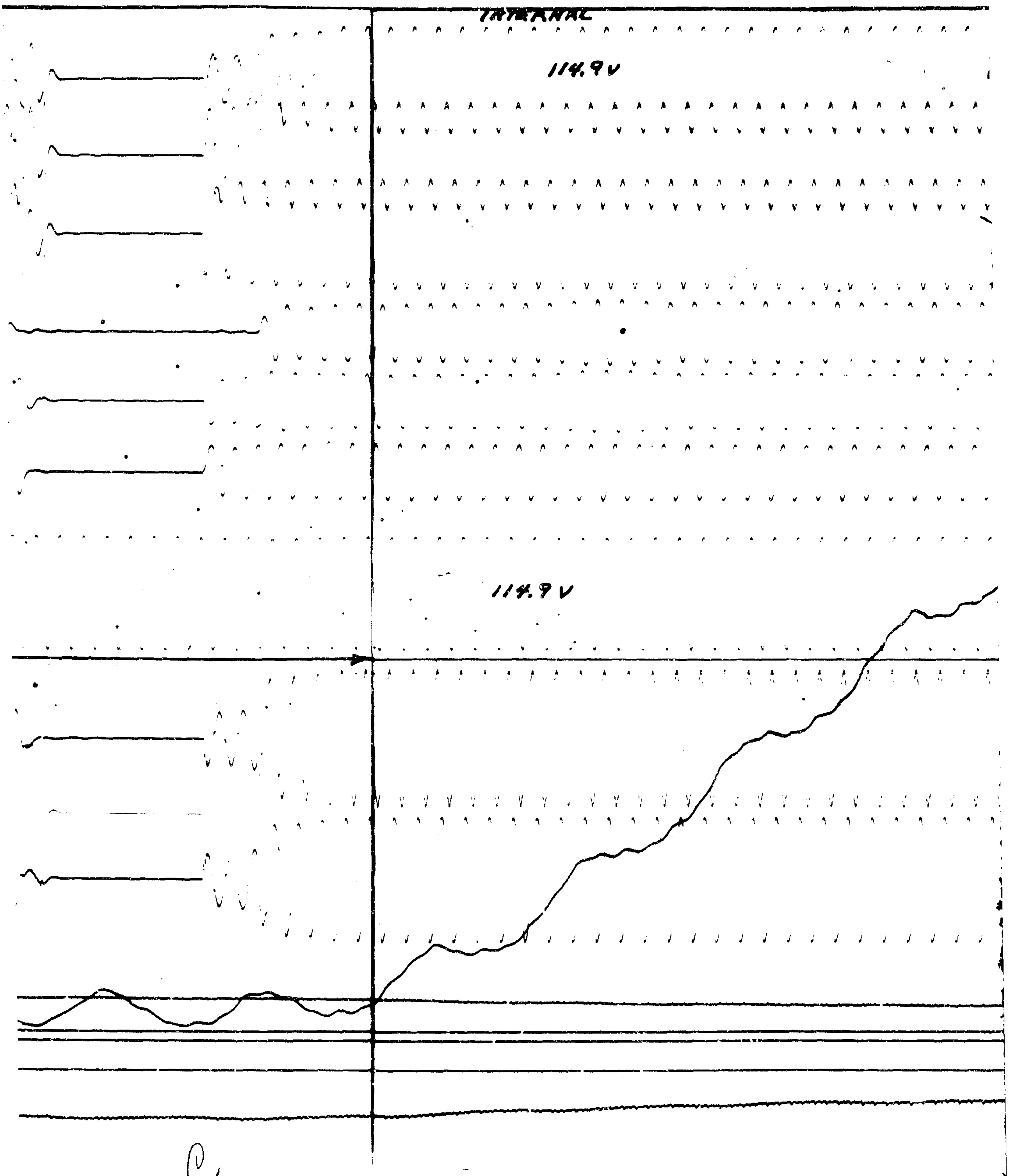


FIGURE 40

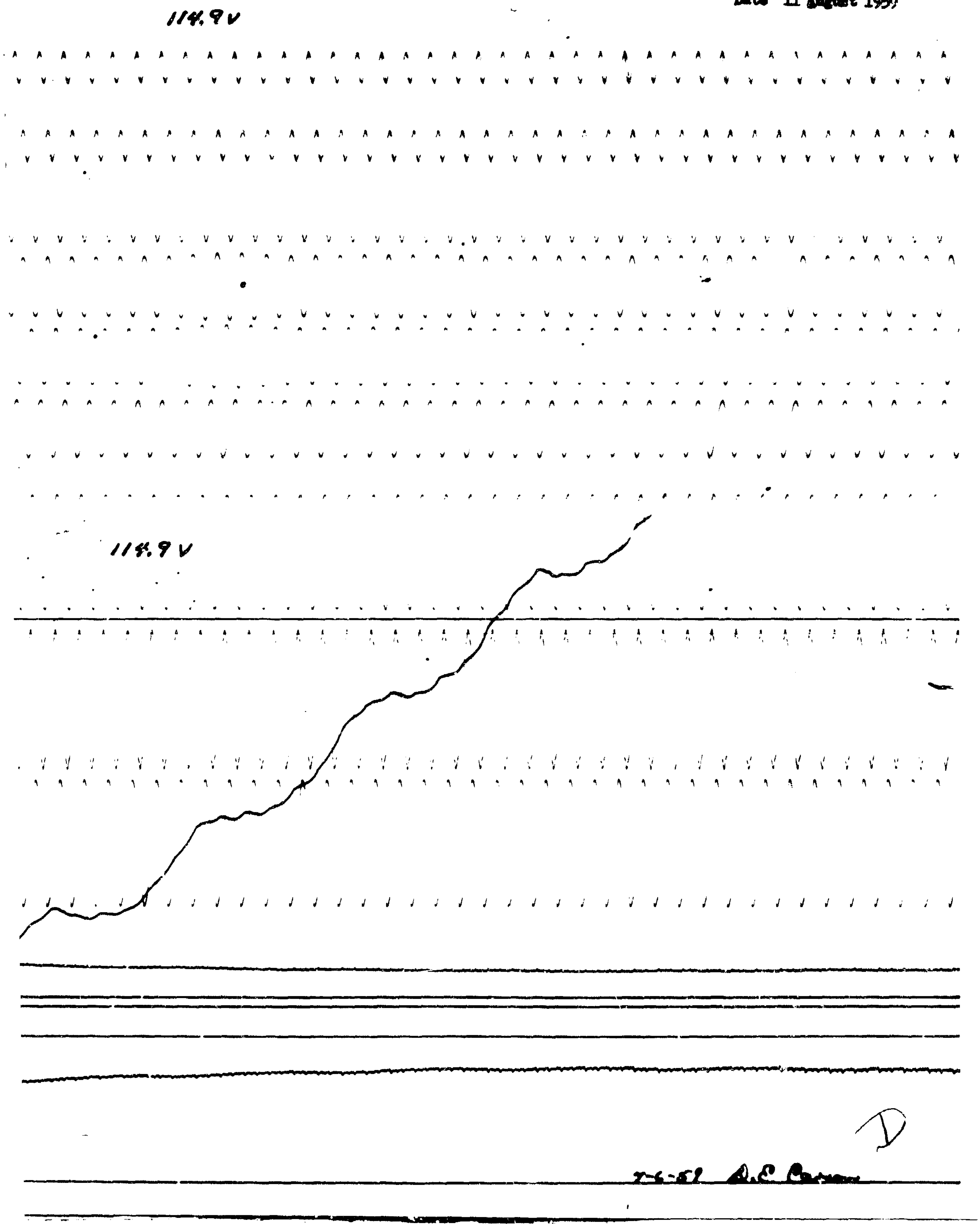
114.9V
114.9V
7-6-59 D.E. [illegible]
D

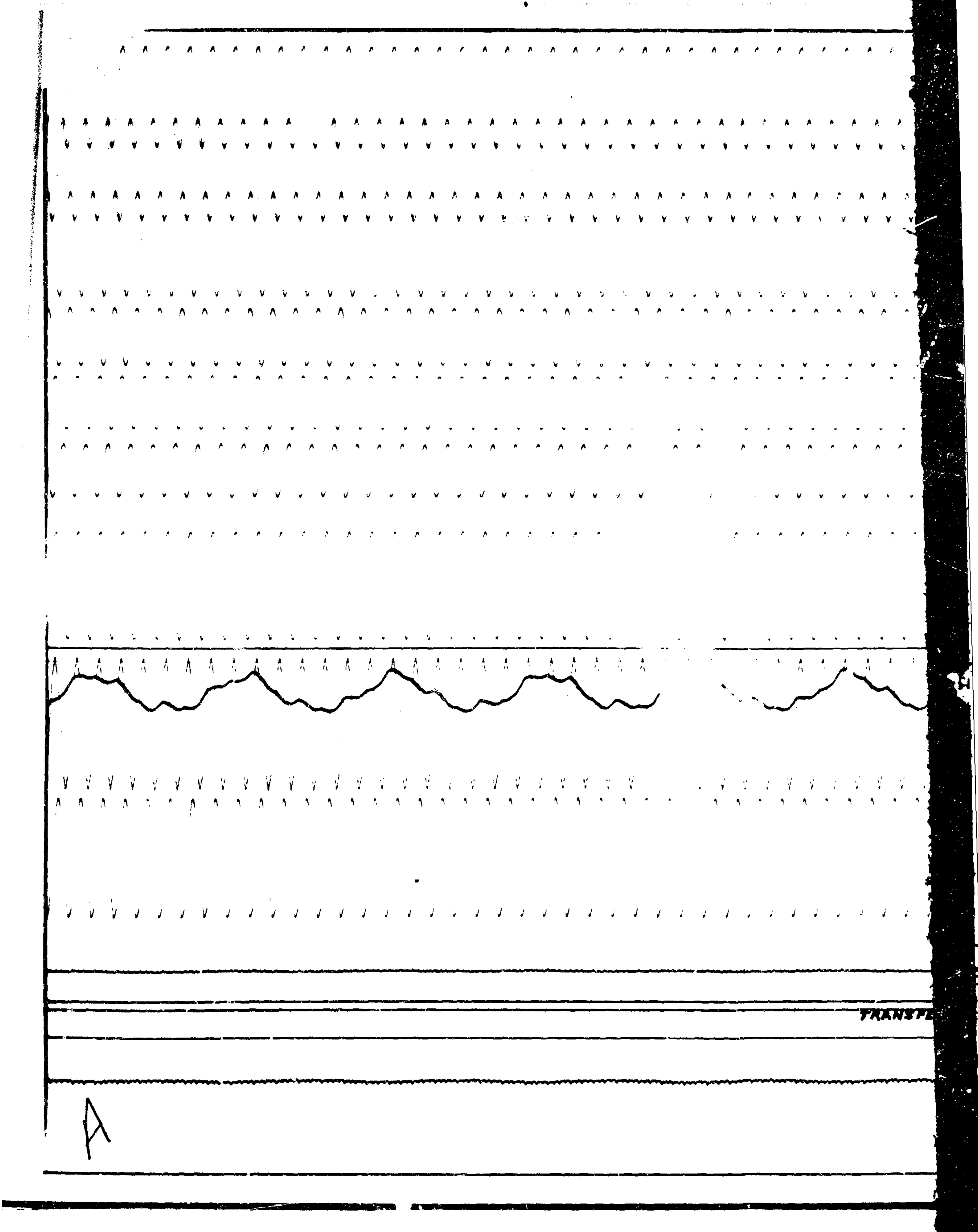
A

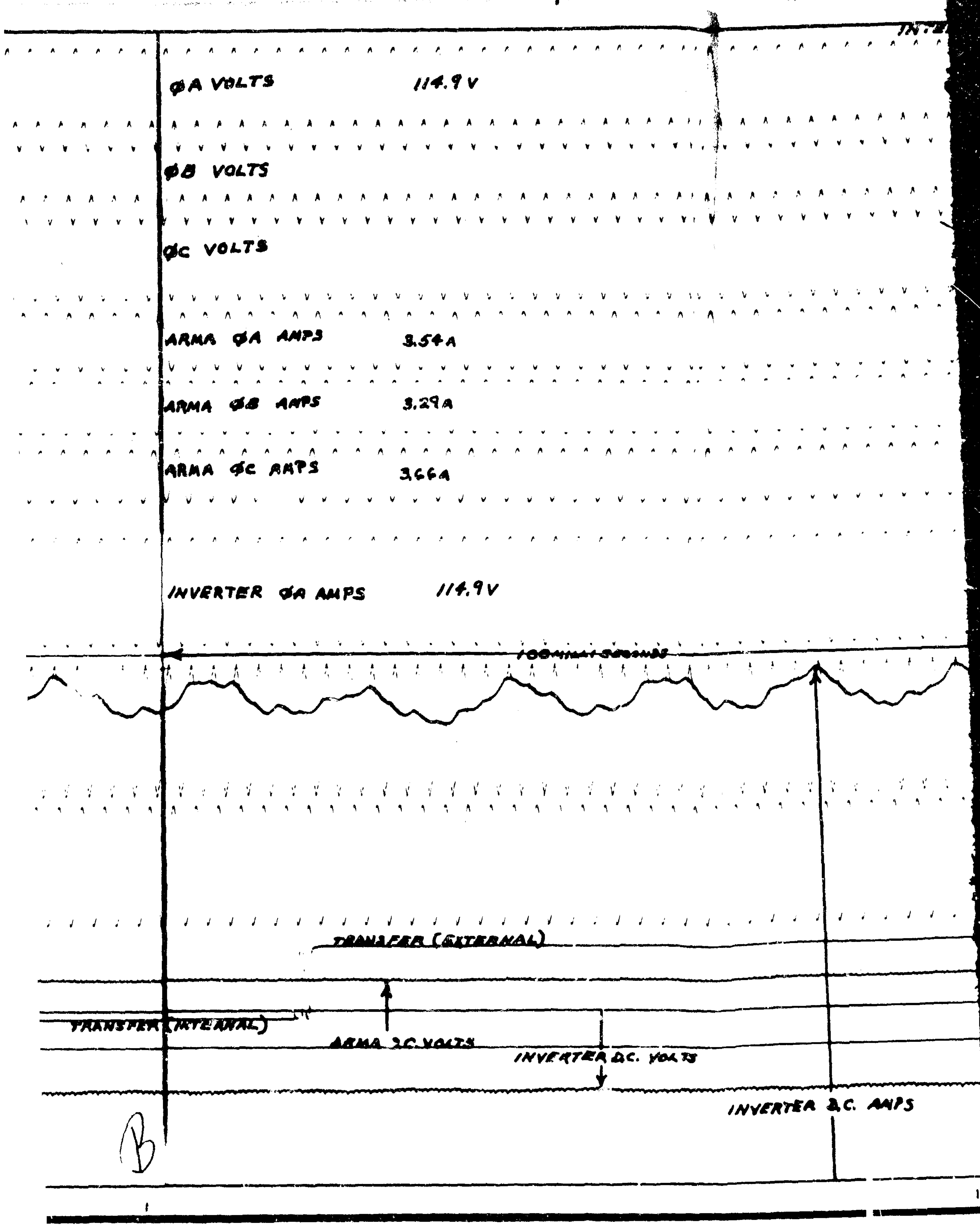

ØA VOLTS 114.9V
ØB VOLTS
ØC VOLTS
ARMA ØA AMPS 3.54A
ARMA ØB AMPS 3.29A
ARMA ØC AMPS 3.66A
INVERTER ØA AMPS 114.9V
TRANSFER (EXTERNAL)
TRANSFER (INTERNAL)
ARMA DC VOLTS
INVERTER D.C. VOLTS
INVERTER D.C. AMPS
B

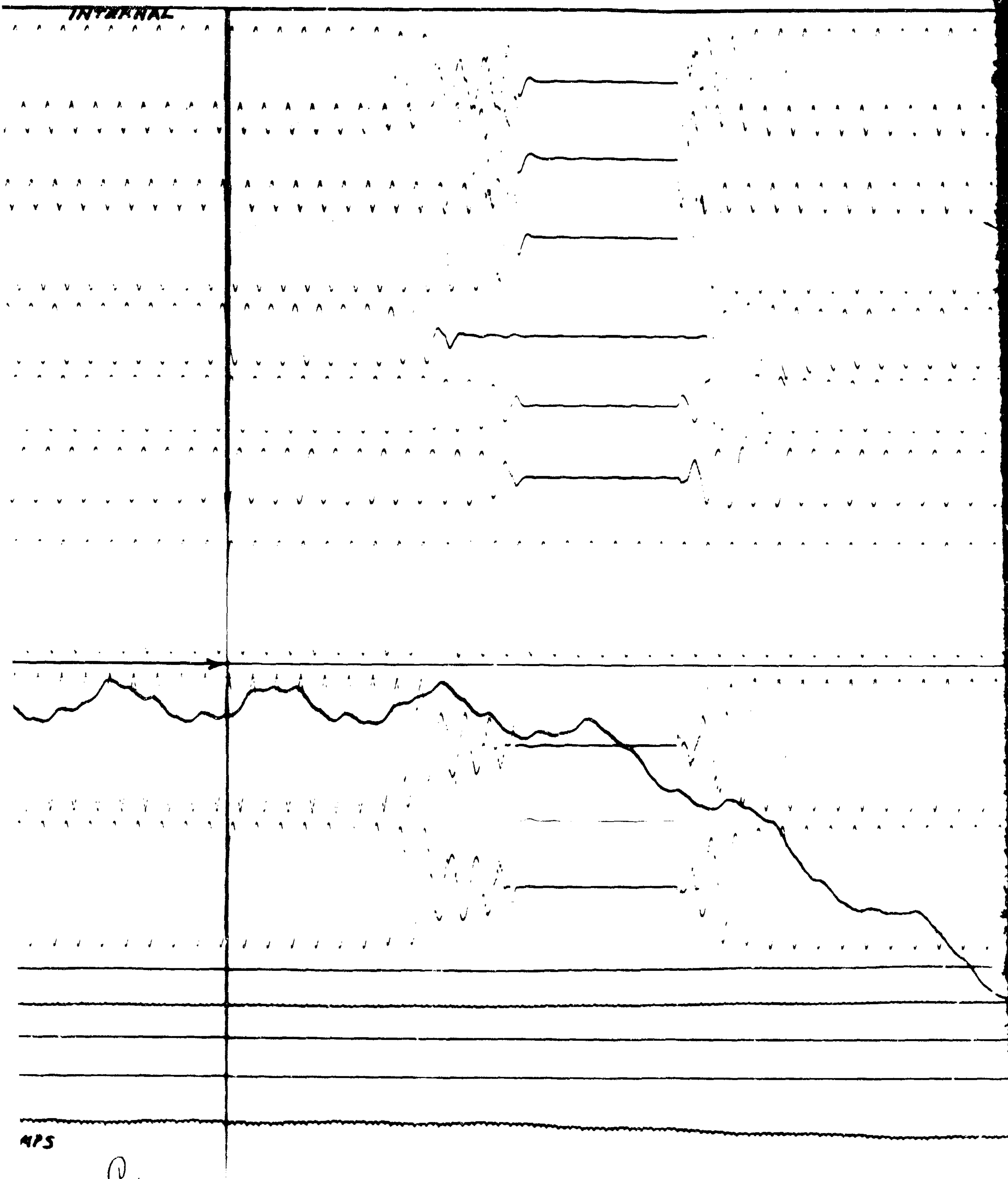


FIGURE 41

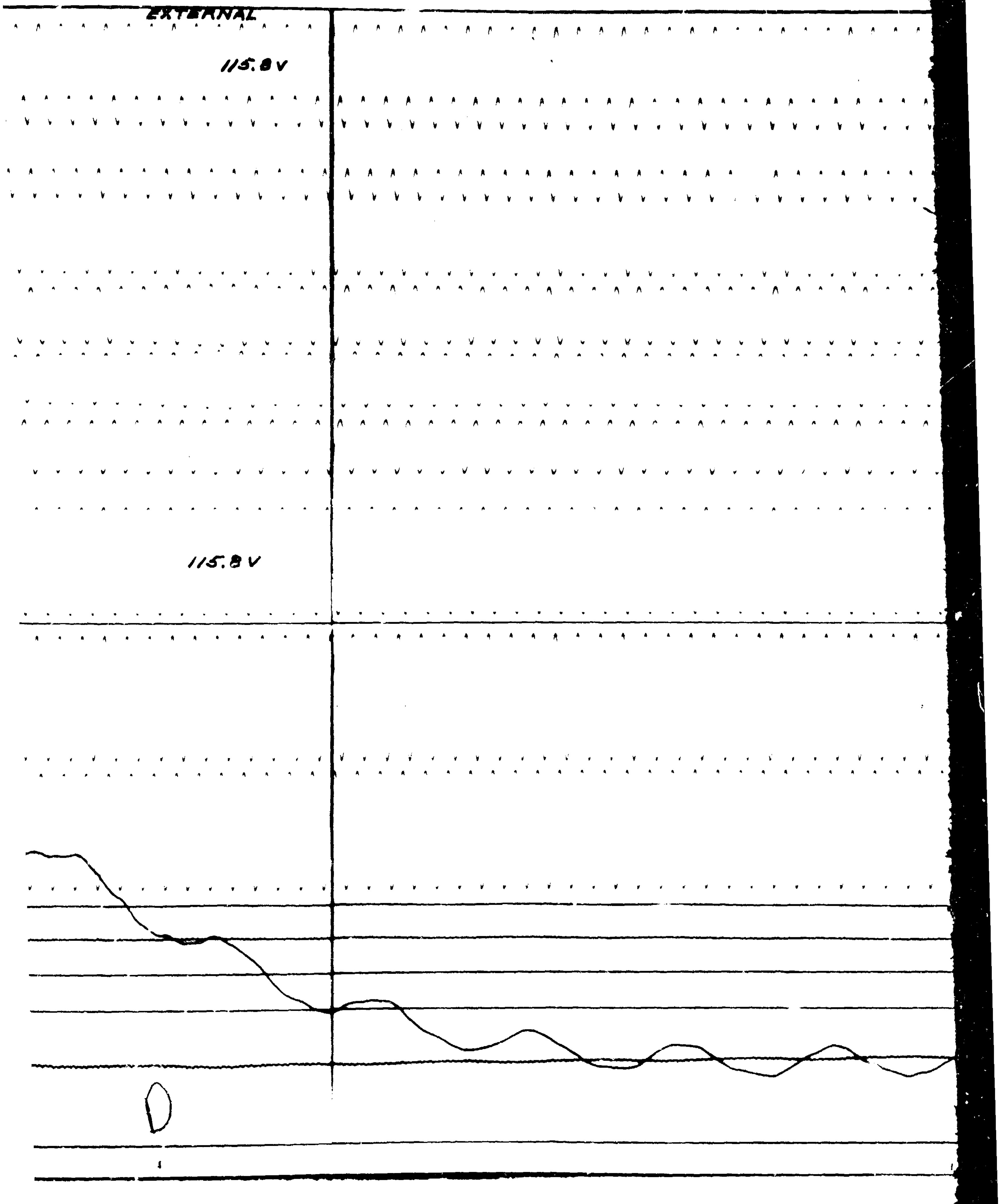
EXTERNAL
115.8V
115.8V
D

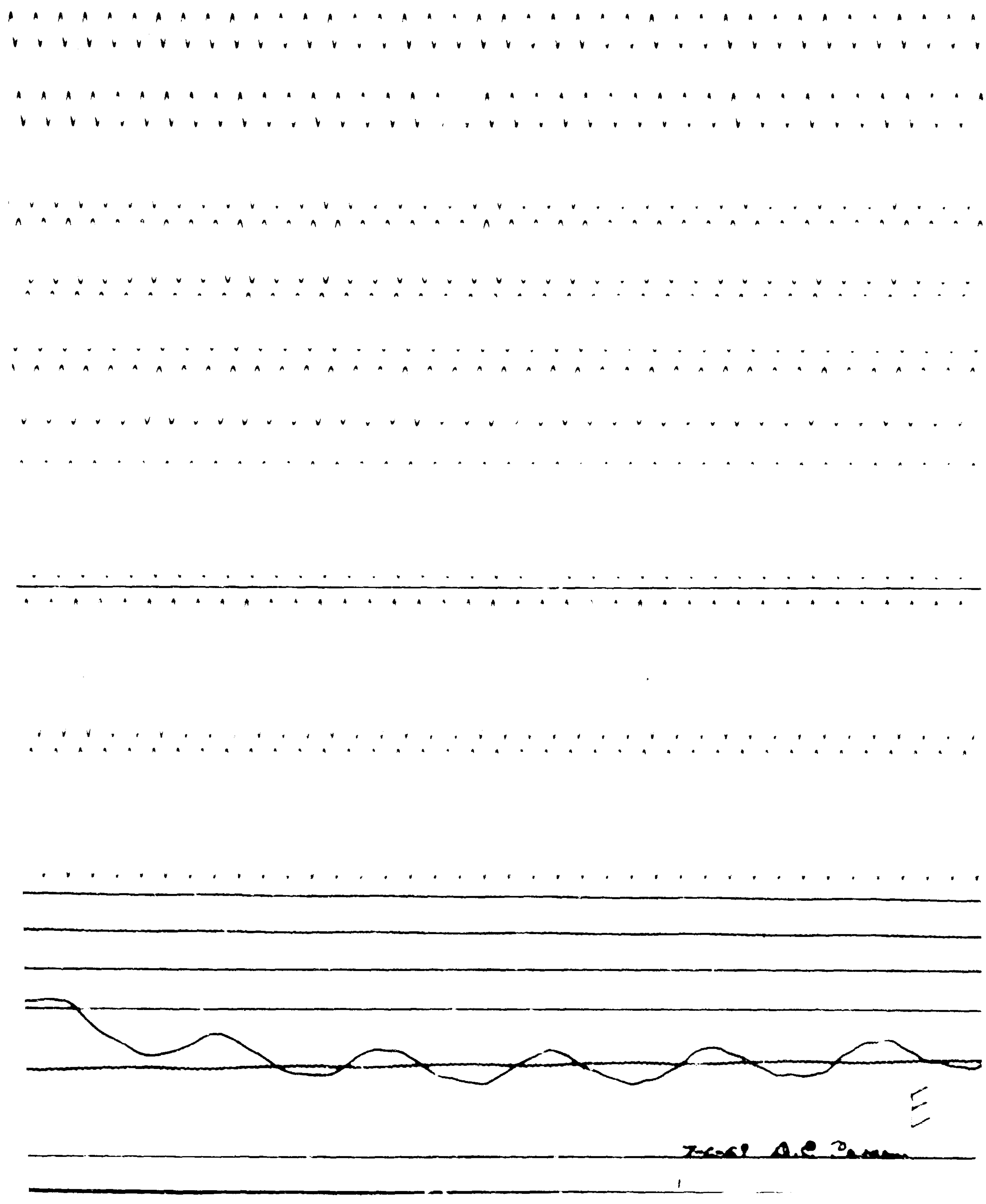

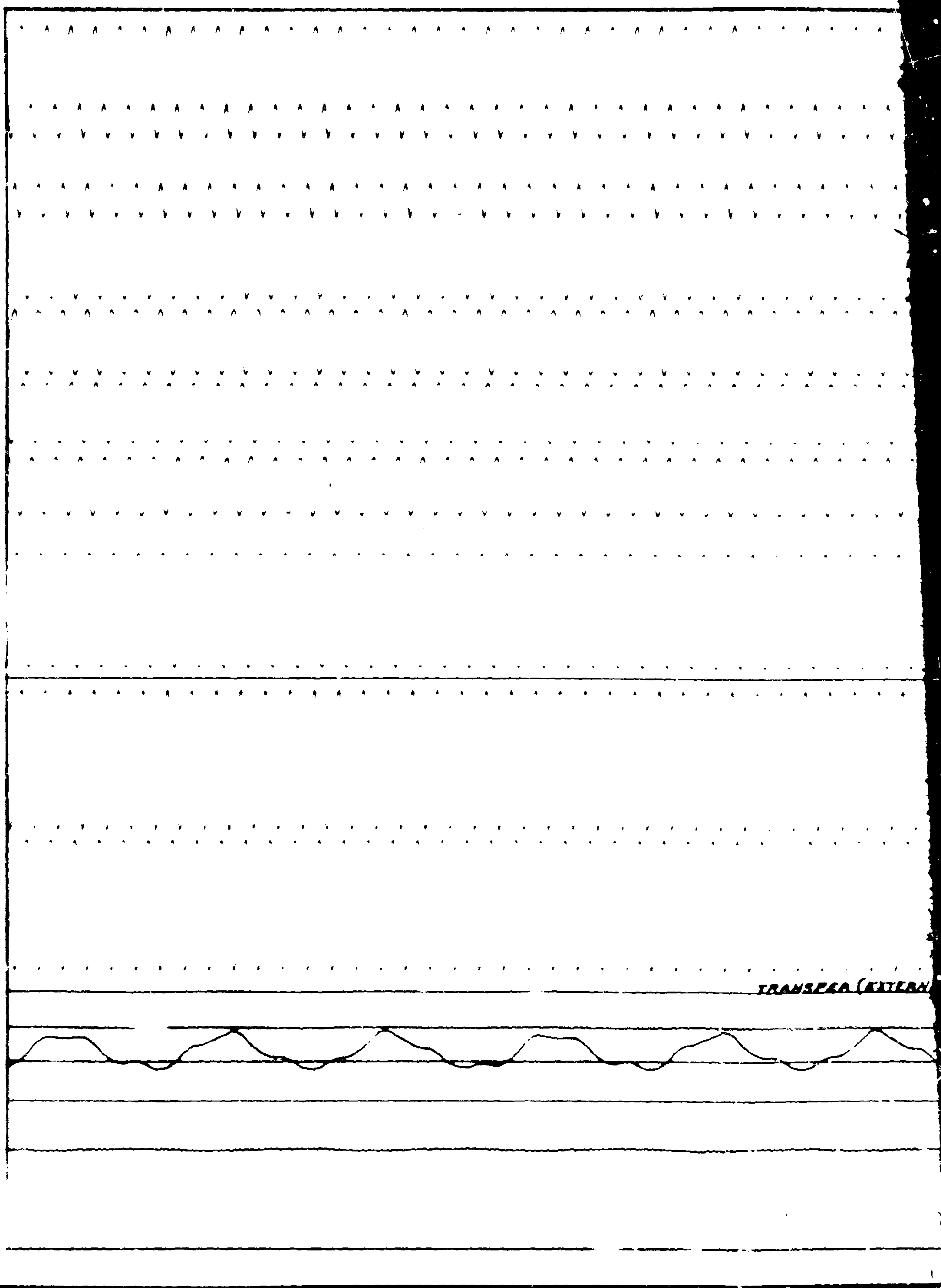
TRANSFER (EXTERN

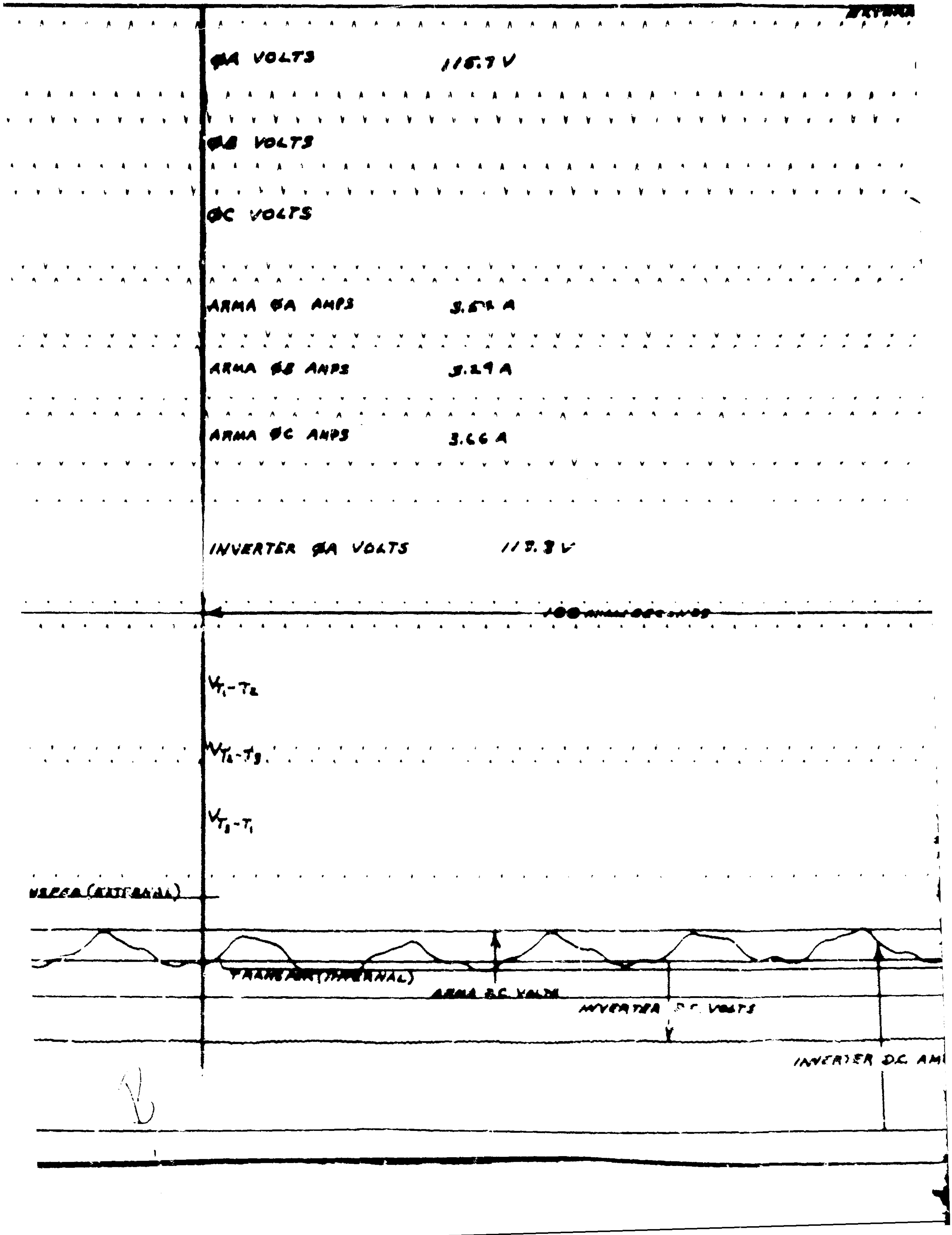

ØA VOLTS 115.7 V
ØB VOLTS
ØC VOLTS
ARMA ØA AMPS
ARMA ØB AMPS 3.29 A
ARMA ØC AMPS 3.66 A
INVERTER ØA VOLTS 118.3 V
$V_{T_1-T_2}$
$V_{T_2-T_3}$
$V_{T_3-T_1}$
ARMA D.C. VOLTS
INVERTER D.C. VOLTS

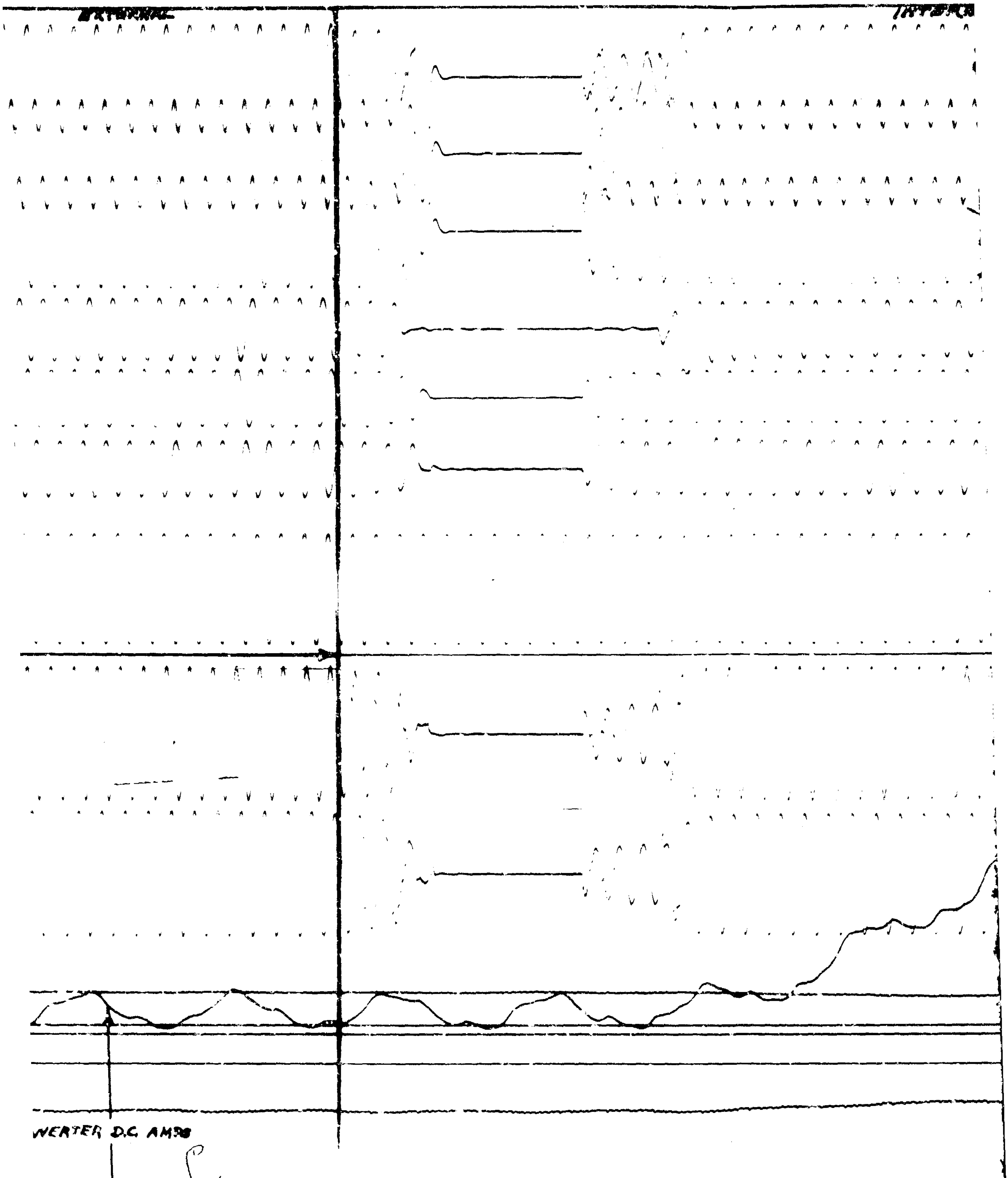


FIGURE 42

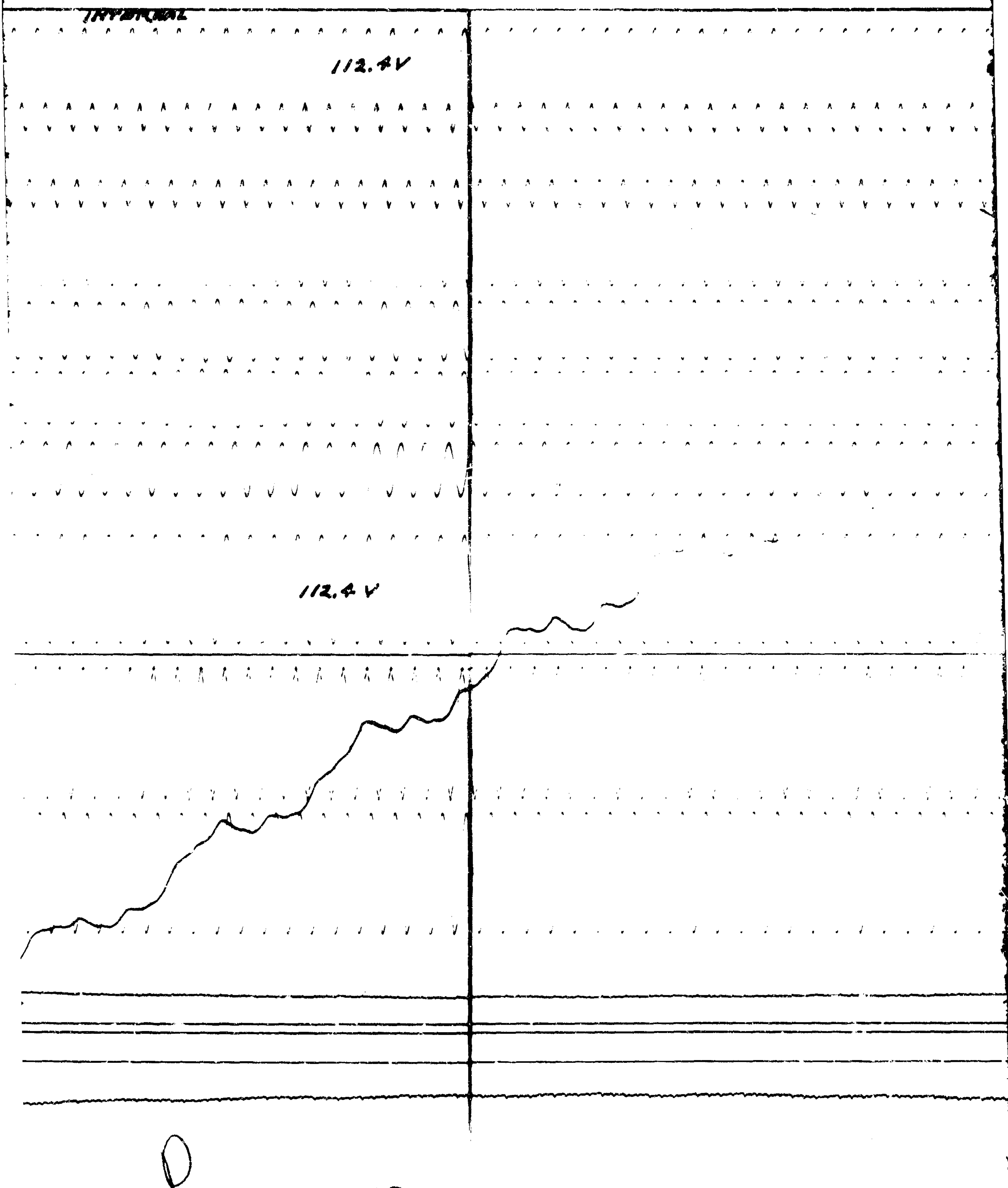

112.4V
112.4 V

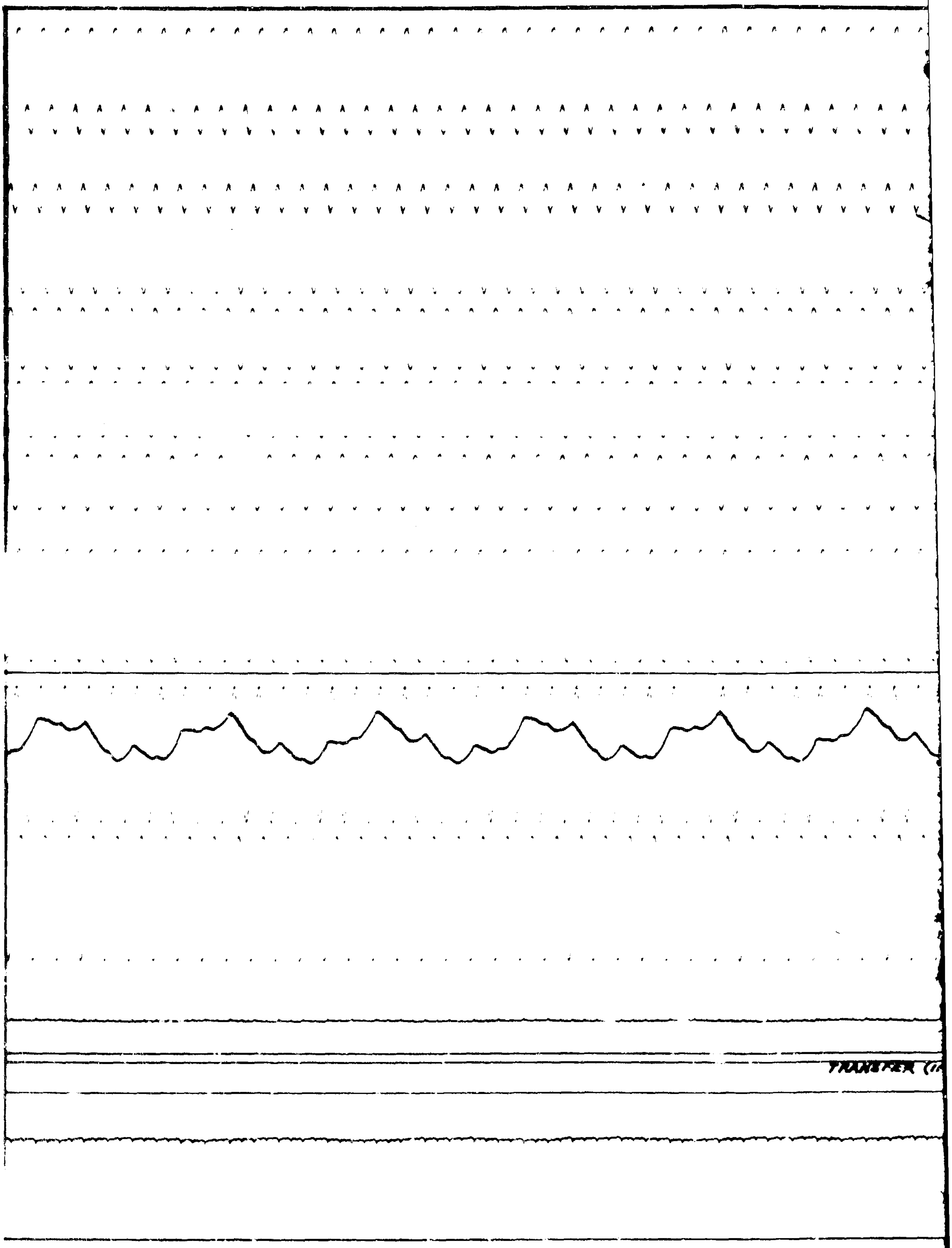


A

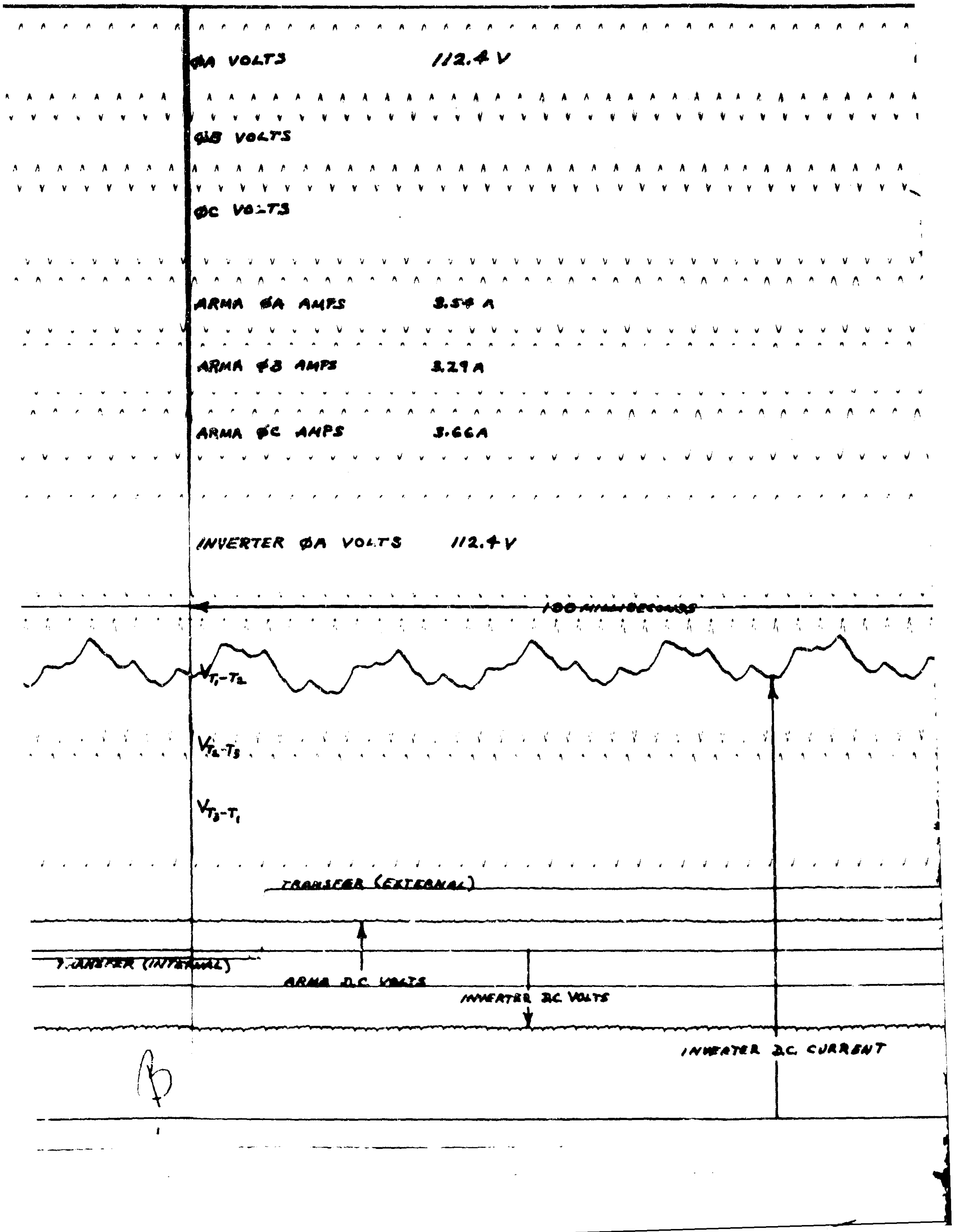

ØA VOLTS 112.4 V
ØB VOLTS
ØC VOLTS
ARMA ØA AMPS 3.54 A
ARMA ØB AMPS 3.29 A
ARMA ØC AMPS 3.66A
INVERTER ØA VOLTS 112.4V
$V_{T_1-T_2}$
$V_{T_2-T_3}$
$V_{T_3-T_1}$
TRANSFER (EXTERNAL)
TRANSFER (INTERNAL)
ARMA D.C VOLTS
INVERTER D.C VOLTS
INVERTER D.C. CURRENT
B

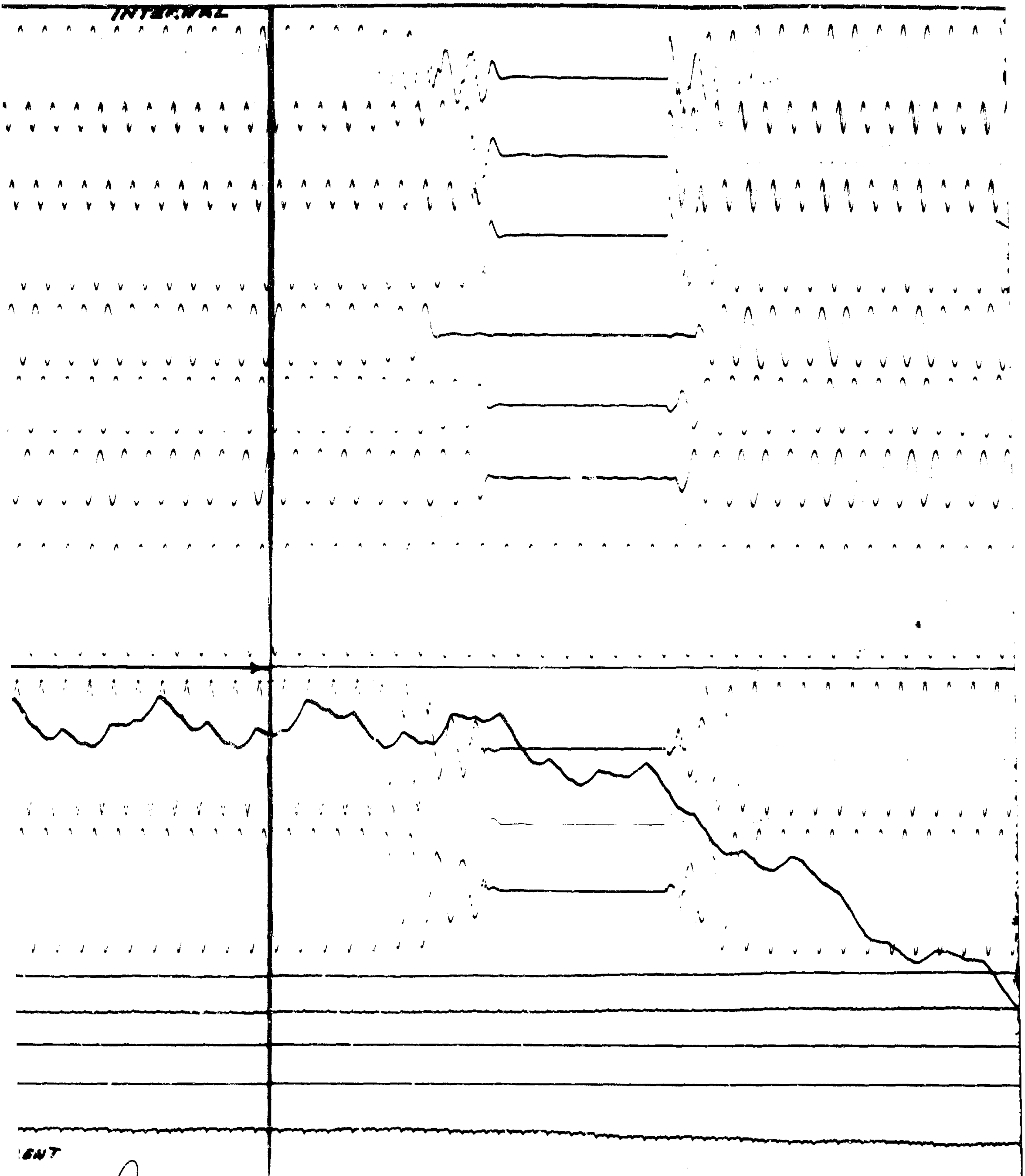


FIGURE 48

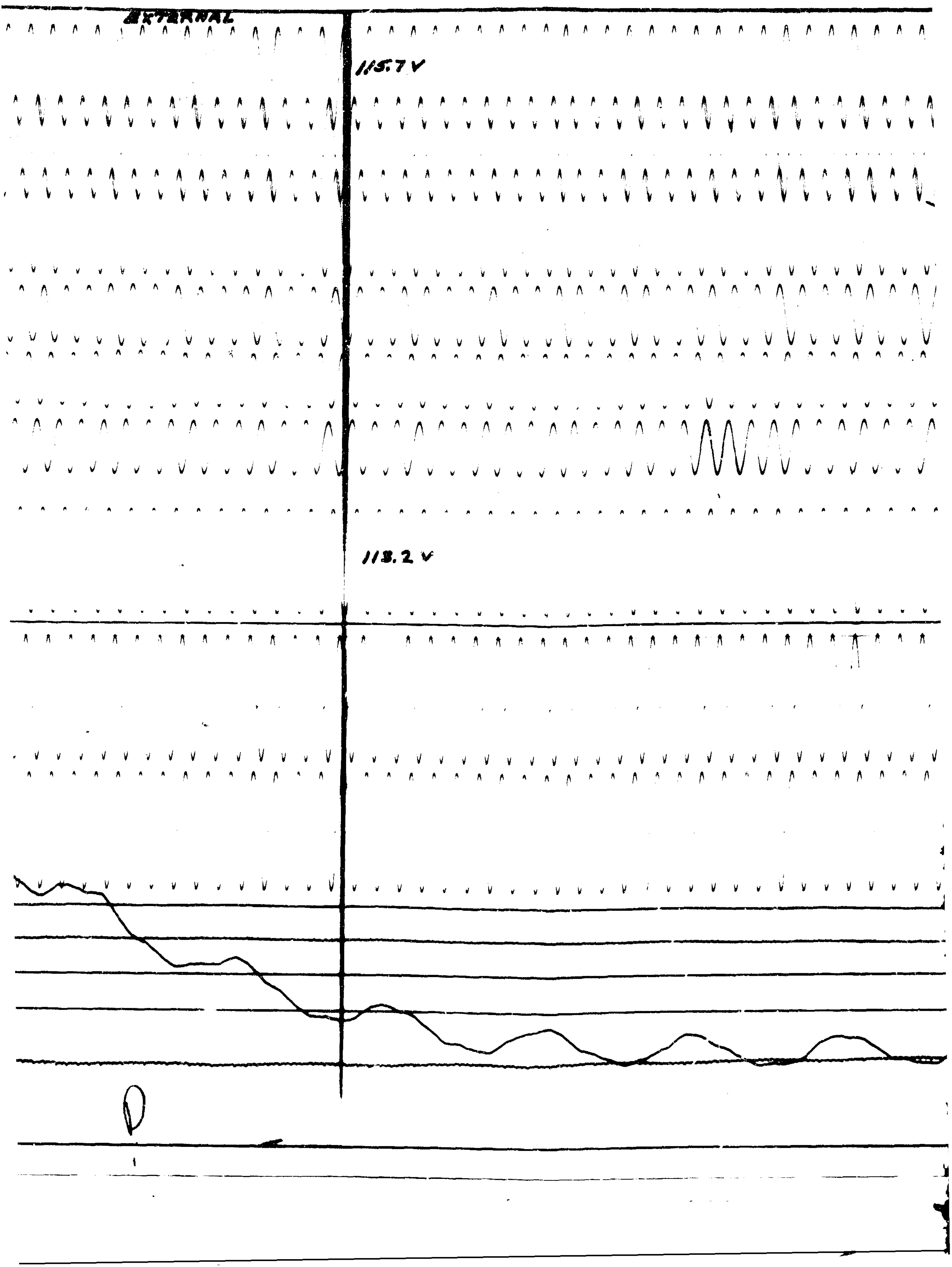
EXTERNAL
115.7 V
113.2 V

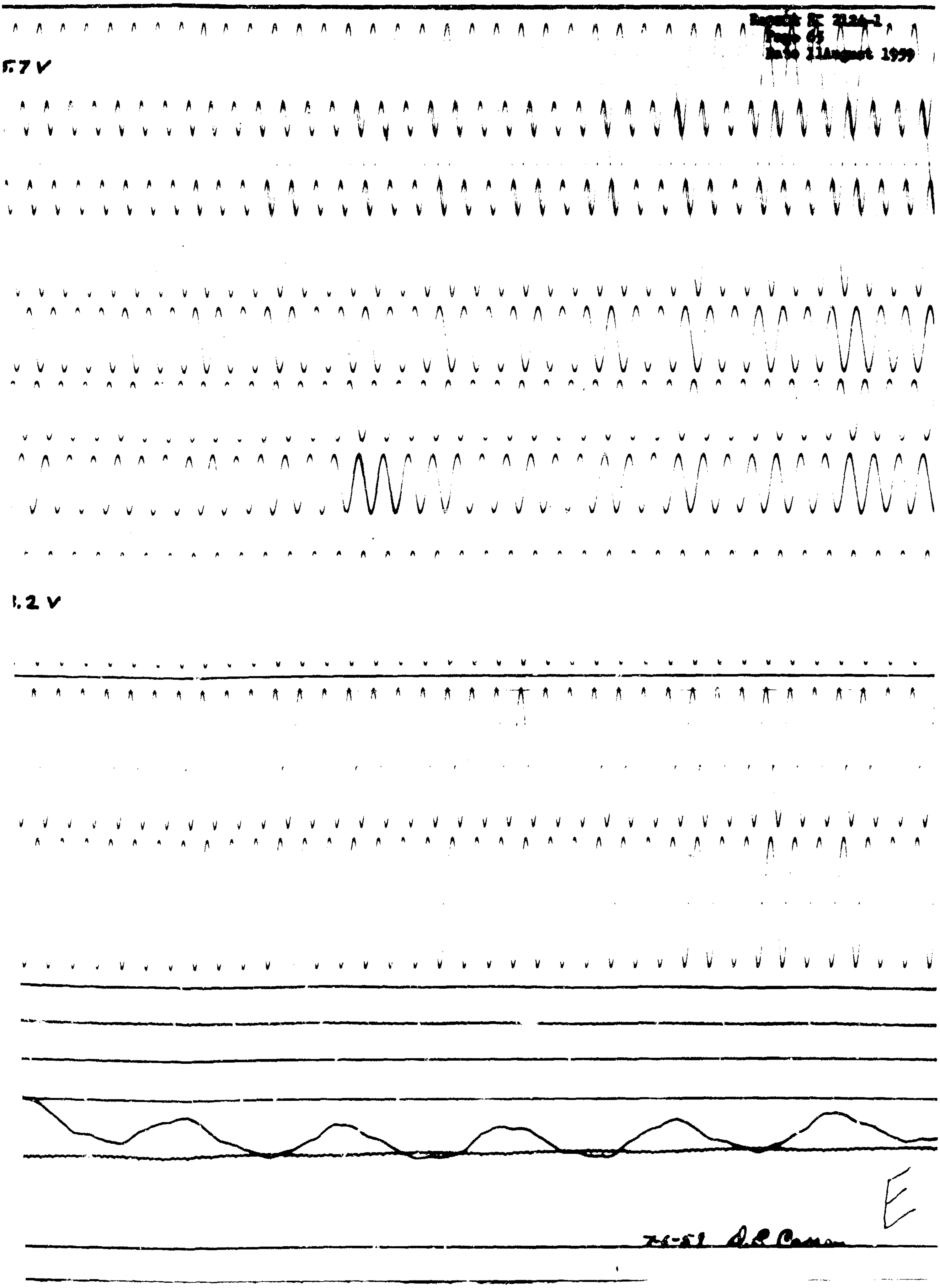
7 V
.2 V
E